17/9/76

THE METAMORPHIC GEOLOGY OF THE WINDMILL ISLANDS AND ADJACENT COASTAL AREAS, ANTARCTICA.

VOLUME 1

by

David Frank Blight, B.Sc.(Hons) (Adelaide)

Department of Geology and Mineralogy

University of Adelaide

October, 1975.

A THESIS SUBMITTED IN ACCORDANCE WITH THE REQUIREMENTS OF THE DEGREE OF DOCTOR OF PHILOSOPHY

C O N T E N T S

SUMMARY

Rocks of the Windmill Islands, Antarctica (long. 110°E, lat. 66°S) consist of a layered sequence of schists, gneisses and migmatites, intruded by a charnockite and a porphyritic granite and cut by two swarms of east-west trending dolerite dykes.

The rocks have undergone four deformations. The first two produced tight isoclinal folds, the third developed broader less appressed concentric folds and the last deformation produced gentle warps which plunge steeply to the south.

The metamorphic grade of the Windmill Islands rocks ranges from (i) upper amphibolite facies (sillimanite-biotite-orthoclase) in the north, through (ii) biotite-cordierite-almandine granulite to (iii) hornblende-orthopyroxene granulite in the south. The boundary between (i) and (ii) above, is marked by the incoming of orthopyroxene and also the outgoing of sphene and that between (ii) and (iii) by the outgoing of cordierite. Other metamorphic variations, apparent in the field are (i), the southward colour change of biotite (sepia → red brown) and of hornblende (blue green → brown green) and (ii), the greater abundance of migmatites and pegmatites in the north of the area.

Major element rock chemistry suggests the pre-metamorphic nature of the schists and gneisses probably consisted of acid and basic volcanics interbedded with sediments ranging from greywacke type sandstones to shales. Partial melting of these rocks produced some of the more acidic gneisses of the area.

The abundances of the elements K, Rb and Th are lower than those of terrains of similar grade elsewhere. This is regarded as representing original rock composition. The ratios K/Rb, Th/K and K/(Rb/Sr), however, are comparable with those from similar terrains elsewhere, and suggest

K, Rb and Th enrichment of these upper amphibolite-lower granulite facies rocks by a prograde crustal fractionation process; thus precluding the derivation of these rocks from the upper granulite facies by retrogradation.

The previously mentioned metamorphic grade changes from north to south are also evident in the mineral chemistry, both in terms of individual mineral compositions and in the distribution co-efficients ($K_D's$) of co-existing minerals. These changes can be accounted for as the result of the recrystallization temperatures being higher in the southern areas than in the northern areas. Load pressures during metamorphism were also higher in the southern areas.

Use of the garnet-cordierite geothermometer and geobarometer (Currie, 1971) coupled with other experimentally determined mineral breakdown curves in P-T space, indicate that the northern part of the Windmill Islands recrystallized under conditions of 5.5-6.5 Kbars load pressure, approximately 3.0 Kbars water pressure and temperatures around 760^{o}C.

This thesis contains no material which has been accepted for the award of any other degree or diploma in any University, nor to the best of my knowledge and belief, does it contain any material previously published or written by any other person except where due reference and acknowledgement is made in the text.

D. F. Blight

ACKNOWLEDGEMENTS

I am deeply grateful to Dr. R.L. Oliver who suggested and supervised the project. Dr. Oliver also critically assessed the final draft of the thesis.

I thank the Australian National Antarctic Research Expeditions who provided the logistic support for the field program. ANARE personnel of the 1970 Casey wintering party and 1971-72 Casey summer party provided considerable help during the field program.

I have benefited from discussions with my colleagues from the Department of Geology and Mineralogy, University of Adelaide, in particular Dr. A.W. Kleeman, Dr. J. Platt and Mr. C.D.A. Coin.

I also thank the following people for help in the fields indicated: Mr. R. Barrat (photography), Mr. R.J. Hill and Mr. M.J. Fitzgerald (computing), Dr. K. Turnbull and Mr. D. Bruce (chemical analyses), Mr. S. Tzrichy (H_2O^+ analyses), Mr. G. Trevelyan and Mr. W. Mussered (thin section preparation), Mrs. K. Bishop and Mrs. J. Gilliland (draft typing) and Miss L. Blight (drafting). Mrs. J. Brumby efficiently and accurately typed the final copy of the thesis.

The study was carried out during the tenure of a University of Adelaide Research Grant. Support for the Microprobe Analyses was obtained from an A.R.G.C. grant to Dr. R.L. Oliver.

CHAPTER 1

INTRODUCTION

1.1 AIM OF THESIS

The aim of this thesis is to examine in detail and document the geology of the rocks outcropping in the Windmill Islands, Antarctica and to elucidate the genesis and history of these rocks. Consequently this study incorporates the petrological, structural and geochemical features of these rocks.

1.2 GEOGRAPHICAL SETTING

1.2.1 Location

The Windmill Islands lie on the coast of "East" Antarctica and are centred at longitude 110° 30'E, latitude 66° 20'S, which is approximately due south of Perth, Australia (Fig. 1.1a). The islands are sited on the west side of the Law Dome, a small ice cap separated from the main continental ice cap by 2 or 3 glaciers (Vanderford, Totten and Fox Glaciers) (Fig. 1.1b). This dome is currently being investigated by glaciologists from the Australian National Antarctic Research Expeditions (henceforth abbreviated to A.N.A.R.E).

The islands occur over a roughly rectangular area, 40 x 15 km in size, with the long side of the rectangle aligned approximately north-south.

1.2.2 Geomorphology

The rocks outcrop as islands and as isolated nunataks on the "mainland". The nunataks are surrounded by ice which is permanently attached to the continent, (Fig. 1.2a), giving the impression that the nunataks are part of the continent. It is suspected that if the mainland ice were removed, the nunataks also would appear as islands.

This impression is supported by the occurrence of a shear moraine (Fig. 1.2b), the Løken Moraine, inland from the nunataks. This moraine may well mark the edge of the continent.

These islands and nunataks vary in height and peak around 90 metres above sea level. Most have low, rounded hills, which are covered in part by ice transported rubble. The valleys between these hills are filled with snow or glacial moraine and exfoliated detritus. Several raised beaches were noted. Exposure is fresh, except in the southern area where a massive charnockite appears to have been susceptible to chemical weathering. Frost action is fairly severe and many massive boulders show strong exfoliation features.

During the height of summer, large melt streams and lakes form (Fig. 1.2c). These severely restrict ground travel.

1.2.3 Vegetation and Animal Life

Vegetation is confined to the lichens and mosses which grow on many of the non-southerly aspect of rock faces. In the summer, large penguin rookeries were observed in five places. These rookeries obscure the geology of a not inconsiderable area with droppings, stone nests and the physical presence of upward of a million closely packed birds.

1.2.4 Climate

The climate is harsh, temperatures ranging between $+6^{o}C$ and $-35^{o}C$. The mean wind speed is around 15 k.p.h., but during blizzards, the wind speed may be in excess of 200 k.p.h.

1.3 HISTORY*

The islands were initially discovered in 1947 by the United States Navy during Operation Windmill. In 1956, the area was visited by A.N.A.R.E., a Soviet Antarctic Expedition, which called the area Grearson Oasis, and personnel of the United States who were involved in Operation Deep Freeze I.

During 1957, the United States set up a temporary station, Wilkes, on the eastern end of Clark Peninsula, for the I.G.Y. In 1959, the administration of Wilkes was turned over to the Australian Government.

---

*See McLeod and Gregory (1966.)

Australia now maintains a permanent base, Casey, on the north side of Bailey Peninsula. Casey was opened in early 1970 to replace Wilkes, which had fallen victim to the elements.

Casey is visited once every summer by a ship carrying relief stores and personnel. Very occasionally, ships of other nationalities call at Casey on goodwill visits.

1.4 PREVIOUS WORK

The first published works on the geology of the Windmill Islands, resulted from the Soviet visit in 1956. Ravich and Voronov (1958), Ravich (1960), and Voronov and Krasik (1963) discuss the petrology and geophysical characteristics of Grearson Oasis, and Starik et. al. (1959 and 1960) document K/Ar dates obtained from rocks of this area.

The results of work by the Americans during the I.G.Y. were published in the early 1960s. Cameron et. al. (1960) details K/Ar dates and Robertson (1961), a glaciologist with the 1957 Wilkes wintering party, published the first geological map and accompanying account of the Windmill Islands.

A brief reconnaissance geology report by A.N.A.R.E. workers, McLeod and Gregory, appeared in 1966 and further K/Ar dates were published by Webb et. al. (1963). More detailed work on the islands was discussed by Oliver (1970) in the context of Antarctic - Australian geological relationships.

1.5 REGIONAL GEOLOGY

These rocks of the Windmill Islands make up part of the Antarctic Shield (Fig. 1.3), a polymetamorphic terrain called by Harrington (1965) the "Basement Complex". This terrain consists mostly of high grade metamorphics (granulite and amphibolite facies) with some lower grade greenschist facies rocks occurring in the Prince Charles Mountains (Trail, 1963). These metamorphics occur as schists, gneisses and migmatites mostly of sedimentary origin, intruded by acid and basic rocks. Large

charnockitic bodies (generally intrusive) are numerous.

Many age determinations have been carried out on the metamorphics of this "Basement Complex". Ravich et. al. (1965) report K/Ar ages between 1525 (Vestfold Hills) and 415 m.y. (Mirny Base). More recently, Arriens (1975), has reported the following Rb/Sr whole rock ages:

George V Land	1500-1700 m.y.
Vestfold Hills	2500 m.y. and 500 m.y.
Prince Charles Mountains	2600-2800 m.y., 1200-1000 m.y., and 700-500 m.y.

East of the Windmill Islands, geophysical work has suggested the existence of a sedimentary basin under the Law Dome (Denham pers. comm.), about 80 km inland from Casey. The presence of sedimentary and volcanic pebbles in the Løken Moraine, support this idea.

K/Ar dates for the Windmill Island rocks have been determined by a number of workers (op. cit.). They fall into two groups, one around 900 m.y. and the other around 1100 m.y. Recent work by Arriens (pers. comm.) using Rb/Sr whole rock data, has yielded isochrons ranging between 1100 and 1400 m.y. Arriens believes the older of these two ages represents the pre-metamorphic age of sedimentation of the rocks, while the younger age corresponds to the high grade metamorphic event which affected them later.

1.6 METHOD OF STUDY

Field mapping and rock sampling was done while the author was wintering at Casey between January, 1970 and February, 1971 and during a brief summer trip in February, 1972.

Because of the scattered nature of the outcrop (Fig. 1.2a), it proved difficult, if not impossible, to use the standard mapping technique of traverses and boundary "chasing". Instead, each outcrop was visited and a geological map pieced together from the data collected. Field data were plotted directly onto "modified" airphotos, which were then collated to

form the map. Airphoto "modification" was necessary since the only airphotos available were a series of different size photos of different scales from different runs, taken by different cameras at different heights during different years. They covered most of the exposed rocks, but many were of poor quality (cold having affected the shutter mechanism) and many were flown when the cloud cover was the order of three oktas. The original airphotos were rephotographed and enlarged to a scale of 1:12000 using base maps produced by the United States Navy in 1957 (reference numbers U.S.H.O. 6656, 6657 and 6658). These United States maps however, are, themselves of dubious accuracy and consequently the accuracy of the resultant map is questionable. It is felt nevertheless to suffice for portraying the geology.

Petrological and geochemical work was carried out in the Department of Geology and Mineralogy at the University of Adelaide, South Australia. Details of the petrographical and geochemical techniques are described in the appendices.

CHAPTER 2

PETROGRAPHY

2.1 SUBDIVISION OF ROCKS

The rocks of the Windmill Islands can be divided into six different compositional groups. They are shown in Table 2.1 with their approximate areal extent. These data are based on an interprative geological map, where outcrop is only about 15%, hence the quoted areal proportion of each rock type is approximate.

Lithological Group	Compositional Group	Areal Extent
Acid Gneiss Granite Gneiss Aplite Pegmatite Porphyritic Granite Migmatite Gneiss	Acidic	50%
Migmatite Gneiss	Pelitic	5%
Charnockite	Charnockitic	40%
Layered Gneiss	Intermediate	3%
Dolerite Dyke Olivine Gabbro Dyke Dolerite Dyke	Mafic	2%
Basic Gneiss	Ultramafic	Trace

TABLE 2.1: Rock Compositional Groups

Mapping was carried out by grouping rock units on the basis of physical appearance, rather than composition. In most cases, what would be a compositionally distinct unit, would also be a unit with a particular physical appearance. However, in the field it is sometimes impossible to distinguish between compositional groups which look similar (e.g. Pelitic and Psammopelitic Migmatite Gneisses). Conversely, it is

possible to distinguish two different rocks in the field, even though they belong to the same compositional class (e.g. Granite of Ford Islands, 335-673, and the Granitic Gneisses elsewhere, 335-313)(see Fig. 4.1 Cluster Analysis). For this reason, the following rock unit descriptions usually apply to rocks which look physically similar, but when possible, various compositional groups of similar looking rocks are described separately.

2.2 TERMINOLOGY AND TECHNIQUES

All plagioclase compositions were determined optically on a four axis universal stage, with sections normal to 'a' using a technique described by Chuboba (1933). Offler (1966, Appendix II), on comparison with X-Ray methods and chemical analysis, found this U-stage technique to be satisfactory.

Perthitic and antiperthitic structure terms are after the classification of Spry (1969). Grain boundary shape description is also after Spry (1969). Other textural classifications are after Moore (1970) with modifications suggested by Collerson (1974). These descriptive terms are illustrated in Fig. 2.1.

Modal percentages of minerals present in each thin section were calculated by point counting of at least 1000 points.

Following are descriptions of the rock units portrayed in Figures 2.2, 2.3 and 2.4. Some of the igneous rocks have been deformed and suffered some recrystallization, so metamorphic textural terms are applied in these cases.

2.3 ACID GNEISSES

2.3.1 Introduction

These rocks make up approximately 50 percent of the total outcrop. They can be divided into two compositional classes on the basis of their FeO+MgO content (viz. (1) the granitic rocks and (11) the quartzofeldspathic rocks, which have a lower FeO+MgO content). However, this dis-

tinction is not sharp. In the field, the rocks were divided into five types on the basis of their physical appearance:

(i)	Leuco Gneiss	Quartzofeldspathic
(ii)	Weakly layered Gneiss	
(iii)	Ribbon Gneiss	Granitic
(iv)	Granite Gneiss	
(v)	Layered Granite Gneiss	

As in the compositional subdivision, it is difficult at times to pigeon-hole some rocks into these classes due to the gradational boundaries.

2.3.2 The Leuco Gneiss and the Weakly Layered Gneiss

These outcrop mainly in the northern area (viz. north of Sparkes Bay), but some occur on Herring, Cloyd and Bosner Islands. The only noticeable difference between the two rock types is in the amount of biotite they contain. The leuco gneisses occur as strikingly white rocks with less than 2% biotite, whereas the weakly layered rocks are slightly darker in colour, with between 2% and 7% biotite. The weak discontinuous layering in the latter is produced by the alignment of clumps of biotite (Fig. 2.5a).

The following assemblage was observed; quartz + plagioclase + microcline + biotite + opaques ± garnet with rare sillimanite and ubiquitous apatite and zircon. Retrograde minerals observed were chlorite, epidote and sericite.

2.3.3 The Ribbon Gneiss

The ribbon gneisses are similar to the weakly layered gneiss described above, but are much richer in ribbon-like biotite schlieren, which have a strong preferred orientation, as does the biotite within the schlieren (Fig. 2.5b). The rock may contain up to 15% biotite. The Ribbon Gneisses are confined to Midgely, Hollin, Warrington and Pidgeon Islands and are thought to represent a strongly metamorphosed granite which was intruded prior to, or during, the main metamorphic event.

The assemblage, quartz + plagioclase + microcline + biotite + opaques with rare garnet, hypersthene, sillimanite, spinel and the pervasive apatite and zircon, was noted.

2.3.4 The Granite Gneiss

Evenly disseminated biotite (up to 7%) with a strong preferred orientation characterises these gneisses. They occur on Hollin, Midgely, Warrington, Pidgeon, Ford and Herring Islands and south of Robinson Ridge. The following assemblage was recognised; quartz + plagioclase + microline + biotite + opaques with rare hornblende and hypersthene and the ubiquitous zircon and apatite. Retrograde minerals observed were sericite, chlorite and epidote.

2.3.5 The Layered Granite Gneiss

The layered granite gneiss occurs only on Clark Peninsula. It resembles the granite gneisses, but is penetrated by long, thin (between 0.5 and 5.0 cm. wide) evenly distributed leucocratic veins (Fig. 2.5c). These veins consist of coarser grained quartz and especially microcline with minor plagioclase. The veins are parallel or sub-parallel to the schistosity (S_1) in the granitic portion of the rock. This schistosity is defined by biotites with a preferred orientation and by flattened quartz and feldspar grains. In the core of the major antiform on Clark Peninsula, the grains defining this schistosity have been recrystallized parallel to the axial plane and a new schistosity (S_3) then is at an angle to the layering (Fig. 2.5c).

Because of the scattered nature of the outcrop and the small width of the veins, it was not possible to trace them for long distances, however they are continuous for at least tens of metres. The genesis of these veins is indicated at one location where a pegmatite was seen with apophyses of leucocratic material penetrating the granite gneiss and comprising the veins in question (Fig. 2.6a). The coarser grain size and the presence of dominant quartz and microcline in these veins, supports

the idea that they represent veins of injected pegmatite. Also, it is possibly more than coincidence that pegmatites are strongly developed only on Clark Peninsula, (Fig. 2.16)the one place where the layered granite gneiss occurs.

The veins have a simple assemblage; quartz + microcline + plagioclase, whereas the granitic material has additional biotite + opaques with some hornblende and garnet and ubiquitous apatite and zircon.

2.3.6 Texture of the Acid Gneisses

The texture under the microscope of the acid gneisses is the same, namely inequigranular - interlobate.

2.3.7 Descriptive Mineralogy of the Acid Gneisses

Quartz comprises of the order of 40% of the rock, but varies between 20% and 65%. The xenoblastic grains with embayed boundaries are between 0.05 and 7.0 mm in size, averaging 1.0 mm. The grains nearly always show strain extinction and are often graphically intergrown with plagioclase. They are commonly elongated but some occur as small rounded inclusions.

The grain boundaries observed in the layered granite gneiss, are perhaps a little more sutured than embayed. This may be a function of the fact that this rock is confined to the core of an antiform and as such, may show more recrystallization features than other rock types.

Plagioclase is commonly antiperthitic (patch form). Grain sizes range from 0.1 to 6.0 mm., averaging 1.0 mm. The xenoblastic crystals have embayed grain boundaries and are often heavily altered to sericite.

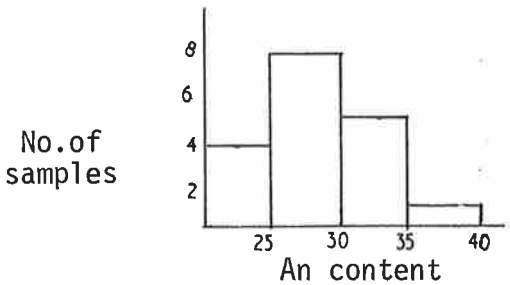

The composition ranges between An_{20} and An_{45}, peaking about An_{27}. (See histogram).

The modal percentages are spread between 5% and 50%, averaging around 25%. As mentioned before, the plagioclase is often graphically

intergrown with quartz. Poorly defined albite and pericline twins are common.

Many of the pagioclases have one or even two rims of plagioclase about them. These rims are particularly evident when the plagioclase is (or was) in contact with microcline (Fig. 2.6b). This phenomenon is well documented (Ramberg 1962, Hubbard 1967 and Byerly and Vogel 1973). Byerly and Vogel (1973) for example, have proposed an exsolution-vacancy hypothesis to explain the formation of these rims. A growing number of workers support, or partly support, this hypothesis (see Phillips 1974) which seems applicable to the plagioclase rims observed in the Acid Gneisses from the Windmill Islands.

Tartan twinning characterises microcline, which occurs as xenoblastic crystals with embayed grain boundaries. Occasionally, the microcline grains show simple twinning. Modal percentage varies between 5% and 60%, averaging around 30%. The grains sometimes occur as porphyroblasts, especially in the leucocratic veins of the layered granite gneiss. The grain size ranges from 0.05 to 12.0 mm, but on an average, is only a little larger than most of the other grains (i.e. 1.3 mm). Some grains are perthitic in stringlet or bead form.

Pleochroic biotite laths have a preferred orientation which gives rise to a schistosity in most of the rocks. The pleochroic scheme depends upon the location of the sample:

		Northern area	Southern area
α	-	Light green	Green
$\beta = \gamma$	-	Sepia	Rusty.

Lath length ranges from 0.05 to 9.0 mm., averaging about 0.5 mm long. The rocks may contain up to 15% biotite (Ribbon Gneiss), but usually have less than 5%. Biotite often occurs in layers with opaques and garnet. These layers are usually parallel to the schistosity. Some grains are poikiloblastic with inclusions of quartz. In the more retrograded rocks,

biotite is partly altered to chlorite.

Garnet occurs as subdioblastic fractured crystals which usually occupy about 1% of the rock, although in rare cases, this may rise to 10%.

Grain sizes vary between 0.05 and 2.0 mm, but average around 0.8 mm. The garnet can be disseminated throughout the rock, but is usually confined to layers with biotite and opaques. These opaques are xenoblastic and are about 0.3 mm in size. They are dominantly magnetic and although they can make up to 7% of the rock, they are usually present in much smaller amounts (viz. about 1%).

Sillimanite occurs in a couple of specimens as small prismatic needles (0.1 mm long) with a preferred orientation parallel to the schistosity.

Where present, hornblende and hypersthene occur in small amounts (<1%).

Zircon and apatite occur in most rocks as small rounded grains, but only in trace quantities.

Secondary epidote occurs in veins while sericite appears to be the retrograde alteration product of feldspars.

2.4 BASIC GNEISSES

2.4.1 General Description

This rock type nearly always occurs as pods or lenses of melanocratic rock completely surrounded by leucocratic gneiss (Fig. 2.6c). The pods range in size from 30 cm up to 30 metres and appear to represent relics of engulfed material caught up during the establishment of the leuco gneisses (discussed later, section 4.3.5). In general, they have a strong schistosity which usually parallels the plane of flattening of the pod. This plane is in turn aligned to the major preferred orientation (S_2) of the leuco gneisses.

The basic gneisses also occur rarely as thin layers (up to 5 m. wide) parallel to the schistosity and layering in the surrounding rock. The layers are traceable for upward of 100 metres along strike and are thought to parallel original sedimentary bedding. They have a strong schistosity parallel to that of the surrounding rock.

2.4.2 Microstructures

The pods have a very strong schistosity (S_2) defined by the preferred orientation of plates of biotite and hornblende and by the flattening of pyroxene grains.

In all these mafic pods, the grain boundaries are straight, curved or more rarely, embayed. This is in contrast to the embayed to sutured grain boundaries exhibited by the leucocratic material surrounding the pods (see Acid Gneisses 2.3). This may imply that the assemblages in the mafic rocks were closer to equilibrium than those in the leucocratic material. However, Spry (1969) cautions that: "Many straight boundaries in regionally metamorphosed rocks have unequal triple points and are not in equilibrium. This is true also for curved boundaries which are typical of textures frozen while in the process of mutual adjustment".

2.4.3 Textures

The texture of these basic rocks is generally equigranular polygonal, although some tend to be inequigranular and interlobate.

2.4.4 Mineral Assemblages

The following primary minerals were observed in thin section - quartz, plagioclase, hornblende, orthopyroxene, clinopyroxene, biotite, garnet, opaques, microcline, apatite and zircon. Some retrograde minerals noted were - a fibrous amphibole, chlorite, epidote and possibly serpentine and talc. The following assemblages of the above minerals were recognised:

(i) biotite + hornblende + plagioclase $\pm$ quartz $\pm$ garnet

(ii) biotite + hornblende + orthopyroxene + plagioclase

(iii) biotite + hornblende + orthopyroxene + clinopyroxene + plagioclase $\pm$ quartz.

(iv) hornblende + orthopyroxene + clinopyroxene + plagioclase $\pm$ quartz.

(v) biotite + orthopyroxene + plagioclase $\pm$ garnet.

(vi) biotite + orthopyroxene + clinopyroxene + plagioclase.

Assemblage (i) occurs only on Clark Peninsula. Assemblages (ii), (iii) & (iv) occur between Bailey Peninsula and Robinson Ridge, whereas (v) & (vi) occur south of Robinson Ridge. This areal distribution of assemblages can be related to the breakdown of hornblende as the metamorphic grade increases from north to south (see section 2.14.2). The breakdown of hornblende can be represented by the reaction:

hornblende (i) + quartz → hornblende (ii) + orthopyroxene + clinopyroxene + plagioclase → orthopyroxene + clinopyroxene + plagioclase (Binns, 1969b).

2.4.5 Descriptive Mineralogy

Generally, quartz occurs in small amounts up to 5%, however, occasionally it may occupy as much as 40%. The grain size ranges from 0.05 to 8.0 mm, averaging about 0.5 mm. The larger size grains occur in narrow veins and most grains are flattened in the plane of the vein. The grains occur as xenoblastic crystals with curved to embayed boundaries and as small rounded inclusions. Some are graphically intergrown with hornblende. Most grains show strain extinction.

Plagioclase is characterised by albite and pericline twinning. Occasionally, it is antiperthitic in stringlet form. Modal volumes vary between 5% and 50% and grain size ranges 0.1 to 3.0 mm, averaging 0.5 mm.

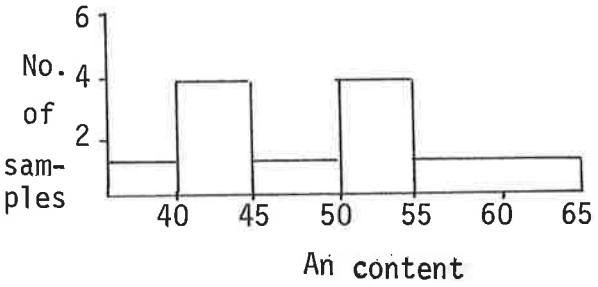

The An content of the plagioclase grades from below An_{40} to above An_{50}. (See histogram).

The plagioclase composition appears not to be related to the mineral assemblage (c.f. with psammopelitic migmatite gneisses). Some grains are poikiloblastic with rounded quartz inclusions. Grain boundaries are straight to curved.

Microcline was observed only in two basic rocks (335/601 and 335/713) and in both of these, it is confined to a leucocratic vein and occupies less than 5% of the rock. It is characterised by tartan twinning and is perthitic in stringlet form.

Pleochroic hornblende with the following scheme has a strong preferred orientation:

	Assemblage	
(i) & (ii)	(iii) & (iv)	(v) & (vi)
α - light green	light green	green
β - green	green	dark green
γ - bluish-green	green	greenish brown
with $\beta > \gamma > \alpha$		

It generally comprises greater than 50% of the rock, but can vary from 3% to 70%. Grain sizes range from 0.1 mm to 2.0 mm, averaging 0.8 mm. It is in places graphically intergrown with quartz and commonly contains inclusions of quartz and plagioclase. Grain boundaries are straight to curved (some slightly embayed).

Subidioblastic garnet may form porphyroblasts up to 12 mm in diameter, but is generally much smaller, about 0.8 mm. It is commonly confined to bands and constitutes between 2% and 15% of the rock, although in most cases, this modal volume is less than 5%.

Hypersthene comprises 5% to 25% of the rock. It ranges in grain size between 0.05 mm and 8.0 mm, averaging 0.5 mm. Together with clinopyroxene, it commonly forms a mineralogical layering. Those hypersthene grains with a high Al content, show a weak pleochroism (see section 5.3.2).

α - pink

β - yellow

γ - pale green.

Grain boundaries are straight to curved. A characteristic feature of the hypersthene is that it is nearly always partly or totally altered (Fig. 2.7a), especially in assemblages (i), (ii) and (iii). The alteration, interpreted as retrograde, is as follows:

orthopyroxene → fibrous amphibole + opaque

or orthopyroxene → talc (?) + serpentine (?) + opaque.

The latter reaction is not definite as the retrograde products are very fine grained making positive optical identification impossible.

The clinopyroxene grains range in size from 0.1 mm to 1.0 mm, averaging about 0.5 mm. They occupy between 1% and 40% of the rock. Some grains are simply twinned. Grain boundaries are straight to curved. Observed $2V's$ grade between 45^o and 55^o.

Biotite commonly occurs in layers with garnet and has a very strong preferred orientation parallel to these layers. It comprises 1% to 25% of the rock, but the modal volume is generally around 5%. The pleochroic laths have embayed grain boundaries and are often retrograded to chlorite. The laths vary in length between 0.2 mm and 3.0 mm, averaging 0.4 mm long. Sometimes it is graphically intergrown with quartz. The pleochroic scheme is as follows:

	Assemblage	
	(i), (ii) & (iii)	(iv), (v) & (vi)
α	- light green	sepia
$\beta = \gamma$	- sepia	rusty brown

Zircon and apatite are almost ubiquitous, but only occur in trace quantities as small rounded crystals.

2.5 MIGMATITE GNEISS

2.5.1 Definition of the terms Pelite, Psammite & Psammopelite

The term pelite was originally defined as "....clastic sediments composed of clay, minute particles of quartz or rock flour". (Holmes 1928). As such, it was essentially a size classification. However, over the years, this has been largely superseded by the term lutite. Instead, the metamorphic petrologists have adopted the term pelite and use it to describe a metamorphosed aluminous rich sedimentary rock, e.g. "Pelitic - derivitive of pelitic (aluminous) sediments. Abundance of micas characteristic". (Turner 1968). Joplin (1968 page 23) gives a very comprehensive glossary on the term pelite : "Mud rock, argillite, lutite. Commonly applied to metamorphic rocks and can be used for this type of rock in any grade of metamorphism. The mud may have a wide range of composition, but it is most commonly aluminous, so the term pelite is usually applied to fine grained aluminous rocks of sedimentary origin and, if not otherwise stated, this composition is inferred". She apparently imposes a grain size condition which is not considered necessary because absolute grain size is really only dependent upon the number of nuclei present and the time of crystallization. It would appear that the phase "fine grained" was probably meant to apply to the original sediment, rather than the metasediment.

It is difficult at times to decide (i) if a metamorphic rock was once a fine grained aluminous sediment and (ii) what boundary conditions define aluminous? For the purpose of the following descriptions, it is felt that the term pelite be restricted to metamorphic rocks and that the only connotation that can be placed on the term is a chemical one. Hence, a pelite is here defined as a metamorphic rock which has 3% or more normative corundum in its catanorm and thus should contain minerals rich in Al such as muscovite, andalusite, sillimanite, staurolite and cordierite. Similarly, the term psammite has now come to mean a metamorphosed, usually

quartz rich, sandstone (Joplin 1968). Thus, a psammopelite is a metamorphic rock presumably derived from a clay rich sandstone.

2.5.2 General Description of Migmatite Gneiss

Migmatite gneisses are confined entirely to the area north of Sparkes Bay. They consist of pods and discontinuous layers (up to three metres wide) of strongly schistose fairly mafic rock, surrounded by and interlayered with anastomosing leucocratic veins (Fig. 2.7b&c).

Chemically, the rock is a psammopelite with interlayered pelites. These pelitic layers, which are up to 50 metres wide, are very difficult, if not impossible, to distinguish in the field from the psammopelites. The only difference is that in the pelites, the more schistosic parts contain aluminous minerals (e.g. cordierite and sillimanite). The original sedimentary bedding is probably manifest in these pelitic layers.

2.5.3 Microstructures

These rocks have a very strong schistosity (S_1) defined by the preferred orientation of plates of biotite, needles of sillimanite and occasionally the flattening of cordierite and quartz grains. Tight microfolds of S_1 are commonly present, being manifest by sillimanite and biotite (Fig. 2.8a). These folds develop a weak axial plane schistosity (S_2), but only with biotite. This S_2 is parallel to the dominant schistosity, S_1 in most cases.

2.5.4 Texture

The texture exhibited by the migmatite gneiss is seriate, interlobate.

2.5.5 Assemblages

The following primary minerals were observed under the microscope: quartz, plagioclase, microcline, biotite, cordierite, garnet, sillimanite, hypersthene, hornblende, opaques, zircon, apatite, spinel and sphene. Some secondary minerals were seen and found generally to be retrograde alteration products of the above and are, chlorite (after biotite), sericite

and muscovite (after feldspar), amphibole (after orthopyroxene) and epidote. From these observed minerals, five assemblages were noted:

(i) Quartz + plagioclase + microcline $\pm$ biotite + opaque.

(ii) Quartz + plagioclase + microcline + biotite + cordierite $\pm$ sillimanite $\pm$ garnet + opaque.

(iii) Quartz + plagioclase + biotite + hypersthene + garnet + opaque.

(iv) Quartz + plagioclase $\pm$ microcline + biotite + garnet + opaque.

(v) Quartz + plagioclase + biotite + hornblende $\pm$ hypersthene + opaque.

Assemblage (i) describes the leucocratic veins, assemblages (ii) and (iii) the pelitic sections and assemblages (iv) and (v) the psammopelitic parts of the migmatite gneisses.

2.5.6 Descriptive Mineralogy

Quartz varies in size between 0.05 mm and 5.0 mm, averaging 1.0 mm. The modal percentage also varies, ranging from 15% to 55%, but has a strong mean around 30%. The grains are xenoblastic with embayed grain boundaries. Quartz also occurs as small rounded inclusions in other minerals. Not surprisingly, it is the dominant mineral in the leucocratic parts of the migmatite gneisses. Most grains show strain extinction.

The An content of the plagioclases varies between An_{22} and An_{48} (see histogram). Assemblages (i) to (iv) have compositions generally less than An_{35}.

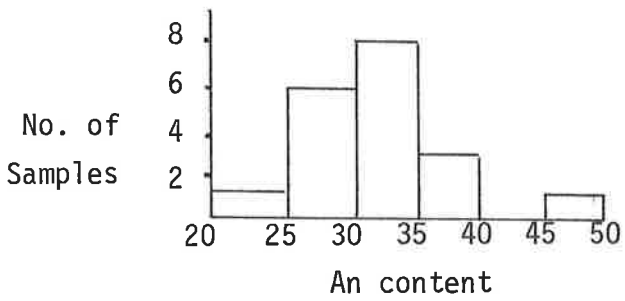

These xenoblastic plagioclase grains have embayed to lobate sutured boundaries and make up between 2% and 50% of the rock.

They vary in size between 0.05 mm and 5.0 mm, averaging about 1.0 mm.

Albite and pericline twinning are common as is string and patch form antiperthite. Some grains are poikiloblastic with small rounded quartz inclusions. Others are graphically intergrown with quartz. Often grains of plagioclase are partially altered to sericite.

Potash feldspar occurs as microcline which has prominent tartan twinning. It can constitute between 1% and 35% of the rock, although in the pelitic assemblages, the amount of microcline is usually around 3%.

Grain sizes vary from 0.2 mm to 0.4 mm, averaging 1.0 mm. It occurs as xenoblastic crystals with embayed to lobate sutured boundaries and is often perthitic in stringlet form.

Pleochroic sub idioblastic biotite laths with ragged ends range in size from 0.05 mm to 4.0 mm, averaging 0.6 mm. The pleochroic scheme is as follows:

α - light green

$\beta = \gamma$ - sepia.

In general, the biotite occupies about 10% of the rock, but can range from 5% to 20%. It is often associated with garnet, concentrated into bands with a strong preferred orientation parallel to these bands. Frequently, biotite is partially altered to chlorite and opaque, along the (001) cleavage plane (Fig. 2.8b). It is rarely poikiloblastic with rounded quartz grains.

Cordierite occurs in most of these pelitic rocks. The modal volume ranges from 10% to 32%. Grain size varies between 0.1 mm to 6.0 mm, averaging 1.0 mm, however, in one location (near barge storage slips at Casey Base), some very large crystals, up to 10 cm in size, were found. Cordierite is difficult to differentiate from quartz and plagioclase in thin section, since its optical properties are similar to both. The distinguishing features of the cordierite in the rocks of the Windmill Islands are:

(i) Yellow pleochroic halos about included zircons (Fig. 2.8c).

(ii) Multiple twinning. These twins are spindle shaped at one end, while the other ends terminate at grain boundaries (Fig. 2.9a&b). They lack the sharpness of the multiple twins of plagioclase.

(iii) Retrograde alteration products (Fig. 2.9c). The cordierite alters at the grain boundaries and along cracks to a fine grained light greenish coloured, fibrous product called pinite (this, presumably, is a mixture of muscovite with chlorite or serpentine minerals).

(iv) Colour a light red to pink when stained with amaranth.

The xenoblastic grains have embayed boudaries and are generally poikiloblastic with inclusions of rounded zircons and quartz and idioblastic sillimanite needles.

In many thin sections examined, the cordierite is intimately associated with fine idioblastic sillimanite needles (Fig. 2.9a). These needles are between 0.2 mm and 0.5 mm long, averaging 0.1 mm and make up to 3% of the rock. They have a strong preferred orientation and in some thin sections define microfolds (Fig. 2.9a).

When garnet occurs, it is usually slightly greenish in colour and highly fractured, and in some cases, has a slightly larger grain size than that of the coexisting minerals, making it porphyroblastic. The grains are usually sub idioblastic, retaining a roughly equidimensional shape. The boundaries are curved to embayed and some alteration is visible at the boundaries and along fractures. Grain sizes range from 0.05 mm to 5.0 mm, averaging 1.5 mm. The garnet usually occurs in quantities less than 5%, however, occasionally it occupies up to 20% modal volume.

The opaque minerals, which are mostly magnetite and ilmenite with a small amount of hematite (possibly exsolved from the magnetite and ilmenite) pyrite and chalcopyrite, occur in flattened xenoblastic grains ranging from

0.005 mm to 3.0 mm in length, averaging 0.6 mm. They are flattened in the direction of the preferred orientation of biotite and sillimanite (viz. S_1) and are often concentrated in layers parallel or sub-parallel to this schistosity.

Normally, the opaques rarely exceed 3% modal volume, but in 335-98 (Shirley Island), it is as high as 14%. 335-98 is also unusual in that it is the only pelitic rock examined which contains spinel. A few small grains of this spinel are intimately associated with the opaque minerals. It is felt that the spinel is probably hercynite because it:

(i) is associated with the Fe opaques;

(ii) is dark green in colour;

(iii) co-exists with free silica (Deer et. al. 1966, p. 430).

Hypersthene occurs very rarely and only in small amounts (viz.<10%). The xenoblastic grains, which have embayed boundaries, are flattened. Their size varies between 0.05 mm and 6.0 mm, averaging 2.5 mm. This is slightly larger than the rest of the minerals, making the hypersthene porphyroblastic. It often shows strong pleochroism presumably because of its high (up to 5.13 wt%) Al content (Howie 1964, Burns 1966). The pleochroic scheme is:

α - pink

β - yellow brown

γ - green.

Some grains are poikiloblastic with rounded quartz and subsidioblastic opaques included. The cleavage shows a moderate preferred orientation in the direction of S_1. Occasionally, the hypersthene has suffered retrograde alteration at the edges to a fibrous amphibole (possibly anthophyllite).

Xenoblastic crystals of hornblende occur occasionally. They have curved to embayed grain boundaries and range in size from 0.2 mm to 1.5 mm, averaging 0.8 mm. Hornblende may occupy up to 50% of the rock.

It is pleochroic in the following manner:

α - light green

β dark green

γ bluish green

with $\beta > \gamma > \alpha$

Zircon and apatite occur as small rounded grains, about 0.1 mm in size, in trace quantities. Sphene was only observed in one thin section (335/400A).

2.6 LAYERED GNEISS

2.6.1 General Description

These gneisses occur over most of the area studied, except north of the hypersthene isograd (namely Clark Peninsula and the Swain Group). They are prominent as xenoliths in the charnockite (see section 2.8.2). The dominant feature of these rocks is the strong mineralogical layering (Fig. 2.10a) defined by the alternation of mafic rich and mafic poor portions (Fig. 2.10b). The non-mafic layers consist predominantly of plagioclase and sometimes quartz. The grain size of the minerals in these leuco layers is generally larger than that in the mafic layers. The layered gneisses are generally dense compact looking rocks, the biotite content being relatively small, and the schistosity consequently is less penetrative than that observed in the migmatite gneisses or the mafic pods.

2.6.2 Microstructures

A fairly strong schistosity (S_1) however is defined principally by laths of biotite and hornblende. Other minerals (e.g. quartz and pyroxenes) are slightly flattened in the plane of S_1. S_1 is folded, usually tightly, and a weak axial plane schistosity (S_2) is developed by the recrystallization of the biotites only.

2.6.3 Texture

The texture of the layered gneisses is equigranular polygonal, tending towards inequigranular interlobate.

2.6.4 Assemblages

The following primary minerals were observed in thin section:

Quartz, plagioclase, microcline, biotite, hornblende, hypersthene, clinopyroxene, garnet, opaques, zircon and apatite.

From these, the following assemblages were recognised:

(i) Quartz + plagioclase + biotite + hypersthene + opaque + garnet $\pm$ microcline.

(ii) Quartz + plagioclase + hornblende + hypersthene + clinopyroxene + opaque $\pm$ biotite.

(iii) Plagioclase + biotite + hypersthene + opaque $\pm$ hornblende $\pm$ clinopyroxene.

2.6.5 Descriptive Mineralogy

Xenoblastic quartz grains with straight to embayed boundaries are often slightly flattened with a preferred orientation. The grain size varies between 0.02 mm and 6.0 mm, averaging about 1.0 mm. Quartz makes up between 10% and 40% of the rock when it occurs (assemblages (i) and (ii) detailed above). Most grains show strain extinction. Rare graphic intergrowth with plagioclase is observed. The quartz also occurs as small rounded inclusions in other minerals.

Plagioclase grains ranging from 0.2 mm to 12.0 mm in size, averaging 1.0 mm. The composition varies between An_{45} and A_{56}, with a mean around An_{52}. The plagioclase occurs as xenoblastic grains with straight to slightly embayed boundaries. It occupies between 10% and 60% of the rock and is often characterised by albite and pericline twinning. Grains are often antiperthitic in patch, string and stringlet form, and rarely are graphically intergrown with quartz.

Microcline occurs in only trace quantities about 0.5 mm in size. It is characterised by tartan twinning. Most grains are perthitic in stringlet form.

Pleochroic biotite laths ranging in length from 0.1 mm to 2.0 mm, averaging 0.7 mm. The pleochroic scheme depends upon the location (see also section 5.3.4):

in the north	α	- light green
	$\beta = \gamma$	- brown
in the south	α	- sepia
	$\beta = \gamma$	- rusty.

The biotite may occupy between 1% and 20% of the rock. It has a strong preferred orientation which imparts a moderate schistosity to the rock. It is usually confined to layers with other ferromagnesium minerals and opaques.

Xenoblastic lath like, pleochroic grains of hornblende also define a schistosity. Once again, the pleochroic scheme depends upon the location. In the north Z - green brown, in the south Z - brownish green. Grain boundaries are straight to embayed, grain size ranges between 0.01 mm and 1.5 mm, averaging about 0.8 mm. The hornblende comprises between 5% and 25% of the rock.

Hypersthene constitutes from 2% to 25% of this rock, but is generally around 5%. The grain size varies between 0.02 mm and 2.5 mm, averaging 0.5 mm. It is often poikiloblastic with inclusions of quartz and feldspar. The grains are generally fresh, but some have suffered retrograde alteration around the rims to a fibrous amphibole. The xenoblastic grains have straight to weakly embayed boundaries. Some of the more aluminous hypersthene grains (as indicated by electron probe analyses) are pleochroic as follows:

α	- pink
β	- yellow green
γ	- light green.

Xenoblastic clinopyroxene grains with straight to slightly embayed boundaries, occupy between 0% and 25% of the rock. Observed 2 V's are unusually low (i.e. approximately 40^{o}). The grain size ranges between 0.02 mm and

2.5 mm, averaging about 0.5 mm.

Opaques are mainly magnetite with minor pyrite and chalcopyrite. The xenoblastic grains are slightly flattened and are about 0.4 mm in size. They occupy up to 10% of the rock.

Garnet was observed in only one rock (335/329), making up 2% of the rock as idioblastic crystals about 0.3 mm in size.

2.7 QUARTZ VEIN

2.7.1 General Description

Located on the north eastern side of Newcombe Bay, striking roughly N.W.-S.E., is a quartz vein. It is about 50 metres wide extending over a distance of nearly one kilometer. The contacts with the country rock are sharp and apparently vertically dipping. The rock is highly strained with one strong schistosity (Sm) visible in the field. It is felt that this quartz vein represents a fault.

2.7.2 Texture

The texture is that of a blastomylonite (Joplin 1968), for the development of which, Joplin regards cataclasis as mainly responsible, with "some recrystallization and/or neomineralization". Recent work (Bell, 1973) suggests that recrystallization may be the dominant process responsible for such a texture. In thin section the rock shows two preferred orientations, Sm and S_4 (see section 3.4 and Fig. 2.10b). Bell (1973) has also shown that two schistosities can be developed in a mylonite during one major deformation.

2.7.3 Assemblage

The vein must have recrystallized under retrograde conditions. The assemblage observed is quartz + muscovite + plagioclase, with some epidote present, whereas the surrounding country rock contains hypersthene.

2.7.4 Descriptive Mineralogy

Quartz is the most dominant mineral, making up 95% of this rock. the xenoblastic quartz grains which are flattened (in the plane of Sm), are

between 0.5 mm and 3.0 mm long, averaging 1.0 mm. They have recrystallized as flattened sub grains, oriented at a moderate angle (about 30^{o}) to the plane of rock flattening resulting in the development of a second schistosity (S_4) visible only in thin section. Some of the large grains have completely recrystallized as smaller grains which range between 0.02 mm and 0.5 mm long, averaging 0.2 mm (Fig. 2.10c). All grain boundaries are embayed to lobate sutured.

Ribbons of slightly pleochroic muscovite flakes, with a strong preferred orientation, run through the rock in the plane of flattening of the larger quartz grains. The flakes comprise about 2% of the rock and range in length from 0.05 mm to 0.3 mm, averaging 0.1 mm.

Kinked plagioclase grains of moderate to low An content (R.I. less than quartz) and showing poor multiple twinning, occur in lensoid aggregates mixed with small quartz grains. These aggregates make up as much as 3% of the rock. The strong schistosity (Sm) shown by the muscovite wraps around these aggregates. The plagioclases occur as xenoblastic crystals with embayed to lobate sutured boundaries and are about 0.8 mm in size.

Epidote occurs as small, slightly flattened, subidioblastic grains with straight boundaries. It occupies about 3% of the rock and grain size varies from minute to 0.2 mm, averaging 0.1 mm. The grains occur in stringlike aggregates with a strong preferred orientation which parallels that of the muscovite.

2.8 THE CHARNOCKITE

2.8.1 General Description

Outcropping in the southern area is a large, apparently folded, intrusive charnockite. It suffers deep chemical weathering up to 30 cm. below the surface. This weathering imparts a rusty brown colour to the rock and produces a very poor soil around the outcrops. The charnockite is also characterised by extremely well developed honeycomb weathering (Fig. 2.11a). This honeycomb weathering is probably a combination of both

salt weathering and the abrasive force of the wind.

The body has a well developed schistosity and contains many planar xemoliths parallel or sub-parallel to the schistosity. The intrusive nature of the charnockite is clearly evident in a number of places where the margin is transgressive to the layering and schistosity in the country rock. At the contact on Bosner Island (Fig. 2.12a), charnockite containing large xenoliths of country rock grades into country rock with apophyses of charnockite. This change occurs over a distance of between 5 and 20 metres.

The charnockite mass is not one homogeneous body, but a cluster of multiple intrusions. Subtle differences in outcrop colour distinguish the individual bodies but the boundaries of the latter are not sharp enough to be mapped. Further evidence for multiple intrusion is seen in the varied modal analyses of charnockites from various localities (Fig. 2.13); samples 335/693 (Holl Island) and 335/317 (Robinson Ridge) for example, being monzonoritic (after Tobi, 1971) in mineral composition compared with more typical charnockites elsewhere. Plagioclase compositions of the charnockite as a whole are fairly consistent (viz. An_{40}) but some give anomalous values (see histogram in section 2.8.5). Hornblende, although generally present, is absent from several specimens.

2.8.2 Textural Features

Distributed fairly evenly through the main charnockite body are many small flattened xenoliths. The flattening of these xenoliths is parallel to the schistosity (S_3?) (Fig. 2.12b). Most of the xenoliths are between 5 cm. and 20 cm. long and 1 cm. to 6 cm. wide in any section normal to the schistosity. On the south west side of Browning Peninsula, a large xenolith of charnockite is contained within the main charnockite body. The xenolith has a leucocratic reaction rim (Figs. 2.11b & c) and includes many relatively undeformed "fragments" of the country rock outside the main charnockite body. In a number of places the charnockite is layered. These layers occur in groups of up to 20 which are apparently randomly scattered

throughout the body (Fig. 2.12c). Six groups of these layers were located. The layers, which do not have sharply defined boundaries, are of alternating light and dark colour and are parallel to the schistosity of the charnockite. The dark coloured, or mafic layers are only 3 to 6 crystals thick. The light coloured, or leuco layers are thicker. Metamorphic differentiation is thought to be responsible for the development of the layering.

In some areas, the charnockite is porphyritic with large porphyroblasts of plagioclase (Fig. 2.14a).

2.8.3 Texture

The texture exhibited by the charnockite is equigranular interlobate.

2.8.4 Assemblage

The following minerals were identified under the microscope from 24 thin sections:

Quartz, plagioclase, microcline, orthopyroxene, clinopyroxene, hornblende, biotite, opaques, zircon and apatite.

Retrograde minerals observed were:

Epidote, sericite, chlorite and a fibrous amphibole (probably anthophyllite).

The above preretrograde minerals occur as the following assemblage:

Quartz + plagioclase + microcline + orthopyroxene + biotite + clinopyroxene $\pm$ hornblende + opaques.

2.8.5 Descriptive Mineralogy

The xenoblastic quartz grains, which are slightly flattened, show strain extinction. Some of the larger grains show recrystallization to smaller sub grains. Most grains show embayed grain boundaries, although a few tend to lobate sutured. They vary in size from 0.2 mm to 5.0 mm, averaging 1.5 mm. Other grains occur as small rounded inclusions in other minerals, especially biotite. These inclusions are commonly in optical continuity. Modal analyses show that quartz is present generally between

25% and 30% by volume, although in a few cases, the figure may be lower (e.g. 10%). A small amount of quartz (less than 1%) is graphically intergrown with plagioclase.

Grains of plagioclase are xenoblastic with embayed boundaries, although some have a remnant rectangular igneous shape in the form of subidioblastic (subhedral) laths. They generally range between 0.2 mm and 0.7 mm, averaging 2.0 mm, but, occasionally, they form large porphyroblasts up to 25 mm. in size. Albite, pericline and simple twins are common; occasionally the grains are deformed, kinking the twin lamellae (Fig. 2.14b.). Patch form antiperthite is frequently present.

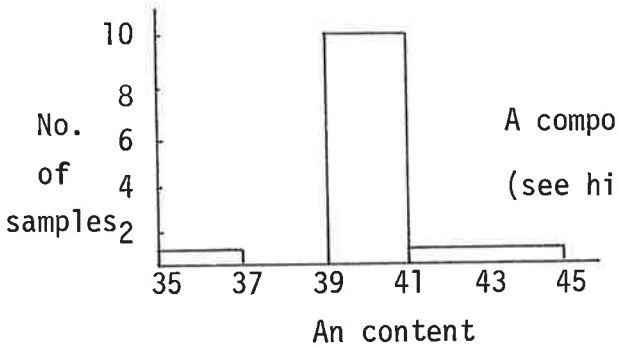

A composition of An_{40} is usual (see histogram).

Plagioclase comprises about 35% of the rock though, where the quartz content is low, this figure is up to around 50%. In most specimens a few grains are graphically intergrown with quartz. Many grains are poikilitic with inclusions of clinopyroxene, quartz and opaques. Partial retrogradation to sericite is relatively common.

Microcline grains are xenoblastic with embayed boundaries. They occupy 20% to 30% of the rock. The size of the grains varies greatly, between 0.2 mm and 12.0 mm, although, unlike plagioclase, they never really form porphyroblasts. Generally the microcline shows well developed tartan twinning but in a few sections observed, what is assumed to be microcline is twin-free. The grains are almost invariably perthitic in stringlet form. Some grains are poikilitic with inclusions of quartz.

Pleochroic laths of biotite with a weak preferred orientation, make up between 5% and 10% of the rock. The pleochroic scheme is:

α - brownish green

β γ - rusty brown

with $\beta = \gamma > \alpha$

Most grains are poikilitic with small inclusions of quartz and pyroxene. The grain size varies between 0.05 mm and 7.0 mm, averaging 1.0 mm.

Hypersthene and clinopyroxene occur in approximately the same proportions, namely 3% to 5%, though, in a few thin sections clinopyroxene is present in only trace amounts. Both pyroxenes occur as xenoblastic grains with embayed boundaries. They range in size between 0.05 mm and 5.0 mm, averaging 0.8 mm. This is noticeably smaller than the size of associated phases. Both types of pyroxene may be altered at the rims to a fibrous amphibole. That surrounding the hypersthene has straight extinction and is thought to be anthophyllite in contrast to that surrounding the clinopyroxene, which has oblique extinction and is presumed to be tremolite. Rarely, both pyroxenes exhibit simple twinning. Specimen B.M.R.2. exhibits topotactic growth of clinopyroxene on orthopyroxene and some of the discreet orthopyroxene grains have a large number of exsolved, aligned plates of opaques. These plates are rich in TiO_2 (scanning electron microscope measurement) and are thought to be rutile or ilmenite.

Laths of hornblende comprise 0% to 10% in most rocks. In those samples where the hornblende is around 10%, the biotite content is lower than normal, suggesting that the hornblende is developing at the expense of the biotite. The grains have a slight preferred orientation and vary in length between 0.1 mm and 6.0 mm, averaging 1.0 mm. The hornblendes form as xenoblastic crystals with embayed grain boundaries and are often poikiloblastic with rounded inclusions of apatite, quartz, plagioclase and opaques. Occasionally the grains are altered at the edges and along cracks to an indeterminable greenish mineral. The pleochroic scheme is:

α - green

β - olive green

γ - greenish brown

with $\gamma > \beta > \alpha$

The opaque minerals are always associated with the ferromagnesium minerals as inclusions, exsolved phases or with common grain boundaries. The grains range in size from 0.1 mm to 3.0 mm, averaging 0.8 mm. They constitute between 1% and 3.5% of the rock. Because of the large magnetic response of the charnockite, it is presumed that most of the opaques are magnetite. The grains are slightly flattened in the plane of the preferred orientation of the biotites and hornblende.

The accessory minerals consist of well rounded elongate apatite crystals and subidioblastic zircons. Epidote occasionally occurs as a presumed retrograde mineral.

2.9 PORPHYRITIC GRANITE

2.9.1 General Description

On both Ford and Cloyd Islands there outcrops a coarse grained porphyritic intrusive granite (Fig. 2.3). It weathers a light pink colour which is due in part, to iron staining (McLeod & Gregory, 1966), and in part to the pink colour of the feldspar phenocrysts. The granite outcrops as very evenly rounded low hills. It is a typical granite in composition (Table 4.1, Analysis 335/673), though it has an abnormally high Th content compared to the other rocks of the Windmill Islands. This was manifest in high readings taken over Ford Island during an airborne scintillation survey carried out by A.N.A.R.E. in 1956 (Dr. P. Law pers. comm.). The body appears extremely homogeneous and has sharp contacts which are not chilled. On the north eastern side of Ford Island, the contact transgresses country rock schistosity (Fig. 2.14c) and dips at about 50^{o} to the west.

2.9.2 Macro Structures

The most characteristic feature of the granite is the presence of aligned tabular feldspar phenocrysts. These impart, to the rock, a weak schistosity which is parallel to the contact, above mentioned, on Ford Island (Fig. 2.15a). The biotite present also defines this schistosity. The granite contains xenoliths of both acid and basic country rock. Most xenoliths observed are small, though one large one was noted (250 metres in diameter). The xenoliths are relatively undeformed.

2.9.3 Micro Structures

The micro structure of this unit is dominated by the large aligned xenoblastic porphyroblasts of microcline, surrounded by smaller interlobate grains of lenticular quartz, plagioclase and aggregates of biotite which have a preferred orientation parallel to that of the microcline porphyroblasts. An extremely weak second schistosity is manifest by the biotites.

2.9.4 Texture

The texture is granoblastic, inequigranular interlobate.

2.9.5 Assemblage

The assemblage is as follows:

Quartz + plagioclase + microcline + biotite + hornblende + opaque $\pm$ hypersthene $\pm$ sillimanite.

2.9.6 Descriptive Mineralogy

Quartz, which constitutes 20% of the rock, occurs as small rounded inclusions and larger xenoblastic grains with embayed to lobate sutured grain boundaries. This indicates that the quartz is in disequilibrium. This is probably a function of the weak deformation (also manifest in the biotites) impressed on the granite after it was emplaced and solidified. The granite occurs in the core of a probable large fold. The grain size varies from minute up to 4.0 mm, averaging 1.5 mm. Most grains show

strain extinction and a moderate amount of quartz is graphically intergrown with plagioclase.

The most dominant mineral, microcline, makes up 60% of the rock. It occurs as both porphyroblasts and in the ground-mass. The size varies between 0.2 mm and 15.0 mm. The porphyroblasts average 7.0 mm in length, while the grains in the ground-mass average 2.0 mm in size. The xenoblastic grains have embayed boundaries. The porphyroblasts which are tabular in shape, are generally twinned simply with the twin plane parallel to the tabular alignment of the crystals (Fig. 2.15b). Most grains show the characteristic tartan twinning. The porphyroblasts are often dusty, presumably with exsolved opaques.

All microcline crystals are strongly perthitic in stringlet form. This accounts for the high CaO + NaO value (4.5 wt%) of the rock, even though discreet plagioclase grains constitute only 10% of the rock. The composition of the plagioclase is An_{30}. The xenoblastic crystals have embayed grain boundaries and are between 0.2 mm and 3.0 mm in size, averaging 1.0 mm. Good lamellar twinning is rare as it is generally weak or diffuse. The plagioclase is antiperthitic also in stringlet form.

Biotite, which constitutes between 3% and 4% of the rock, is occasionally altered to chlorite. It ranges in size between 0.1 mm and 1.0 mm, averaging 0.5 mm, and is rarely poikiloblastic with included zircons around which are characteristic pleochroic halos. The biotite occurs as pleochroic laths in elongate aggregates. The pleochroic scheme is:

α - green

$\beta = \gamma$ - rusty brown.

Pleochroic hornblende occupies 2% of the rock. Its pleochroic scheme is:

α - light green

β - green brown

γ - dark green

with $\beta > \gamma > \alpha$

It occurs as xenoblastic crystals with embayed boundaries and is between 0.05 mm and 1.0 mm in size, averaging 0.5 mm.

Up to 1% hypersthene is present. Grain sizes vary between 0.05 mm and 1.0 mm, averaging 0.5 mm. The xenoblastic crystals have embayed grain boundaries. Commonly the rim of the grains show alteration (retrogradation) to a fibrous amphibole. Less commonly it shows a weak pleochrism from pink (α) to pale green (γ). All the ferromagnesium minerals tend to form clusters.

Sillimanite and garnet both occur as rare accessories. The sillimanite occurs as idioblastic crystals surrounded by biotite, whereas the garnet, although not surrounded, also is intimately associated with the biotite. The garnet is also graphically intergrown with the quartz and is flattened in the plane of schistosity. It is thought that the sillimanite and garnet are remnants of pelitic xenoliths, almost totally consumed by the magma.

Opaque minerals in the form of magnetite and pyrite make up 1% of the rock. The grains are flattened in the plane of schistosity and are up to 1.00 mm long. They always occur with the ferromagnesium minerals.

Accessory minerals are zircon and apatite, which occur as small rounded grains.

2.10 PEGMATITES

Pegmatites are developed extensively on Clark Peninsula (Fig. 2.16) and some, to a much lesser extent, occur on Pidgeon, Ford (McLeod and Gregory, 1966) and Herring Islands (Oliver, 1970). They consist of mainly quartz and microcline with some plagioclase and rarely contain muscovite. The pegmatites on Clark Peninsula are characterised by large (up to 20 cm) perthitic (in band or ribbon form) microcline crystals in symplectic intergrowth with quartz.

2.11 APLITES

2.11.1 General Description

Intrusive aplite dykes occur over most of the area. Three types have been recognised and these are described in Table 2.2. All are pre-

sumed intrusive; xenoliths of country rock are found in types (i) and (ii) (Fig. 2.15c); type (iii) occurs in the charnockite on Browning Peninsula and it is difficult to visualize any other process other than intrusion to emplace it. The type (iii) aplite is folded with an axial plane parallel to the charnockite schistosity (Fig. 2.18a). It is possible that the type (iii) may represent a late fraction of the charnockite melt, but this is considered unlikely. It may also represent a xenolith caught up in the charnockite, but this is also improbable as its length to width ratio is more than 35 compared with a ratio of less than 5 for all other observed xenoliths. Thin section photographs of all three aplite types are shown in Fig. 2.17.

2.11.2 Subdivision of Aplites

The three types of aplites recognised have been subdivided on the basis of chemistry, texture, grain size and assemblage. This is summarised in Table 2.2 below:

	Type (i) (e.g.335/15)	Type (ii) (e.g.335/400B)	Type (iii) (e.g. 335/219)
Location	Ford and Cloyd Islands	North of Sparkes Bay	Browning Peninsula
Major mineralogy	Mesoperthitic (54%) Quartz (43%) Microcline (2%) Biotite (1%)	Microcline (40%) Quartz (40%) Plagio-clase (19%) Biotite (1%)	Microcline (50%) Quartz (37%) Plagioclase (10%) Biotite (3%)
Texture	Weakly foliated Equigranular - interlobate	Non foliated Inequigranular-interlobate	Non foliated Inequigranular-interlobate
Average grain size	0.3 mm	1.0 mm	3.0 mm
Chemistry SiO_2	74.23 wt.%	74.41 wt.%	69.76 wt.%
TiO_2	0.11 wt.%	0.12 wt.%	0.69 wt.%
Sr	25 ppm	77 ppm	188 ppm
Rb/Sr	13.0	3.87	1.29

TABLE 2.2. Subdivision of Aplites

2.12 OLIVINE GABBRO DYKE

2.12.1 General Description

This dyke intrudes the charnockite on Browning Peninsula and Peterson Island. It is displaced in two places by faults (Fig. 2.2). The dyke which is traceable for 7 km. and is up to 50 meters wide trends in a direction of 280^{o}.

2.12.2 Texture

The rock is a holocrystalline, equigranular cumulate.

2.12.3 Assemblage

The assemblage observed is:

Plagioclase + olivine + augite + biotite + opaque.

2.12.4 Descriptive Mineralogy

Plagioclase is the dominant mineral present, making up between 65% and 70% of the rock. It occurs as subhedral laths between 0.2 mm and 6.00 mm long, averaging 1.5 mm. The composition is An_{61}. Multiple and simple twins are common. Inclusions of other smaller plagioclase grains are present in some larger grains.

Cumulus olivine grains, comprising 10% of the rock, are generally altered at the rims to what is thought to be talc and opaques, as well as a brownish material, possibly iddingsite. The grains are between 0.3 mm and 1.5 mm in size, averaging 0.5 mm. They are optically negative with a 2V of approximately 80^{o} indicating they are moderately iron rich (Fa_{30}).

Anhedral augite, although constituting only 10% of the rock, occurs in larger crystals than the other constituents. The grains are anhedral and range in size from 0.3 mm to 12.0 mm, averaging 2.0 mm. The grains are light green in colour and do not show pleochroism, 2V is approximately 50^{o}. Some grains are poikilitic with inclusions of rounded olivine and subhedral opaques.

Subsidiary biotite occurs as subhedral pleochroic laths between 0.1 mm and 3.0 mm long, averaging 1.0 mm. The pleochroic scheme is:

α - light green

$\beta = \gamma$ - red brown.

It comprises 5% of the rock. The biotite is intimately associated with the opaque grains, partially or totally surrounding them (Fig. 2.18b). This is considered to represent a reaction corona, in the cooling magma, between ilmenite and the potassium rich portion of the last portion of the liquid magma, forming biotite.

i.e. ilmenite + K rich liquid → biotite.

Such an iron rich biotite is stable at low temperatures. The biotite is very reddish indicating a high Ti content (Binns, 1969b).

The opaque minerals constitute 5% of the rock. They occur as euhedral to subhedral crystals, ranging in size from 0.1 mm to 5.0 mm, averaging 1.0 mm. They are generally associated with the ferro magnesium minerals. The dominant opaque mineral is ilmenite with a lesser amount of magnetite. Traces of pyrite, chalcopyrite and pyrrhotite were observed.

2.13 DOLERITE DYKES

2.13.1 General Description

Two dolerite dyke swarms occur in the Windmill Islands. One swarm is centred around O'Brien Bay along the crest of an antiform. The other swarm occurs at the northern ends of Browning Peninsula and Peterson Island. This second swarm post dates the olivine gabbro dyke as the swarm is not displaced by the fault, which affects the gabbro dyke, between Browning Peninsula and Peterson Island. The dykes are usually thin (up to two metres thick) and vary in length, the longest being about 2 kms. Most are discontinuous over their length. Distinctive features of the dykes are:

(i) fine grained chill margins;

(ii) flow structures in the form of aligned plagioclase phenocrysts (Fig. 2.18c) and alignment of the microlitic ground mass;

(iii) they are strongly magnetic.

2.13.2 Texture

The texture of the dykes is typically doleritic.

2.13.3 Assemblage

Primary minerals observed in thin section are plagioclase, clinopyroxene and opaques with epidote and calcite occurring as secondary minerals. The dolerite assemblage is:

plagioclase + clinopyroxene + opaque.

2.13.4 Descriptive Mineralogy

The plagioclase comprises 60% of the rock and occurs as both glomeroporphyritic euhedral phenocrysts, some of which are weakly zoned, and as subhedral laths in the ground mass. The composition of the cores is approximately An_{50}. The length of the phenocrysts ranges from 0.5 mm to 3.5 mm, averaging 1.5 mm, compared with the ground mass plagioclase from 0.05 mm to 1.0 mm, averaging 0.2 mm.

Clinopyroxene occurs as anhedral crystals between 0.05 mm and 2.0 mm in size, averaging 0.1 mm. It is probably subcalcic augite as the 2V is approximately 20^{o}. The crystals are often altered to a fibrous amphibole. They also have exsolved needles of an unidentified opaque mineral.

Opaques occur in the ground mass as small discreet subhedral crystals, averaging 0.03 mm in size. Because of the high magnetic response of these dykes, it is probable that most of the opaques are magnetic

2.14 METAMORPHIC GRADE

(Further consideration of metamorphic grade, based on mineral compositions and distribution coefficients is given later - Chapter 5).

2.14.1 Metamorphic Facies

Utilizing the somewhat limited, but nevertheless convenient, facies concept; these rocks show characteristics of both amphibolite and granulite facies (Turner, 1958 & 1968). Applying the classification of

de Waard (1965) the Windmill Islands rocks have been grouped into three subfacies. The rocks in the north correspond to the sillimanite-biotite-orthoclase subfacies of the almandine amphibolite facies whereas those in the middle of the area correspond to the biotite-cordierite-almandine subfacies of the granulite facies. The rocks in the southern part of the Windmill Islands have assemblages diagnostic of the hornblende - ortho-pyroxene-plagioclase subfacies of the granulite facies.

2.14.2 Grade Changes

The areas representing the above three subfacies are bounded by mineral isograds which, traversing southwards are:

1) the outgoing of sphene;

2) the incoming of hypersthene;

3) the outgoing of cordierite, (refer to Fig. 2.19).

The orientation of these isograds is somewhat speculative because of limited outcrop. They are thought to have been folded by D_4 (see Chapter 3).

The outgoing of sphene is probably represented by the reaction sphene → rutile + wollastonite. Yoder and Tilley (1962) have determined the approximate experimental position of the sphene stability curve in P-T space for a wet basalt composition. This curve is a fairly pressure independant reaction, occurring at about $800^{o}C$.

The orthopyroxene isograd is determined by the reaction hornblende (1) + quartz → hornblende (2) + orthopyroxene + Ca - clinopyroxene + plagioclase + H_2O in basic rocks (Binns, 1969b). The incoming of orthopyroxene in basic rocks marks the lower boundary of the granulite facies (Binns, 1969b).

Further south and up-grade from the orthopyroxene isograd, at the north end of Mitchell Peninsula the southernmost occurrence of cordierite is as shown (Fig. 2.19). Cordierite breaks down as follows:

3 cordierite → 2 garnet + 4 sillimanite + 5 quartz (Currie 1971). It may be argued that cordierite does not occur south of the indicated isograd because rock compositions are unfavourable. However, at least one rock south of this isograd, V12 288-30 (from Herring Island), is of suitable composition (see section 4.2). Thus it is felt that the cordierite isograd is a significant metamorphic indicator.

One other variation (already referred to) is that pegmatites are almost entirely confined to Clark Peninsula, north of the hypersthene isograd (see Fig. 2.16). Migmatites and "lit-par-lit" gneisses also are more abundant in the northern areas (viz. north of Sparkes Bay). Both the pegmatites and the migmatitic rocks probably represent partial melts of acid portions of country rock (see section 4.3.5). The presumed higher water content of the amphibolite facies compared with that of the granulite facies (Winkler, 1967, Touret, 1971b) is thought to have facilitated melting preferentially in the northern areas.

These changes are the result of differing P-T conditions during progressive metamorphism from almandine amphibolite facies in the north to lower granulite facies in the south. Trace element study shows that this metamorphism was not retrogressive (see section 4.4.8). This conclusion is supported by the fact that the Mg/Fe ratios of the hornblendes from the northern area are related to the Mg/Fe ratios of the host rocks (see section 5.2.1), indicating, according to Sen (1970), that the hornblendes are primary rather than breakdown products of orthopyroxene (i.e. the amphibolite facies rocks are not retrograded granulites). More ambiguous is the relationship shown in Figure 2.9a, namely folded sillimanite in a relatively undeformed cordierite grain suggesting that the cordierite is "syn" or "post" the sillimanite development. If it is "post" this is not in keeping with the metamorphism being prograde, thus in this case the cordierite development is essentially "syn" with the sillimanite, due to metamorphic conditions being close to equilibrium for the breakdown of cordierite to sillimanite and garnet. The cordierite

appears to post date the sillimanite and garnet because of local fluctuations in physical conditions (e.g. PH_2O).

Some of the orthopyroxene grains have retrograded rims of a fibrous amphibole (Fig. 2.7a). As these rims are present in all parts of the Windmill Islands it is suggested they formed during the latest deformation (i.e. D_4 - see Chapter 3) at lowish temperatures, which led also to the development of chlorite from biotite (Fig. 2.8b) and of muscovite in the quartz vein.

CHAPTER 3

STRUCTURAL INTERPRETATION

A reconnaissance structural interpretation of the Windmill Islands metamorphics is shown in figure 3.1.

3.1 TERMINOLOGY AND NOMENCLATURE

The terminology of structural elements as defined by Turner and Weiss (1963, pages 100-105) is used. The symbols S, L and F are used to refer to surfaces (schistosities and layering), lineations and folds respectively. Deformative events are symbolized by D. All of these symbols are subscripted by an integer which refers to a particular event (hopefully in chronological order). Size classification used is that defined by Turner and Weiss (1963, pages 15-16).

3.2 DEFORMATION 1

The earliest recognisable surface in the area, So, is a metamorphic layering. This layering is produced by compositional segregation or by grain size variations (Fig. 2.10a & b). Because of the strong chemical segregation this metamorphic layering is thought to be an expression of original sedimentary bedding.

Paralleling S_o is a schistosity S_1, which is strongly penetrative. S_1 is defined by the alignment of platy or tabular minerals (e.g. biotite and sometimes hornblende), the strong preferred orientation of sillimanite needles and the flattening of quartz, feldspar and rarely pyroxene grains. Since S_1 is such a strongly developed schistosity, it is unlikely that it was produced by primary sedimentation. Thus it is assumed that S_1 was developed axial plane to tight isoclinal folds during a first deformation D. However, no closures of such postulated F_1 folds were found.

3.3 DEFORMATION 2

D_2 produced tight, often rootless, folds, in some cases with discontinuous limbs and with a wavelength seldom exceeding 30 cm. (Fig. 3.2a, b & c, Fig. 2.6c and Fig. 3.4a).

This D_2 deformation folded S_1, commonly defined by biotite and silli-

manite, to produce a weak axial plane schistosity S_2 by the recrystallization of biotite (Fig. 2.8a). S_2 is only recognisable in the cores of F_2 folds; it is not easily seen on the mesoscopic scale but is generally visible in thin section.

No macroscopic F_2 folds were observed. The orientation of F_2 folds appears random as subsequent deformations have obscured their original attitude.

3.4 DEFORMATION 3

The third deformation D_3 produced broader, less appressed macroscopic folds, F_3, and associated smaller folds, with vertical axial planes (Fig. 3.3a,b,c & d and Fig. 3.4b). These F_3 folds, fold $S_0 // S_1$ and in most cases $/ S_2$.

The best exposed area showing a macroscopic F_3 antiform occurs along the northern coastal areas of Clark Peninsula (Fig. 3.1). Another macroscopic F_3 antiform occurs in the O'Brien Bay area, though this is not as well exposed. Separating the two antiforms is a synform, the core of which is marked by a highly deformed, vertically dipping quartz vein. The significance of this quartz vein is discussed in section 3.6.

Both antiforms have curved axial plane traces which appear to be displaced by faults (Fig. 3.1). A weak, vertical, axial plane schistosity S_3, manifest in biotite, and a mineral lineation L_3 (Fig. 3.5b) are developed in the core of the macroscopic F_3 antiform on Clark Peninsula. Minor F_3 folds on the southern limb of this antiform have folded the acid veins of layered granite gneiss producing pinch and swell structures with the expected vergence. (Figs. 3.3a & 3.5a). Pegmatites are commonly developed in the cores of mesoscopic F_3 folds. One overprinting relationship was found at the head of O'Brien Bay where an F_3 fold has folded an F_2 fold (Fig. 3.2d).

The distribution of the large intrusive charnockite body outcropping in the southern part of the Windmill Islands is interpreted as an expression of F_3 (see figure 2.1). Although the contact of the charnockite with the country rock can only be observed on Robinson Ridge and Boffa and Bosner Islands, the general shape of the fold has been interpreted from airborne magnetics. Voronov and Krasik (1963) have published four east-west magnetic profiles over the southern area of the Windmill Islands. The charnockite gives a very strong positive magnetic response. Unfortunately these magnetic profiles are not detailed enough to determine the dip of the contacts, although a faint suggestion of an easterly dip of the western contact is present in two of these profiles.

The charnockite has a strong schistosity and elongate xenoliths which roughly parallel the likely east-west axial plane trace of the macroscopic fold suggested by the outcrop distribution of the charnockite. This axial plane trace approximates the rough east-west trend of the macroscopic F_3 antiforms observed in the northern areas.

3.5 DEFORMATION 4

This fourth deformation produced broad macroscopic warps which plunge steeply to the south. These warps can be seen folding the axial plane trace of the F_3 antiform on Clark Peninsula. The plunge and plunge direction of this F_3 antiform as determined from poles to planes of $S_1 /\!/ S_2$ schistosities and from the direct measurement of mesoscopic F_3 folds, swings from 15^{o} to 67^{o} at the western end of Clark Peninsula, through 20^{o} to 106^{o}, to 30^{o} to 129^{o} (sub-areas 1, 2, 3 and 4 of Fig. 3.1).

Sub-area 5 of Figure 3.1 gives a rough indication of the orientation of F_4 warps which plunge about 70^{o} to 195^{o}.

The F_4 warps also fold the muscovite bearing quartz vein outcropping on the northeastern side of Newcombe Bay, indicating that D_4 post dates the development of this quartz vein.

The relationship of the folding on Herring Island to the previously

mentioned deformative events is uncertain. Oliver (1970) has recognised at least two folding episodes on Herring Island. His tight isoclinal folds are tentatively correlated with the F_2 folds which occur in the northern areas. The broader more open macroscopic folds which plunge to the south-east at about 50^o (see Fig. 2.4) may correspond to the F_3 folds of the northern area.

3.6 FAULTING

A probable major fault (or slide?) is marked as a zone defined by the deformed muscovite bearing quartz vein (already mentioned) which outcrops on the north-eastern side of Newcombe Bay. The quartz vein has a strongly developed schistosity (S_m) and has recrystallized later(?) to give another schistosity (S_4?) at a moderate angle to S_m (Fig. 2.10c). The dominant schistosity (S_m) is thought to have developed during D_3. The development of muscovite, limited to this quartz vein, is thought to reflect a higher water content than in the surrounding rocks. Such would now be inconsistant with faulting.

Faults of small movement displace the F_3 antiformal axial plane traces in the northern part of the area. In the south, approximately north-south trending faults displace the olivine gabbro dyke by approximately 1 kilometre (Fig. 2.2). These north-south faults predate to dolerite dyke swarm as the latter are not displaced.

The structural history of the Windmill Islands metamorphics is detailed in Table 3.1.

Deformation	Fold style	Features	Other details	Metamorphic grade
D_1	F_1? tight isoclinal	S_1 dominant axial plane penetrative schistosity. Sillimanite lineation.		Amphibolite to granulite facies.
D_2	F_2 tight isoclinal	Weak S_2 axial plane schistosity manifest in hinge zones by biotite.		
			Intrusion of charnockite	
D_3	F_3 broad open concentric folds.	Weak S_3 axial plane schistosity and L_3 developed in hinge zones. Pegmatites developed in some hinge zones. S_m schistosity developed in quartz vein-manifest in flattened quartz and muscovite	Shallow easterly plunge.	
			Faulting of F_3 axial plane traces.	Low to Middle Amphibolite facies.
D_4	F_4 gentle warps.	S_4 axial plane schistosity developed in quartz vein.	Steeply plunging to south.	
			Intrusion of Olivine Gabbro Dyke.	?
			Faulting of Olivine Gabbro Dyke	
			Intrusion of Dolerite Dykes.	

TABLE 3.1: Structural History of the Windmill Islands Metamorphics.

CHAPTER 4

ROCK CHEMISTRY

4.1 INTRODUCTION

Fifty six rocks were chosen for analyses. These were then divided into the following three groups on the basis of chemistry: twenty nine acid, ten pelitic and intermediate and seventeen basic to ultrabasic rocks. The petrographic details of these rocks are listed in Appendix I. The sample preparation and the analytical techniques are described in Appendix II.

The major and trace element chemistry of these rocks are listed in Tables 4.1, 4.2 and 4.3. C.I.P.W. norms of the acid rocks are listed in Table 4.4 and catanorms of the pelitic, intermediate, basic and ultrabasic rocks are listed in Tables 4.5 and 4.6

4.2 CLUSTER ANALYSES

The cluster analysis presented here is a computer analysis whereby each object is compared with every other object by calculation of a "similarity coefficient" which is stored as a "similarity matrix". This "similarity matrix" is normally too large for interpretation so it is subject to a "sorting strategy" to identify groups of similar attribute structures. The objects in each group being more similar to each other than to objects in all other groups. Pair by pair comparison is represented graphically on a dendogram (J. Barry, pers. comm.).

A cluster analysis was performed on the major element chemistry of all analysed rocks from the Windmill Islands. 288-30 clustered with pelitic rocks 335-19, 335-274, 335-402 and 335-519, all of which have catanormative cordierite and modal cordierite. In order to reduce the overriding effect of the more abundant elements (e.g. Al_2O_3) on less abundant minor elements, (e.g. TiO_2) all data was logged prior to the clusters analysis. Then in order to minimise the effect of SiO_2 on these analyses the rocks were reduced to the three groups mentioned above; acid - pelitic and intermediate - basic and ultrabasic. These three groups were then subjected independently to cluster analyses. The resultant dendograms are displayed in Figs. 4.1, 4.2 and 4.3.

TABLE 4.1

WHOLE ROCK ANALYSES: ACID LITHOLOGIES

(Located in the pocket at the back of Volume 2)

TABLE 4.2

WHOLE ROCK ANALYSES: PELITIC AND INTERMEDIATE LITHOLOGIES

(Located in the pocket at the back of Volume 2)

TABLE 4.3

WHOLE ROCK ANALYSES: BASIC LITHOLOGIES

(Located in the pocket at the back of Volume 2)

TABLE 4.4

C.I.P.W. NORMS: ACID LITHOLOGIES

(Located in the pocket at the back of Volume 2)

TABLE 4.5

CATANORMS: PELITIC AND INTERMEDIATE LITHOLOGIES

(Located in the pocket at the back of Volume 2)

TABLE 4.6

CATANORMS: BASIC LITHOLOGIES

(Located in the pocket at the back of Volume 2)

In Figure 4.2, 288-30 correlates particularly closely with 335-274. 335-274 is a pelitic rock which contains 12.5% modal cordierite and has 13.23% cordierite in its catanorm. 288-30 contains 4.25% catanormative cordierite but no modal cordierite. It is presumed that although 288-30 is a pelitic rock (see section 2.5.1) metamorphic conditions were not conducive to the formation of modal cordierite. This supports the existence of the cordierite isograde (see section 2.14.2).

In the group of acid rocks (Fig. 4.1), two subgroups can be easily recognised. On comparison with the analytical data (Table 4.1) the group containing 335-50, 335-321, 335-24, 335-30, 335-21 and 335-445 have higher CaO and Na_2O values and lower K_2O values, which is a reflection of the dominance of plagioclase over microcline in the rock. Within the other subgroup a subsidiary two-fold division appears to reflect slightly higher K_2O values in the samples 335-15 to 335-219 than in the samples 335-113 to 335-151.

Within the basic rocks (Fig. 4.3) no marked grouping is evident though the cluster 335-307 to AN71-3B can be correlated with relatively high CaO and MgO values (Table 4.3).

4.3 PREMETAMORPHIC NATURE OF THE WINDMILL ISLANDS ROCKS

4.3.1 Discriminant Analyses

Shaw (1972) has proposed a discriminative function (D.F.) by means of which he believes the premetamorphic nature of leucocratic gneisses may be determined. This discriminative function is defined as

$$D.F. = 10.44 - 0.21\ SiO_2 - 0.32\ Fe_2O_3\ (\text{total Fe}) - 0.98\ MgO + 0.55\ CaO + 1.46\ Na_2O + 0.54\ K_2O$$

Acid Rocks				Pelitic & intermediate rocks	
Sample No.	D.F.	Sample No.	D.F.	Sample No.	D.F.
335- 1	4.13	335-151	3.34	335- 19	-2.89
335- 21	6.69	335-313	2.74	335- 73	-3.85
335- 24	3.81	335-321	0.21	335- 83	-5.27
335- 30	4.01	335-324	3.87	335-274	-4.16
335- 32	1.78	335-375	4.44	335-402	-5.56
335- 35	2.80	335-380	1.38	335-519	-1.44
335- 50	2.52	335-445	3.84	335-329	-6.70
335- 74	4.64	335-495	2.60	335-160	-1.55
335- 82	4.36	288- 12	1.16		
335-100	2.66	335- 15	3.22		
335-113	2.20	335-144	3.83		
335-114	4.28	335-219	3.25		
335-115	3.55	335-400B	2.52		
335-122	1.41	335-673	1.96		

TABLE 4.7: Shaw's D.F. values of leucocratic gneisses from the Windmill Islands.

Positive values of D.F. suggest igneous parentage and negative values of D.F. suggest sedimentary parentage.

This discriminative function was applied to the leucocratic rocks of the Windmill Islands. The results are detailed in Table 4.7.

The pelitic and intermediate rocks all display negative D.F. values indicating sedimentary parentage. This is most likely as the chemistry of pelites arises from sedimentary processes (e.g. weathering, deposition of clay particles and leaching; see also section 2.5.1). However the acid rocks all have positive D.F. values indicating igneous parentage. This "igneous" nature may be inherited from the original rock or it may be the result of a melting or partial melting phenomena to which these rocks may have been subjected. The obviously intrusive granites (see section 4.3.5) all give positive values of D.F. as would be expected.

Shaw and Kudo (1965) have also derived a similar discriminatory function which can be applied to basic rocks. However it utilizes trace element chemistry and as the particular trace elements it uses were not determined for the Windmill Islands rocks, this D.F. for basic rock was not applicable.

4.3.2 Comparison with "Average" Rocks

A comparison of the Windmill Islands rocks with selected "average" rocks was made by using ACF, and where possible AKF and AFM, diagrams (Figs. 4.4a to 4.4g). These "average" rocks are detailed in Table 4.8. The ACF, AKF and AFM values were calculated, following the technique described by Winkler (1967) As modal analyses were not available for the "average" rocks, no correction could be applied to account for ilmenite, hematite, magnetite and sphene.

These comparisons are only valid if the metamorphism was essentially isochemical. No evidence for extensive migration of major

	A	B	C	D	1	2	3	4	7	8	9
SiO_2	58.10	78.33	76.37	64.7	49.78	50.19	48.11	72.08	66.27	63.58	54.02
Al_2O_3	15.40	4.77	10.63	14.8	15.69	17.58	15.55	13.86	15.39	16.67	17.22
Fe_2O_3	4.02	1.07	2.12	1.5	2.73	2.84	2.99	.86	2.14	2.24	3.83
FeO	2.45	.30	1.22	3.9	9.20	7.19	7.19	1.67	2.23	3.00	3.98
MgO	2.44	1.16	.23	2.2	7.79	9.31	9.31	.52	1.57	2.12	3.87
CaO	3.11	5.50	1.30	3.1	11.93	10.43	10.43	1.33	3.68	5.53	6.76
Na_2O	1.30	.45	1.84	3.1	1.21	2.85	2.85	3.08	4.13	3.98	3.32
K_2O	3.24	1.31	4.99	1.9	.29	1.13	1.13	5.46	3.01	1.40	4.43
MnO	-	-	0.25	.01	.35	.16	.16	.06	.07	.11	.12
TiO_2	0.65	.25	.41	.5	.68	1.72	1.72	.37	.66	.64	1.18
P_2O_5	.17	.08	.21	.2	.07	.56	.56	.18	.17	.17	.49
H_2O^+	5.00	1.63	.83	2.4	-	-	-	.53	.68	.56	.78

A - Shale (Mason, 1958, page 147)
B - Sandstone (Mason, 1958, page 147)
C - Arkose (Pettijohn, 1957, page 324)
D - Greywacke (Pettijohn, 1957, page 307)
1 - Tholeiite (Kuno, 1960)
2 - High alumina Basalt (Kuno, 1960)
3 - Alkali-olivine Basalt (Kuno, 1960)
4 - Calc-alkali Granite (Nockolds, 1954)
7 - Rhyodacite (Nockolds, 1954)
8 - Dacite (Nockolds, 1954)
9 - Latite (Nockolds, 1954)

TABLE 4.8: Analyses of "Average" Rocks

elements was found in the rocks of the Windmill Islands and thus it is felt that these comparisons may give an idea of the parentage of these rocks.

In figures 4.4a to 4.4g the pelitic rocks show a greater affinity to shales, arkoses and greywackes than any other rock type and probably represent metasediments. The basic rocks cluster close to basalts and may well represent metamorphosed basic igneous rocks (see also section 4.3.4). The acid rocks cluster near both acid igneous rocks and near most detrital sedimentary types. Their genesis remains obscure. The high K_2O group of acid rocks (section 4.2) is also evident in Fig. 4.4b.

4.3.3 Oxidation Ratios

Chinner (1960), in a detailed study of pelitic and semi-pelitic gneisses of sedimentary origin at Glen Clova, Scotland, found that the oxidation ration O.R = Mol $\frac{2Fe_2O_3 \times 100}{(2Fe_2O_3 + FeO)}$ was related to the opaque iron oxide mineral assemblage. Further, increasing oxidation ratios of the gneisses was accompanied by increasing amounts of muscovite and iron oxides, decreasing amounts of biotite and garnet and major increases in the MgO/FeO ratios of biotites and in the MnO/FeO ratios of the garnets. He also showed that there is a strong positive linear correlation between oxidation ratio and total Fe (as Fe_2O_3) and also total MnO of the rock. These relationships he concluded were inherited from the original sedimentary composition of the gneisses, which behaved as "closed systems" to oxygen during metamorphism (Chinner 1960, page 210 and abstract).

Oxidation ratios for the Windmill Islands rocks were calculated and are listed in Tables 4.1, 4.2 and 4.3. Most of these oxidation ratios are less than thirty five, although some are as high as fifty. On the basis of Chinner's (1960) classification, most of the Windmill Islands rocks should have ilmenite-magnetite-bearing assemblages, with some hematite. Based on the limited number of polished sections and

slabs examined, this prediction seems in accord with observations. The dominant oxide is magnetite with some ilmenite and very occasionally hematite.

In a plot of oxidation ratio against MnO and against total Fe (as Fe_2O_3) (Figs. 4.5a and 4.5b) only the pelites show a positive correlation; probably reflecting their sedimentary parentage. The basic gneisses show no correlation and if they were once sediments, this characteristic has been completely removed. The acid gneisses possibly show a very weak positive correlation in the plot of oxidation ratio against total Fe (Fig. 4.5b).

The oxidation ratios of rocks from the areas north of Sparkes Bay were compared with those to the south (Fig. 4.6). No correlation between metamorphic grade and oxidation ratio was found. This is in contrast to the findings of Wilson (1960) and Miyashiro (1964) who demonstrated that the oxidation ratio decreases with increasing metamorphic grade.

The relationship of oxidation ratios to rock chemistry suggests that the pelitic rocks have retained some of their original sedimentary characteristics, but the acid rocks, if they were sediments, have not.

4.3.4 Niggli Plots and Origin of the Basic Rocks

4.3.4.1 Introduction

The origin of amphibolites and other basic metamorphic rocks has long been a subject of discussion. Many attempts have been made to show that those derived from sedimentary rocks (para) have recognisable chemical differences from those derived from igneous rocks (ortho) (Shaw & Kudo, 1965). Shaw and Kudo (1965), as previously mentioned (section 4.3.1) believe they can discriminate between these two types on the basis of a multivariant statistical analysis of certain trace elements. Evans and Leake (1960), Leake (1963, 1964 and 1969) and Van der Kamp (1968) plotted Niggli numbers of various rocks against

each other and against trace elements. Further, Evans and Leake (1960), showed that the presence of layering within an amphibolite does not necessarily imply a sedimentary origin. This is not surprising in the light of many meta-sedimentary rocks having metamorphic layering or striping which bear no relation to the sedimentary layering (e.g. Talbot & Hobbs, 1968).

4.3.4.2 Application to Windmill Islands Rocks

Following the procedure outlined by Barth (1966), Niggli numbers were calculated for the basic rocks of the Windmill Islands (Table 4.9). These were then plotted on diagrams following the method of Leake (1964) (Figs. 4.7a, 4.7b & 4.8). In all these plots, the Windmill Islands basic rocks show strong affinities with igneous trends. In Fig. 4.7a nearly all plot within the field of the Karoo dolerites and on the low c side of the pelite-dolomite join. In Fig. 4.8 some plot on the high mg side of the pelite-dolomite join but all tend to follow the igneous trend. In Fig. 4.7b nearly all plot on or near the Karoo dolerite trend.

From these plots it appears likely that the Windmill Islands basic rocks have igneous parentage.

Where a basic layer is parallel to regional layering field evidence for either igneous or sedimentary parentage is lacking. 335-307, however, has contacts transgressive to layering and schistosity of the surrounding rock (Fig. 4.9a) and appears to be a dyke-like structure of igneous origin. 335-111 is a thin ultra-basic unit up to five metres thick which extends for a few hundred metres along strike parallel to the lithological layering and adjacent to a pelitic unit. It may well represent a volcanic flow or an intruded sill on the basis of its chemical composition.

Sample	mg	al	alk	c
335- 12A	.56	15.15	6.89	22.79
335- 45	.46	23.17	7.16	22.52
335-110	.46	19.67	4.78	22.79
335-254	.44	20.33	7.98	23.97
335-307	.69	9.31	3.33	26.57
335-483	.51	23.92	9.70	23.81
335-601	.65	17.88	5.96	19.51
335-602	.68	11.88	4.09	22.41
335-640A	.72	18.92	11.56	17.23
335-641	.50	24.00	12.36	22.67
335-648	.58	26.28	10.35	23.80
335-716	.57	28.02	12.79	24.19
335-717A	.49	20.34	6.88	22.86
AN71-3B	.52	15.19	3.59	23.91
288- 19	.48	17.76	3.85	23.58
288- 46	.42	27.21	12.50	22.90
288- 76	.45	28.04	3.80	23.94

TABLE 4.9: Niggli Numbers for Basic Rocks

Having established a probable igneous parentage for the Windmill Islands basic rocks, it may be interesting to speculate upon their parental magma. Table 4.3, shows a diverse range of compositions, some of which could represent alkali basalts (e.g. 335-12A & 288-19), hornblendites (e.g. 335-307), or tholeiites (e.g. 335-254, 335-641, 335-648, 335-717A & 288-46) and, because of their low TiO_2 content, fragments of layered differentiates, (e.g. 335-601, 335-602, 335-640A & 335-716).

4.3.5 Origin of the Acid Rocks

There are two types of acid rocks in the Windmill Islands (excluding the intrusive charnockite). One type shows obvious intrusive field relationships and the other does not. The intrusive types are discussed first.

The porphyritic granite from Ford and Cloyd Islands (335-673) has sharp cross cutting contacts (Fig. 2.3), flow foliation (manifest by tabular feldspar phenocrysts) parallel to the contacts and contains obvious xenoliths (see section 2.9.2). The aplites (335-15, 335-219 & 335-400B) are also intrusive as they have cross cutting relationships and also contain xenoliths (see section 2.11.1). The granite gneiss (335-144) of Midgely, Warrington, Hollin and Pidgeon Islands also falls into this category. Although its boundaries are difficult to locate (probably because they have been through a high grade metamorphic event) its gross outcrop trace is transgressive to the layering and schistosity in the surrounding rocks indicating its intrusive nature.

The second type, comprises the rest of the leucocratic rocks of the Windmill Islands. In places, on a mesoscopic scale they sometimes show magmatic features, such as small apophyses intruding into basic rocks, but on a megascopic scale are generally concordant with the layering of the surrounding rocks.

On a normative An-Ab-Or triangle (Fig. 4.10) using data from Table 4.4 the obviously intrusive types all plot in or close to the low temperature trough of Kleeman (1965).

The above mentioned field relationships of the obviously intrusive types, suggest that they may well have crystallized from an almost completely liquid magma, and because of their conformity with the low temperature trough it is most probable that this magma was derived from the partial remelting of country rock, which may or may not have been located close to the final emplacement position.

Acid rocks of the second type generally plot away from the low temperature trough towards the An-Ab side. This suggests that unless temperatures were exceptionally high, these rocks could not have crystallized from a complete melt. It is probable that they have formed by partial remelting of country rock resulting in the development of only a small amount of liquid. The existence of a melt fraction is supported by field evidence. On Hollin Island a large skialith of similar material to the surrounding Ribbon Gneisses was observed (Fig. 4.9b). These Ribbon Gneisses are considered to be an example of the non intrusive type. The skialith has a leucocratic rim suggesting reaction between magmatic liquid and the skialith. Further, the "ribbons" of biotite in this surrounding Ribbon Gneiss resemble strongly the basic and biotitic schlieren portrayed by Didier (1973) in Figures 155, 156 and 159. Didier (1973) presumes that these schlieren are the result of the partial destruction of basic enclaves by a magma. Additional evidence of partial melting is provided by the development of migmatites.

Having established that the intrusive type of acid rock was probably once almost completely liquid, and assuming that it formed as a result of the remelting of the country rock, it is of interest to know this country rock's original nature. Chappell and White (1974) have suggested they can discriminate between granites formed by partial melting of igneous rocks on the one hand and sedimentary rocks on the other. The properties of these

two types of granites, viz. "S" (sedimentary) and "I" (igneous), are listed in Table 4.10a.

Values of these properties for rocks 335-15, 335-144, 335-144, 335-219, 335-144 and 335-673 (Table 4.10b) suggest that 335-400B, 335-673 appear to be "S" types and 335-144 appears to be an "I" type. 335-15 and 335-219 could be either "S" or "I" type.

4.3.6 Conclusions

The Windmill Islands gneisses and schists pre-metamorphic nature probably consisted of acid and basic volcanics interbedded with sediments ranging from dirty sandstones to shales and possibly intruded by basic bodies of varying types. The quartzo feldspathic portions of these rocks were partially melted, probably in situ. The area was then intruded by granitic magmas probably derived nearby by the remelting of igneous and sedimentary rocks.

No major element chemical differences were detected between the northern amphibolite facies and the southern granulite facies rocks.

4.4 TRACE ELEMENT GEOCHEMISTRY

4.4.1 Introduction

It has now been well established that medium high pressure granulite facies rocks (which probably represent low crustal material) are depleted to varying degrees in the more lithophile elements (e.g. K, Th, Rb & U) compared with the upper amphibolite-lower granulite facies rocks (upper crustal material) (Heier 1964, 1965, 1965b, 1973a & 1973b; Heier and Adams 1965; Heier and Thoresen 1971; Lambert and Heier 1967, 1968a, 1968b; Sighinolfi, 1970 & 1971 and Lewis and Spooner 1972). This relationship has been explained in terms of a crustal fractionation utilizing melts and/or the expulsion of hydrous phases in the production of "dry" upper granulite facies rocks (of subacid composition) from relatively wet upper amphibolite lower granulite facies material (of more acid composition) (Lambert and Heier 1968a, Sheraton, 1970 and Drury, 1973).

"I" type	"S" type
Relatively high sodium Na_2O normally >3.2%	Relatively low sodium Na_2O normally <3.2%
Molecular $\left(\frac{Al_2O_3}{Na_2O+K_2O+CaO}\right)$ <1.1	Molecular $\left(\frac{Al_2O_3}{Na_2O+K_2O+CaO}\right)$>1.1
C.I.P.W. normative diopside or <1% normative corumdum	>1% C.I.P.W. normative corundum
Broad spectrum of compositions from felsic to mafic	Relatively restricted in composition to high SiO_2 types

TABLE 4.10a: Distinctive chemical properties of "I" and "S" type granites from Chappell & White (1974)

Sample	Mol $\left(\frac{Al_2O_3}{Na_2O+K_2O+CaO}\right)$	CIPW Normative Corundum	Na_2O	SiO_2	"S" or "I" type
335- 15	0.98	.01	3.63	74.23	"S" or "I"
335-144	0.94	-	4.34	74.13	"I"
335-219	0.99	0.23	2.78	69.76	"S" or "I"
335-400B	1.10	1.14	3.63	74.41	"S"
335-673	1.01	1.01	2.80	69.47	"S" or "I"

TABLE 4.10b: Chemical feature of "intrusive" type granites from the Windmill Islands.

The trace element chemistry of Windmill Islands rocks, which all show petrological characteristics of the upper amphibolite and lower granulite facies (see chapters 2 & 6), are compared with data from rocks of similar grade reported elsewhere. Sixteen basic rocks and twenty four acid rocks from the Windmill Islands were used to obtain "averages", the pelitic, intermediate and the previously mentioned intrusive acid rocks being omitted. These sets of data are detailed in Table 4.11. Because of the relatively small number of rock analyses, it was considered undesirable to attempt an estimate of the average composition of the Windmill Islands schists and gneisses. Hence the "average" values of the rocks listed in Table 4.11 are not weighted, as such, they probably have a bias towards basic compositions (assuming acid rocks make up 80-90% by volume as in other similar terrains).

4.4.2 Comparison of Different Grades

Windmill Islands rocks of the upper amphibolite facies (i.e. north of the orthopyroxene isograd - see section 2.14) were compared with those of similar composition in the lower granulite facies south of this isograd.

With the limited number of samples, no observable geochemical differences were found between these two facies thus supporting the findings of Lambert and Heier (1968a). Whitney (1969), in contrast, found a small difference in the mean K/Rb ratio between the upper amphibolite (231) and the lower granulite (307) facies rocks in the Northwest Adirondacks, which he attributed to the previously mentioned fractionation process.

4.4.3 Comparison with the Data from Other Terrains

As can be seen from Table 4.11, the Windmill Islands rocks have generally lower K, Th and Rb values than similar rocks from elsewhere. However, the Th/K, Rb/Sr, K/Rb and K/Pb ratios are compatible with these other values. The low K, Th & Rb values probably reflect the premetamorphic chemistry of the rocks. Sheraton (1970) believes that the low K, Th and Rb values he obtained from the Lewisian gneisses of Drumbeg reflect

	MUSGRAVE BLOCK		EYRE PENINSULA	CAPE NATURALISTE	NORTH NORWAY	WINDMILL ISLANDS (This study)		
	Lambert & Heier(1968a)	Collerson (1972 & 1975)	Lambert & Heier(1968a)	Lambert & Heier(1968a)	Heier & Thorensen(1971)	Acid	Basic	(Acid & Basic)
K%	2.8	3.6	3.65	3.8	3.1	3.3	.85	2.4
Rb ppm	140	163	185	185	155	152	64	120
Sr ppm	400	235	130	175	338	1.83	306	230
Th ppm	11	16	27	30	14	13	3	9
Pb ppm	25	-	30	32	24	51	14	37
Th/K($X10^4$)	2.1-5.0	6.4	2.8-9.5	3.2-9.6	4.5	6.5	8.7	7.4
K/Rb	144-688	310	175-232	182-686	198	274	132	222
K/Pb	701-1992	-	960-1785	861-1509	1300	911	726	842
Rb/Sr	.01-1.39	1.08	.21-3.16	.03-4.55	.46	.84	.35	.64

TABLE 4.11: "Average" Potassium and Trace Element values of upper amphibolite - lower granulite facies terrains.

partly the premetamorphic composition, and partly the subsequent crustal fractionation process to which these high pressure granulites had been subjected. It is unlikely that the low values are the result of a fractionation process having operated for only limited time (i.e. presumed deep crustal material under the Windmill Islands rocks being depleted in K, Th & Rb, and thus enriching the higher Windmill Islands rocks), because the ratios of K/Rb, Rb/Sr, Th/K and K/Pb would have different values compared with those rocks where the process was more complete.

4.4.4 Potassium/Rubidium Ratio

K/Rb ratios have increasingly become used and quoted in reference to the genesis of various rock types and in estimates of the composition of the upper mantle and lower crust (Shaw 1968). In relation to this problem of the lower crust, many granulite and upper amphibolite facies terrains have been studied (Lambert & Heier 1968a, Sheraton 1970, Heier & Thoresen 1971, Sighinolfi 1971a, Drury 1973 and Lewis & Spooner 1973). As K is really the only element for which Rb can substitute (Taylor 1965), the Rb content of rocks should be related to the K content. Taylor (1965) ascribes the varying K/Rb ratios observed in nature to the varying response of K and Rb during fractionation. High K/Rb ratios are observed in upper granulite facies rocks with respect to upper amphibolite-lower granulite facies rocks presumably because Rb is depleted relative to K during crustal fractionation processes.

Fig. 4.11 shows log log plots of K against Rb for each of the three chemical rock types of the Windmill Islands. A linear regression analysis was carried out on these data using the method described by Shaw (1968). The "Main Trend" of Shaw (1968) for igneous and quasi-igneous rocks ($\log_{10}$ Rb ppm = 1.115 $\log_{10}$ K% + 1.597) and the "Metamorphic Trend" of Lewis and Spooner, (1973) for upper granulite facies rocks ($\log_{10}$ Rb ppm = 1.136 $\log_{10}$ K% + 1.497) are also plotted on this diagram for comparison. The results of the linear regression analyses are detailed below.

$$\log_{10} \text{Rb ppm.} = a(1 + \log_{10} K\%) + b$$

	a	b	Number of samples
Acid rock	.886	.829	30
pelitic & intermediate rocks	.679	1.332	9
basic rocks	.513	1.388	17
all rocks	.586	1.314	56

Two observations are evident from this log log plot. Firstly, Rb is much enriched with respect to K when compared with the metamorphic trend of Lewis and Spooner (1973). This suggests that the upper amphibolite-lower granulite facies rocks of the Windmill Islands have been enriched in Rb with respect to K in contrast to other upper granulite facies rocks which are characteristically relatively depleted in Rb with respect to K (due to crustal fractionation). Secondly the basic rocks are very much enriched in Rb compared with the Igneous "Main Trend" of Shaw (1968), suggesting that they are not showing their original igneous trace element (Rb) chemistry. White (1966) and Lange, Reynolds and Lyons (1966) have shown that in metamorphic rocks, Rb may be concentrated by a factor of three to four in biotites, relative to feldspars. Because the basic gneisses of the Windmill Islands are generally fairly high in modal biotite (>10%) enrichment in Rb from a deeper source by fractionation would result in an increased Rb content being more noticeable in these basic gneisses than in the acid gneisses (see Fig. 4.11).

4.4.5 Thorium/Potassium Ratio

Log log plots of Th against K are displayed in Fig. 4.12. Heier and Adams (1965, fig. 2) on a similar plot found that:

1) Upper granulite facies rocks have Th/K ratios generally less than 1.0×10^{-4}

2) Upper amphibolite - lower granulite facies rocks have Th/K ratios between 1.0×10^{-4} and 10.0×10^{-4}.

3) Low amphibolite facies rocks have Th/K ratios around 10.0×10^{-4},

and thus postulated a depletion of Th in higher grade rocks and an enrichment in lower grade rocks.

The Windmill Islands upper amphibolite-lower granulite facies rocks have Th/K ratios between 1.0×10^{-4} and 10.0×10^{-4}, corresponding to values given by Heier and Adams (1965), for rocks of this metamorphic grade, indicating some enrichment of Th with respect to K.

4.4.6 Potassium against Rubidium/Strontium

Log K% is plotted against log (Rb/Sr) in Fig. 4.13. The line dividing upper granulite facies from upper amphibolite-lower granulite facies is from Sighinolfi (1971a). With reference to this, the plot of most of the Windmill Islands rocks is in the Upper Amphibolite-Lower Granulite field in confirmation with indications provided by Thorium and Rubidium (N.B. 335-254 contains anomalously high Sr, i.e. 1063 ppm).

4.4.7 Calcium and Potassium against Strontium and Rubidium/Strontium

Figures 4.14a & b show that in the acid rocks, a positive correlation exists between Calcium and Strontium and a negative correlation between Calcium and Rb/Sr. The acid rocks also show a weak negative correlation between Potassium and Strontium and, for low values of Rb/Sr, a slight positive correlation (Figs. 4.14c & d); i.e. Potassium and Calcium behave in opposite sense with respect to Strontium and Rb/Sr. There is no correlation between these elements in the basic rocks (Figs. 4.15a, b, c & d).

In the acid rocks the dominant mineralogy is quartz + plagioclase + microcline. The two feldspars provide sites for Rb and Sr. As previously mentioned Rb prefers the K sites, substituting quite easily (Taylor, 1965) and most of the Rb would thus be expected in the micro-

cline. As shown in figures 4.14b & d, as Ca decreases, so does Sr, whereas a decrease of K corresponds to an increase of Sr. This suggests that the Sr is located in the plagioclase, substituting for Ca. Sr^{2+} is intermediate in size between Ca^{2+} and K^{+} and supposedly enters plagioclase preferentially, the Sr/Ca ratio increasing during fractionation (Taylor, 1965). However, Virgo (1966) suggests on geometrical considerations that Sr prefers the K sites in potash feldspar to the Ca sites in plagioclase. He also showed that as temperature increases the Sr is preferentially substituted in the potash feldspar. This is not in accord with the observations of this work and those of Taylor (1965). In the Windmill Islands, additional Rb, due to enrichment, must substitute for K in the microcline, thus forcing Sr into the plagioclase lattice. This would account for the "flattening off" of the K versus Rb/Sr curve at higher Rb/Sr ratios, Rb being preferentially, compared with Sr, incorporated into microcline.

Taylor (1965) has shown that Sr^{2+} does not enter the K^{+} sites of biotite, but the Windmill Islands basic rocks, which usually contain considerable biotite, show high Sr values. These high values may be the result of *adsorption* of Sr onto the growing biotite surfaces (de Vore, 1955).

4.4.8 Conclusions

No geochemical differences between the northern upper Amphibolite facies rocks and the southern Granulite facies rocks could be detected.

The Windmill Islands rocks show slightly lower K, Th and Rb values than other rocks of similar metamorphic grade elsewhere. This is interpreted as reflecting the premetamorphic nature of the rocks. The K/Rb, Th/K and K/(Rb/Sr) plots, on the other hand, are compatible with those of rocks of similar metamorphic grade elsewhere. The ratios shown by the latter rocks are interpreted as being due to enrichment of the more

lithophile elements due to a crustal fractionation process. The Windmill Islands rocks are assumed to have undergone a similar enrichment process. The basic rocks of the Windmill Islands do not display their original igneous trace element geochemistry in keeping with this postulation of enrichment.

If this assumption of enrichment is correct, then these upper amphibolite-lower granulite facies rocks of the Windmill Islands are *not* retrogressed upper granulite facies rocks.

CHAPTER 5

MINERAL CHEMISTRY

5.1 INTRODUCTION

Ninety two minerals were chosen for analysis, 26 biotites, 23 orthopyroxenes, 13 clinopyroxenes, 13 hornblendes, 7 garnets, 5 cordierites and 5 secondary amphiboles. These analyses, together with the appropriate structural formulae are listed in Table 5.1 to 5.6. The analyses were performed by the author at Melbourne University, using a Jeol Electron Microprobe X-Ray Analyser, utilising the technique developed by Dr. D.K.B. Sewell at Melbourne University. FeO and Fe_2O_3 values were assumed to be similar to average values published in the literature. This ratio is listed in Tables 5.1 to 5.6.

5.2 MINERAL CHEMISTRY - ROCK CHEMISTRY RELATIONSHIPS

5.2.1 $^{Mg}/_{(Mg+Fe+Mn)}$ and $^{Mn}/_{(Mg+Fe+Mn)}$ Ratios

A rough correlation of the values of these ratios for hornblende, biotite, orthopyroxene and clinopyroxene with the value for the respective containing rocks, is shown in Figure 5.1a-f. Garnet and cordierite, which are confined to pelitic lithologies, show no apparent correlation.

Control of host rock composition on the $^{Mg}/_{(Mg+Fe+Mn)}$ ratios of some ferromagnesium minerals has been established by other workers (e.g. Leake, 1965b; Sen, 1970 & 1973, and Maxey & Vogel, 1974).

The $^{Mn}/_{(Mg+Fe+Mn)}$ ratios of rock versus mineral are detailed in Figure 5.2. Only minerals with an $^{Mn}/_{(Mg+Fe+Mn)}$ ratio generally larger than 0.010 were used, because it was felt that at lower values of Mn, the scatter of points, due to analytical error, would mask any trend, if present. Thus, only the Mn content of the host rock with relation to the Mn content of orthopyroxene, clinopyroxene and garnet were examined. A positive correlation between rock Mn content and the Mn content of orthopyroxene and of clinopyroxene is discernable, but not that of garnet.

The Ca content of the host rock and that of the appropriate garnet

TABLE 5.1

GARNET ANALYSES AND STRUCTURAL FORMULAE

(Located in the pocket at the back of Volume 2)

TABLE 5.2

CORDIERITE ANALYSES AND STRUCTURAL FORMULAE

(Located in the pocket at the back of Volume 2)

TABLE 5.3

HORNBLENDE ANALYSES AND STRUCTURAL FORMULAE

(Located in the pocket at the back of Volume 2)

TABLE 5.4

CLINOPYROXENE ANALYSES AND STRUCTURAL FORMULAE

(Located in the pocket at the back of Volume 2)

TABLE 5.5

BIOTITE ANALYSES AND STRUCTURAL FORMULAE

(Located in the pocket at the back of Volume 2)

TABLE 5.6

ORTHOPYROXENE ANALYSES AND STRUCTURAL FORMULAE

(Located in the pocket at the back of Volume 2)

was examined but no correlation between the two was found.

The non correlation between garnet chemistry and host rock chemistry (especially Mn and Ca) is not in accord with the generally widely held opinion that such elements would be concentrated in the garnet (e.g. Weisbrod, 1973).

5.2.2 Dependence of Mineral Composition on Rock Oxidation Ratio

Chinner (1960) first showed that the $[^{Mg}/(Fe+Mg)]$ ratio of some iron-magnesium silicate minerals depends upon the rock oxidation ratio (or the PO_2). This has been substantiated by subsequent workers, both through experiments (Wones & Eugster, 1965 and Gilbert, 1966) and by examination of natural assemblages (Himmelberg & Phinney, 1967, Annersten, 1968 and Butler, 1969). However, the buffering affect of the assemblage magnetite-hematite has been shown to limit the activity of O_2, and under these circumstances, the Fe/Mg ratio of the mineral then becomes purely a function of pressure and temperature (Annersten, 1968 and Butler, 1969).

The $mol(\frac{Mgx100}{Fe+Mg})$ of the analysed silicate minerals from the Windmill Islands are plotted against their host rock oxidation ratio in figures 5.3a-c. Although the Fe^{2+}/Fe^{3+} ratios of the minerals is estimated and not analysed, the wide variation in $^{Mg}/(Fe^{2+}+Mg)$ for minerals from rocks with approximately the same oxidation ratio indicates that the composition of these minerals is probably independent of the oxidation ratio of the rock. It is presumed then that the activity of O_2 in the rocks of the Windmill Islands was buffered by the presence of an iron oxide assemblage(s). Collerson (1972) came to a similar conclusion regarding high grade metamorphic rocks from Central Australia.

Chinner (1960) also found a relation between the $mol(\frac{Mnx100}{Fe+Mg+Mn})$ value of a mineral and the oxidation ratio of the host rock. A similar examination of the rocks of the Windmill Islands found no such relationship

(Figs. 5.4a-d) probably because of the previously mentioned buffering.

5.3 CHEMISTRY OF SELECTED MINERALS

5.3.1 Secondary Amphiboles

Secondary amphiboles, identified as anthophyllite, developed presumably, in response to retrograde metamorphism (see Chapter 2) as fine grained aggregates rimming orthopyroxene. The fine grained aggregates are mixed with quartz and minor plagioclase. Analysis (by electron probe) of individual amphibole grains was precluded because of the fine grain size. The probed Fe/Mg ratio of the aggregate, however, is considered a close approximation to its true value in the anthophyllite. This ratio is lower in the anthophyllite than in the primary hornblende, indicating that Fe has been lost during the retrogression. In thin section, the anthophyllite rims are, in turn, seen to be rimmed by opaque, presumably an iron oxide (Fig. 2.7b). Thus the retrograde reaction is interpreted as:

orthopyroxene → anthophyllite + Fe oxide

A similar alteration of hypersthene was noted by Himmelberg and Phinney (1967) in granulites from Minnesota.

5.3.2 Orthopyroxene

All orthopyroxenes are hypersthene except those from the charnockite which are ferro-hypersthene (Deer, Howie & Zussman, 1966). The range of composition is shown in Table 5.6. Variation of Al is of particular interest. It is noteworthy that the more aluminous orthopyroxenes, listed in Table 5.7, are all contained in rocks which have a normative corundum content greater than 0.5. There is a close correlation between their Al content and the normative corundum content of the rock. The Windmill Islands orthopyroxenes thus conform to the postulations of Howie (1964) and Binns (1969a) which state that the host rock controls the amount of Al in orthopyroxene. Earlier Eskola (1957) and Boyd and England (1960)

had suggested that high Al in orthopyroxenes is a function of a high pressure environment of recrystallization. Binns (1965), also felt that high Al in orthopyroxene is associated with relatively high soda in plagioclase, but this is not substantiated by the Windmill Islands rocks (see Table 5.7). More recently, Wood (1974) has shown experimentally that in the temperature range 900-1200°C the weight percent Al_2O_3 of the orthopyroxene in fact decreases with increasing pressure.

Sample	Wt%Al_2O_3 in orthopyroxene	Coexisting plagioclase An content	C.I.P.W. normative corundum in host rock
335-115	3.01	21	0.81
335-329	5.13	40	1.86
335-380	5.24	23	1.00
288-12	3.15	-	0.66
288-30	7.48	35	3.56

TABLE 5.7: High Aluminium Orthopyroxenes

All the Windmill Islands high aluminium orthopyroxenes are strongly pleochroic: α - pink, γ - pale green. Correlation of pleochroism with Al content was first suggested by Howie (1964). More recently, Burns, (1966) has ascribed the pleochroism to the entry of Al^{3+} into M_1 sites* and distorting the coordination of Fe^{2+} in the M_2 sites surrounding the M_1 sites.

5.3.3 Hornblende

5.3.3.1 Titanium

The colour of the pleochroic hornblendes from the Windmill Islands changes from the northern area to the south, (Fig. 2.19), the Z absorption colour being bluish green in the rocks of Clark Peninsula

*The significance of M_1 and M_2 sites in pyroxenes is discussed more fully in section 5.4.4.1.

ranging through green (Bailey Peninsula) to greenish brown in the rocks of Ford Island. Leake (1965b) and Binns (1969a) believe that such a colour change is associated with increasing TiO_2 and decreasing ferric iron content of the hornblende. That this general increase in the TiO_2 content of hornblendes is related also to increasing metamorphic grade has been established by Leake (1965b), Binns, (1969a) and Raase, (1974). Leake, (1965b) considers that increasing temperature is the important factor. In figure 5.5.a the weight percent TiO_2 of the hornblendes from the Windmill Islands is plotted against distance from the Swain Group of Islands in the northern part of the area. This shows a weak but discernable TiO_2 increase southwards paralleling the change from green to brown in the hornblendes, as the metamorphic grade of the rocks progresses from amphibolite to granulite facies. Probably the control of host rock chemistry has partially masked this trend.

5.3.3.2 Aluminium

Leake (1965a, 1971) and Raase (1974) suggest that the amount of Al^{VI} and Si in hornblende increases with pressure. Binns (1969a) feels however, that ".... changes in amphibole composition appear more highly influenced by temperature than pressure" and postulates that with increasing temperature, Al^{VI} in amphibole decreases.

In the plot of Si against Al^{VI} (Leake 1971, fig. 2) there is little difference between volcanic hornblendes and other igneous hornblendes. If pressure is a dominant factor in deciding the amount of Al^{VI} in the hornblende, one should be able to distinguish between these two types. Thus it is probable that unless the pressure is high (e.g. 10 Kbars) the temperature of crystallization is more likely to influence the Al^{VI} content of hornblendes.

Figure 5.6a is a plot of Al^{VI} against Si for hornblendes from the Windmill Islands. All of these plot in the "low pressure" region of Raase (1974), as would be expected. However, Si and Al^{VI} values decrease

as the grade (presumably both temperature and pressure) increases: a contrary trend to that expected with pressure being the factor controlling the amount of Al^{VI} in the amphiboles (as suggested by Leake, 1965 a & b, 1971 and Raase, 1974).

Binns (1969a, Fig. 2) found that A^{VI} in hornblendes decreases in conformity with increase of "edenitic alkalis" ($Na+K$). This he related to the fact that....."with increasing metamorphic grade hornblende progressively breaks down, the tschermakitic component more rapidly than the edenitic, to produce a relatively calcic plagioclase. Iron and magnesium either remained concealed in the hornblende as the actinolite or cummingtonite component, or are released into separate cummingtonite or pyroxene phases depending on the grade reached". This idea is supported by the work of Engel and Engel (1962) who recorded higher K_2O values in hornblendes from the granulite facies relative to the amphibolite facies.

Figure 5.6b is a plot of Al^{VI} against "endenitic alkalis" for the hornblendes of the Windmill Islands. Although the samples do not fall into the fields demarcated by Binns (1969a) they do show the trend he envisages, namely that of increasing "edenitic alkalis" and decreasing Al^{VI} with increasing grade.

The author concludes, following Binns (1969a), that unless pressures are high, temperature becomes the deciding factor in the amphibole composition of a metamorphic terrain.

5.3.4 Biotite

Like the hornblendes, the biotites of the Windmill Islands rocks show variation of the Y-Z absorption colour, this being sepia in the north (Clark Peninsula), grading to a rusty colour in the south (Ford Island) (Fig. 2.19). Similarly also the change in absorption colours of the biotite is due to an increasing TiO_2 content of the biotites along with increasing grade (Binns 1969a). As can be seen in Figure 5.5b, the TiO_2

content of the amphibolite facies biotites from the northern area are distinctly less than that in the granulite facies biotites to the south.

5.4 COEXISTING MINERALS*

5.4.1 Introduction

The theory of elemental distribution amongst coexisting minerals was first outlined by Ramberg and De Vore (1951) and Ramberg (1952) and then developed further, with application to rocks, by Mueller (1960 & 1961) and Kretz (1959, 1961, 1963 & 1964). Excellent reviews of this theory and its applications have been presented in many papers dealing with elemental distribution (e.g. Saxena, 1968).

A short resume of the theory is as follows:

The distribution of two components, i and j, between two phases, A and B, may be represented as an exchange reaction:

$$(i)A + (j)B \rightleftarrows (j)A+(i)B$$

At equilibrium $\Delta G=0=\Delta G^{o}+RT\ \ln K$

where ΔG = Change in Gibbs Free Energy of reaction

ΔG^{o} = Change in Gibbs Free Energy of reaction in the standard state

K = Equilibrium constant

R = Gas constant

T = Temperature (^{o}K)

Thus $K = \exp\left(\frac{-\Delta G^{o}}{RT}\right)$

The distribution co-efficient K_D can be related to the equilibrium constant in that $K = K_f K_D$ where K_f is a function involving the activities of components (i) and (j) and a pressure effect. Under "ideal" conditions, $K_f = 1$.

Thus $K_{D_i}^{A-B} = \frac{\chi_i^A}{(1-\chi_i^A)} \cdot \left(\frac{1-\chi_i^B}{\chi_i^B}\right) = \exp\left(\frac{-\Delta G^{o}}{RT}\right)$

χ_i^A = mole fraction of component i in phase A.

---

*The following abbreviations are used throughout this thesis, especially in the figures: Gnt - garnet, Opx - orthopyroxene, Cpx - clinopyroxene, Hbl - hornblende, Biot - biotite, Cord - cordierite.

Hence the Distribution coefficient, K_D, is a function of temperature

$$(\ln K_D = \frac{-\Delta G^o}{R} \cdot \frac{1}{T})$$

Following the procedure of other workers it is convenient to represent the elemental distribution among coexisting phases on a "Roozenboom distribution diagram" (Kretz, 1961) where the mole fraction of a component in phase A is plotted against the mole fraction of the same component in phase B.

5.4.2 Dependence of K_D on Composition

As shown in section 5.2 the mole fraction of Mg and Mn of a mineral is commonly related to the rock composition. Does a relationship exist between the K_D and the mole fraction?

Despite a fair degree of scattering, Maxey and Vogel (1974) believe that, in rocks they examined, the $K_{D_{Fe}}^{opx-cpx}$ is correlatable with the composition of the coexisting phases (i.e. with increasing MgO in Fe rich pyroxenes, K_D increases whereas in Fe poor pyroxenes the opposite trend is evident - the influence of Ca and Al is considered minor). Scharbert and Kurat (1974) similarly examined the influence of mole fraction* on K_D for orthopyroxene - biotite and for orthopyroxene - garnet. They found that for orthopyroxenes more Fe rich than fs40, K_D is compositionally dependant. This, they concluded, supports the findings of Davidson (1968) that in low Fe orthopyroxenes, Fe occupies the M_2 sites preferentially until the M_2 sites are saturated, at which stage Fe tends to enter the M_1 sites in competition with the Mg. Saxena and Hollander (1969) found when examining the pairs garnet-cordierite and biotite-cordierite that, for low grade rocks, K_D is not dependant upon χ_{Mg} but, in high grade rocks, there is a dependence.

---

*Scharbert and Kurat(1974) do not define their mole fraction, i.e. it could be $\chi_{Mg} = (\frac{Mg}{Mg+Fe})$ or $\chi_{Mg} = (\frac{Mg}{Mg+Fe+Mn+Ca})$

K_D's for various co-existing pairs from the Windmill Islands are calculated as follows:

$$K_{D_{Mg}}^{A-B} = \frac{\chi_{mg}^{A}}{(1-\chi_{mg}^{A})} \cdot \frac{(1-\chi_{mg}^{B})}{\chi_{mg}^{B}} \quad \text{where} \quad \chi_{mg} = \left(\frac{Mg}{Mg+Fe}\right)$$

$$= \left(\frac{Mg}{Fe}\right)_A \left(\frac{Mg}{Fe}\right)_B$$

$$K_{D_{Mn}}^{A-B} = \frac{\chi_{mn}^{A}}{(1-\chi_{mn}^{A})} \cdot \frac{(1-\chi_{mn}^{B})}{\chi_{mn}^{B}} \quad \text{where} \quad \chi_{mn} = \frac{Mn}{(Mg+Fe+Mn)}$$

These K_D's are plotted against the composition (as mole fraction) of one of the mineral phases comprising the co-existing pair (Fig. 5.7a & b). No compositional dependence of K_D is apparent. On the basis of the above discussion, the Windmill Islands rocks are thus not in accord with those examined by other workers. This is thought to be due to the much greater range of χ_{mg} exhibited by the latter than those of the Windmill Islands. The effect of rock composition on the Windmill Islands K_D's was also examined and no relationship was found.

5.4.3 Garnet-Biotite

Because there is only one crystal lattice site available for Mg^{2+} and Fe^{2+} in both garnet and biotite, the $K_{D_{Mg}}^{Gnt-Biot}$ should be almost entirely temperature dependant, although it is admitted that the presence of other ions (e.g. Ca&Mn) can affect the K_D. Evans (1965) and Albee (1965) maintain that K_D increases only $2\frac{1}{2}$ - 3% per kilobar decrease in pressure. It follows that because of this assumed strong temperature dependence, the K_D increases with increasing grade (Lyons & Morse 1970, Fleming, 1972). Various corrections for the presence of the previously mentioned other ions have been attempted by a number of workers. Albee (1965) incorporated a correction for Mn defining a new K_D^1 ($K_D^1 = K_D + 0.7 \left(\frac{Mn}{Fe+Mg+Mn}\right)_{Gnt}$. Sen and Chakraboty (1968) corrected for both Mn and Ca, deriving a constant $C = 10.44\ K_D + \left(\frac{Ca}{Mn}\right)_{Gnt}$, the value of C depending upon the grade. Dahl(1972)

also corrected for Ca and Mn by making use of the cell volumes of the garnets. The correction suggested by Dahl (1972) was attempted for the rocks of the Windmill Islands but was discarded. It necessitates the drawing of a curved line of best fit through a plot of the garnet cell edge against the K_D. In the case of the Windmill Islands data the scatter of points is too great for such a line to be drawn.

The varions K_D's incorporating the above mentioned corrections are listed in Table 5.8.

Correction	335-19	335-83	335-274	335-329	335-402	335-519	288-30
$K_D=(Fe/_{Mg})_{Gnt}\ (\frac{Fe}{Mg})_{Biot}$	.312	.294	.277	.274	.313	.246	.254
$K_D^1=K_D+0.7(\frac{Mn}{Fe+Mg+Mn})_{Gnt}$ (Albee, 1965)	.310	.363	.309	.387	.423	.342	.280
$C = 10.44K_D+(\frac{Ca}{Mn})_{Gnt}$ (Sen & Chakraboty, 1968)	3.57	3.47	4.03	3.24	3.53	2.92	3.77

TABLE 5.8: Corrected Garnet-Biotite K_D's.

For the sillimanite metamorphic zone; Lyons and Morse (1970) suggest K_D >0.274, Albee (1965) obtained values of K_D's = 0.30-0.37 and Sen and Chakraboty (1968) believe C should be greater than 3.4. Thus, as can be seen from Table 5.8, the garnet-biotite pairs from the Windmill Islands suggest the rocks reached at least sillimanite zone metamorphism, which is in keeping with their mineralogy (see section 2.14). No systematic variation of these corrected values with metamorphic grade is observable.

Saxena (1969) examined the garnet-biotite pair and derived a transformed K_D (Ktranf.) which incorporated many other ions which could feasibly affect the distribution of Fe and Mg.

$$K_{tranf.} = 0.5013\ K_D - 0.4420\ \chi_{Fe}^{Gnt} + 0.1506\ \chi_{Fe}^{Biot} - 0.3474\ \chi_{Mn}^{Gnt} +$$

$$0.0865\ \chi_{Ca}^{Gnt} - 0.0333\ \chi_{Al}^{Biot\ IV} - 0.3165\ \chi_{Al}^{Biot\ VI} + 0.5488\ \chi_{Ti}^{Biot}$$

where $\chi_{Fe}^{Gnt} + \chi_{Fe}^{Biot} = mol\left(\frac{Fe}{Fe+Mg}\right)$ Gnt or Biot

χ_{Mn}^{Gnt} & χ_{Ca}^{Gnt} = no. of Mn & Ca atoms in garnet for O=12

$\chi_{Al}^{Biot\ IV}$, $\chi_{Al}^{Biot\ VI}$ & χ_{Ti}^{Biot} = no. of Al^{IV}, Al^{VI} & Ti atoms in biotite for O=22.

Tentative temperatures reached during the Windmill Islands metamorphism can be derived using values of $K_{tranf.}$ calculated for the Windmill Islands rocks plotted on the graph of Saxena (1969, Fig. 7). A steady temperature increase from the northern amphibolite facies to the southern granulite facies is indicated (Fig. 5.8a). The temperature estimate for the amphibolite facies (450°C) is well below the beginning of melting for a wet granite; and as abundant migmatites, however, in the amphibolite facies area suggest that metamorphic temperatures were probably on the high temperature side of this melting curve (i.e. probably >500°C), it is felt that the initial assumed temperatures of Saxena (1969) are too low (upper amphibolite - 500°C; charnockite-600°C).

Perchuck (1969) has computed the theoretical temperature dependence of the Fe-Mg distribution between garnet and biotite at pressures between 3 and 12 kilobars. Using this calibration (Fig. 5.8b) temperatures between 620°C and 650°C are obtained for the Windmill Islands as a whole.

5.4.4 ORTHOPYROXENE-CLINOPYROXENE

5.4.4.1 Introduction

The elemental distribution between co-existing pyroxenes has probably been studied more than any other co-existing mineral pair. The pair appears to show almost "ideal" behaviour for low Fe contents, but for

high Fe values K_D is dependant upon the mole fraction of Fe^{2+} in orthopyroxene (Mueller, 1960, Binns, 1962, Davidson, 1968 & 1969 and Scharbet & Kurat (1974). This has been accounted for by the presence of two non-equivalent sites, M_1 and M_2, in the orthopyroxene lattice. Fe^{2+} is preferred strongly at the M_2 site (Ghose 1965 and Ghose & Hafner, 1967). The relative attraction of orthopyroxene and clinopyroxene for Fe^{2+} remains fairly constant until the M_2 sites are saturated with Fe^{2+} beyond which stage the clinopyroxene progressively attracts more Fe^{2+} with increasing Fe. The "cut off" value for the "ideal" behaviour (up to M_2 saturation) of Fe^{2+}-Mg^{2+} distribution between co-existing pyroxenes is about χ_{Fe}^{opx} =0.4 (Davidson, 1968, 1969). Saxena and Ghose (1971) have determined the Fe^{2+} - Mg^{2+} distribution between the M_1 and M_2 sites at varying temperatures.

5.4.4.2 Mg^{2+}-Fe^{2+} Distribution

Ray and Sen (1970) and Saxena (1971) examined the effect of Ca and Al on the distribution of Fe^{2+}-Mg^{2+} between co-existing pyroxenes. Following the procedure adopted by Ray and Sen (1970) it was found that Ca and Al do not appear to exert an influence on the Fe^{2+}-Mg^{2+} distribution between co-existing pyroxenes from the Windmill Islands.

K_D's as defined by Davidson (1968) were calculated for the rocks of the Windmill Islands and plotted against χ_{Fe}^{opx} (Fig. 5.9a). As can be seen, most of these specimens have χ_{Fe}^{opx} less than 0.4 and according to Davidson, (1968 & 1969) they should show close to "ideal" behaviour.

Figure 5.9b is a"Roosenboom"diagram of the co-existing pyroxenes from the Windmill Islands. There are two groups of rocks. One has an average $K_{D_{Mg}}$ of 0.58 and comprises specimens north of and including Robinson Ridge. The other group, with an average $K_{D_{Mg}}$ of 0.68, is from Herring, Cloyd and Ford Islands, which are south of Robinson Ridge. Atkins (1969), on comparing $K_{D_{Mg}}^{opx\text{-}cpx}$ values for the Bushveld Complex

with those from the Skaergaard Complex estimated that a difference in K_D of 0.06 could represent a pressure difference of nearly 6 Kbars or a temperature difference of 200°C. Thus temperature would be expected to have a dominating influence over pressure in determining K_D. It is probable then, that the difference of $K_{D_{Mg}}$ between pyroxenes in the northern areas and those in the south is a function primarily of temperature; the rocks in the south equilibrating under higher temperatures than those in the north. An anomaly is that 335-254, which is located even further south than Herring Island, has a $K_{D_{Mg}}$ with close affinity to those of the northern rocks. An explanation for this might be that 335-254 is in chemical disequilibrium. On the other hand, the anomalous $K_{D_{Mg}}$ may in fact reflect the original P-T conditions prior to the deformative event which folded the charnockite. 335-254 is located on Bosner Island on the southern limb of the "charnockite fold", which, if unfolded would relocate 335-254 with a "southing" equivalent to that of 335-307 and 335-308 (Robinson Ridge). (See also section 5.4.6).

5.4.4.3 Mn^{2+} Distribution

Scharbet and Kurat (1974) believe that the distribution of Mn is most susceptible to changes of temperature. However, because of its general low concentration analytical errors are likely to be relatively great. Lindh (1974) examined from the literature the Mn distribution between co-existing pyroxenes and found that for a mole fraction of Mn $\left(= \frac{Mn}{Mg+Fe+Mn}\right)$ less than 0.008, Mn is distributed evenly between the pyroxenes, but for higher Mn contents, the orthopyroxene is weakly enriched in Mn.

The Mn distribution between co-existing pyroxenes of the Windmill Islands shows (Fig. 5.9c) an approximation to the general trend proposed by Lindh (1974), namely that, for χ_{mn}^{opx} greater than 0.008, the orthopyroxene is slightly enriched in Mn. No discernable grouping, similar to

that exhibited by $K_{D_{Mg}}^{opx\text{-}cpx}$, relating to metamorphic grade, is present. It is felt that such grouping, if present, is likely to be masked by scatter due to analytical error.

5.4.5 Hornblende - Pyroxene

5.4.5.1 Mg^{2+}-Fe^{2+} distribution

Perchuck (1969) has derived theoretical isotherms based on the distribution of Mg^{2+} between (i) hornblende and orthopyroxene and (ii) hornblende and clinopyroxene. Applying the data from the Windmill Islands to this geothermeter the following (Table 5.9) estimated temperatures for these rocks are found.

Sample		Hbl-Cpx Pair	Hbl-Opx Pair
335-602	order of	750°C	675°C
335-601	increasing	750	690
335- 45	southing	-	690
335-110	↓	750	690
335-307		900	790
335-308		700	660
288- 19		700	740
335-629L		-	630
335-629M		-	630

Table 5.9: Estimated temperatures from Hbl-Cpx and Hbl-Opx mineral pairs using the theoretical geothermometer of Perchuck (1969).

No correlation between temperature variation and metamorphic grade based on other evidence (see section 2.14) is apparent; in fact, some of the assumed highest grade rocks (e.g. 228-19) show some of the lowest temperatures (700°C for Hbl-Cpx).

Ray and Sen (1970) in a study of elemental distribution, showed that, in the Fe^{2+}-Mg^{2+} distribution between (i) hornblende and clinopyroxene and (ii) hornblende and orthopyroxene, that Al^{IV}_{Hbl} exerts a major control whereas Ca^{2+}cpx and Fe^{3+}_{Hbl} is a minor influence. Ray and Sen (1970) maintained that if the effect of Al^{IV}_{Hbl} was taken into account, a close approximation to an ideal mixture model should be achieved for the Fe^{2+}-Mg^{2+} distribution.

On the other hand, Hubregtse (1973), in a similar study, did not make any correction for Al^{IV}_{Hbl}, despite variation in the amount of this constituent. Although his data deviated from ideal distribution, he felt that the K_D's he obtained were, in each case, a true indication of equilibration under similar P-T conditions.

Ray and Sen (1970, Fig. 6) showed that for rocks which have equilibrated under the same pressure and temperature, there is a straight line relationship between $K^{Hbl\text{-}Cpx}_{D_{Mg}}$ and Al^{IV}_{Hbl}. This relationship was applied to the rocks of the Windmill Islands and it was found that for a constant Al^{IV}_{Hbl} value, $K^{Hbl\text{-}Cpx}_{D_{Mg}}$ and $K^{Hbl\text{-}opx}_{D_{Mg}}$ (and, if ideality is assumed, temperature) increases from the north to the south (Fig. 5.10a&b). Thus provided the effect of Al^{IV}_{Hbl} is taken into account, the Mg^{2+}-Fe^{2+} partitioning between hornblende and pyroxene shows that the grade change (indicated by mineral assemblage differences) from upper amphibolite facies in the north to the granulite facies in the south is accompanied by a temperature increase.

5.4.5.2 Ca —Na Distribution

Using the theoretical geothermometer of Perchuck (1969), the distribution of Ca^{2+} between hornblende and clinopyroxene in the Windmill Islands rocks yields unrealistic temperatures of the order of $1200^{o}C$. Hubregtse (1973), however, was able to distinguish between meta-gabbros and clinopyroxene gneisses from an area in Spain using plots of $(\frac{Ca}{Na+K})_{Hbl\text{-}Cpx}$ and $(\frac{Na}{Ca})_{Hbl\text{-}Cpx}$, a difference which he inferred resulted from differing

physical conditions operating during equilibration of these rock types. Similar plots have been employed for the Windmill Islands rocks and are shown in Figures 5.11a & b. Only the $(\frac{Na}{Ca})_{Hbl-Cpx}$ plot shows any relation between K_D (which is related to temperature) and metamorphic grade. The scatter of points in the $(\frac{Ca}{Na+K})$Hb-Cpx plot could well be attributed to the high content of Ca in the minerals and the relatively large errors which could accumulate in the analyses of the low concentrations of Na and K.

5.4.5.3 Mn^{2+} Distribution

As can be seen from figures 5.12a & b, there is a reasonable correlation between (i) χ_{Mn}^{Hbl} and χ_{Mn}^{Opx} and (ii) χ_{Mn}^{Hbl} and χ_{Mn}^{Cpx} from the Windmill Islands, indicating Mn is following Nernst's Law approximately. However, no indication of grade variation is apparent. $K_{D_{Mn}}^{Hbl-Opx}$ range from 0.360 to 0.733 and $K_{D_{Mn}}^{Hbl-Cpx}$ from 0.433 to 0.665. Ray and Sen (1970) found no correlation between χ_{Mn}^{Hbl} and χ_{Mn}^{Opx} and attributed this to the low Ca content of the orthopyroxenes (Ca-Mn diadochy).

5.4.6 Biotite-Pyroxene

The distribution of Mg^{2+} and Mn^{2+} between (i) biotite and orthopyroxene and (ii) biotite and clinopyroxene is portrayed in figures 5.13a & b and 5.14a & b. In all these plots, particularly that depicting $\chi_{Mg}^{Opx-Biot}$, a distinction between the mineralogically low grade, (higher K_D), northern and the higher grade, (lower K_D), southern rocks is noted. Greater scatter in the plot of the Mn^{2+} distribution is thought due to the low Mn content of the biotite and hence the large relative analytical error.

Table 5.10 lists the calculated $K_D^{pyroxene-biot.}$ of the Windmill Islands rocks and those recalculated from the literature.

Source	$K_{D_{Mg}}^{Opx\text{-}Biot}$	$K_{D_{Mg}}^{Cpx\text{-}Biot}$	$K_{D_{Mn}}^{Cpx\text{-}Biot}$
Windmill Islands (low pressure granulites)	0.44-1.05	0.66-1.66	1.14-12.79
Scharbet & Kurat (1974) (high pressure granulites)	0.63-1.0	-	0.45- 2.5
Saxena (1969b)(charnockites)	0.70-1.09	1.27-1.68	-

TABLE 5.10: Various values of $K_D^{Pyroxene\text{-}Biot}$

The Windmill Islands K_D's are similar to the granulite facies data available from the literature, but are generally slightly lower: this appears to be a reflection of a higher temperature of crystallization of the Windmill Islands rocks, although the affect of pressure is unknown.

The differing K_D's of the pyroxene-biotite pairs from the northern and southern areas of the Windmill Islands are regarded as a reflection of different physical conditions operating during recrystallization, temperature probably being the dominant influence. It is noted that specimens 335-254 and 335-160 show affinities with the lower grade rocks, even though they are the most southerly outcropping specimens. The significance of this has already been discussed (section 5.4.4.2).

Applying the geothermometer of Perchuck (1969), the clinopyroxene-biotite Mg^{2+} distribution yields temperatures ranging from 630-740^{o}C; no correspondence, however, between the temperatures indicated by individual rocks and their relative metamorphic mineralogical grade being shown.

5.4.7 Hornblende-Biotite

Co-existing hornblende and biotite in basic rocks is confined to the northern areas (see section 2.4.4). The distribution of Mg^{2+} and Mn^{2+} between these two minerals is portrayed in figures 5.15a & b. Mg^{2+} appears to be distributed fairly evenly, only 335-601 being anomalous, indicating that the rocks equilibrated under similar physical conditions. The distribution of Mn^{2+}, which is more random, may be accounted for by the low concentration and consequent analytical error.

Most literature values for $K_{D_{Mg}}^{Hbl\text{-}Biot}$ are close to unity (Hollander, 1970; Annersten & Ekström, 1971) although those of Rivalenti and Rossi (1973) show considerable scatter. Hollander (1970) believes that deviations from K_D=1 can be explained in terms of the Al^{IV}_{Hbl} Al^{IV}_{Biot} ratio. The higher this ratio the greater the deviation of $K_{D_{Mg}}$ from unity. Examination of the Windmill Islands data reveals that Al does not appear to influence this $K_{D_{Mg}}$, at least not in the manner suggested by Hollander (Fig. 5.16a & b). In fact, the rock with the lowest Al^{IV}_{Hbl} Al^{IV}_{Biot} ratio (viz. 335-601) has the greatest deviation from unity!

Following Hollander (1970), Mn^{2+} distribution was examined as wt.% MnO hornblende against wt.% MnO biotite. Hollander (1970) recognises two trends on this plot; one for amphibolite facies rocks and one for granulite facies rocks. These projected trends are incorporated in figure 5.17a. Excepting 335-601, which is thought not to be in equilibrium, all samples fall within these projected trends as would be expected.

Similarly the distribution of Ti between hornblende and biotite was examined (Fig. 5.17b). The points all fall close to the trend determined by Hollander (1970) for similar grade rocks.

Unfortunately as biotite and hornblende do not occur together in the basic rocks of higher grade in the Windmill Islands, it was not possible to determine what effects, if any, the metamorphic grade would have upon these elemental distributions.

5.5 CONCLUSIONS

It is evident that there are systematic differences in both individual mineral chemistry and in the distribution of elements in co-existing minerals, between the northern amphibolite facies and the southern granulite facies rocks. This variation, can in most cases be ascribed primarily to an increase southward of the crystallization temperature. The influence of load pressure is not well understood, however, it must increase southwards (see section 6.5). The distribution of Mn between co-existing mineral phases is of limited use unless accurate analytical determinations are made. The role of PH_2O is impossible to decipher using this approach, but because of the progressive breakdown of the hydrous minerals, it probably decreased southwards (see also discussion in section 6.5). It is probable that PO_2 remained fairly constant due to the buffering affect of certain oxide assemblages.

CHAPTER 6

COEXISTING CORDIERITE AND GARNET AS A GUIDE TO METAMORPHIC CONDITIONS

6.1 INTRODUCTION

Since the turn of the 1960's, the stability field of cordierite in pressure-temperature space has invoked considerable interest. Initially, experimental workers confined themselves to studying the breakdown of either the iron or the magnesium end member of cordierite (Schreyer 1965a, 1965b, Schreyer and Schairer 1961; Schreyer and Yoder 1960, 1964; Schreyer and Seifert 1969a, 1969b; Richardson 1968; Newton 1972, 1974). However, recently, experimental data have been published regarding the breakdown of cordierite at varying compositions. The two most notable contributors in this field have been Hensen and Green (Hensen 1971, 1972; Hensen and Green 1969, 1970, 1971, 1972, 1973), and Currie (Currie 1971, 1973).

Hensen and Green examined a variety of breakdown reactions of synthetic cordierite at varying pressures and temperatures whereas Currie only examined the experimental equilibrium position of the reaction:

$$3\ \text{Cordierite} \rightleftarrows 2\ \text{Garnet} + 4\ \text{Sillimanite} + 5\ \text{Quartz} \quad \ldots\ (1)$$

This assemblage, cordierite + garnet + sillimanite + quartz, is present in some of the rocks from the Windmill Islands and consequently the author has directed attention to the cordierite breakdown reaction (1) mentioned above. From experimental data, both Hensen and Green, and Currie devised a geothermometer and geobarometer utilizing the compositions of coexisting cordierite and garnet to estimate equilibrium temperatures and pressures of natural assemblages. Hutcheon, Froese and Gordon (1974) also presented a calibration of reaction (1).

6.2 THE DIFFERENT CALIBRATIONS

Each calibration is discussed under the heading of the author(s) of the calibration.

6.2.1 Hensen and Green

Hensen and Green (1971, 1972 and 1973) took synthetic glasses of varying Fe to Mg ratios and ran them in graphite bombs under anhydrous conditions. They examined the types and compositions of the products

with an electron microprobe at varying pressures and temperatures. They presented their results in a P-T diagram with mole fraction of magnesium end member contours for the divariant reaction (1). (Hensen and Green 1973 page 154).

6.2.2 Currie

6.2.2.1 Method

Currie (1971) prepared synthetic cordierite of differing Fe to Mg ratios. He experimented with this synthetic cordierite in platinum bombs with 5 weight % water present. He examined and determined the products and their compositions in immersion oils and with X-Rays. He presented his results in tabular form and graphically (Currie 1971 pages 221 and 222).

6.2.2.2 Thermodynamic Considerations

Currie discussed the thermodynamics of reaction (1) and related his experimental data to these thermodynamics as follows:

At equilibrium, reaction (1) becomes an exchange reaction which can be written

1/2 Fe - cordierite + 1/3 Mg - garnet $\rightleftarrows$ 1/2 Mg - cordierite + 1/3 Fe - garnet .... (2)

Assuming ideality for reaction (2),

$$\Delta G^{o} = -RT \ln K_D^{*} = -RT \ln \left[\frac{X^{c}_{m}}{(1-X^{c}_{m})} \cdot \frac{X^{g}_{f}}{(1-X^{g}_{f})} \right]^{*}$$

$$= 1/2\ G^{c}_{m} + 1/3\ G^{g}_{f} - 1/2\ G^{c}_{f} - 1/3\ G^{g}_{m}$$

where G = Gibbs Free Energy

ΔG^{o} = change in Gibbs Free Energy at Standard Temperature and Pressure

K_D = Equilibrium Constant (or Partition Coefficient)

R = Gas Constant

---

*This K_D, as defined, is used throughout this chapter.

χ_j^i = Mole fraction of component j in phase i

m = Magnesium end member component

f = Iron end member component

c = Cordierite and g = Garnet

By studying the end member reactions of (1) viz.

1/2 Fe - cordierite $\rightleftarrows$ 1/3 Fe - garnet + 2/3 sillimanite + 5/6 quartz .... (3)

and

1/2 Mg - cordierite $\rightleftarrows$ 1/3 Mg - garnet + 2/3 sillimanite + 5/6 quartz .... (4)

Currie was able to derive information on the value of K_D

i.e.

$$RT \ln K_D = (P_e^p - P_e^a)\, d\, V \quad \ldots\ (5)$$

where P_e^p = equilibrium pressure for reaction (4)

and P_e^a = equilibrium pressure for reaction (3)

Equation (5) may be rewritten as

$$T = \frac{\Delta P . \Delta V}{R} \left(\frac{1}{\ln K_D}\right) \quad \ldots\ (6)$$

where $\Delta P = (P_e^p - P_e^a)$

He was also able to derive an expression relating the composition to the equilibrium pressure,

i.e. $P = P_e^a + \frac{\Delta P}{2} (\chi_m^g + \chi_m^c)$ .... (7)

From equation (6) $\Delta P = \frac{RT \ln K_D}{\Delta V}$

Currie obtained a value for ΔV from the literature,

$\therefore \Delta P = 0.003138\ T \ln K_D$

Currie examined his experimental data and found that

$\Delta P = 0.020T - 14.18$. So by substituting in (6)

$$T = 4515/(6.37 - \ln K_D) \quad \ldots\ (8)$$

Thus knowing the composition of the coexisting cordierite and garnet, K_D may be determined and using equation (8) T, the equilibrium temperature, may be calculated. P_e^a at this temperature

may be obtained from Currie's experimental data and so utilizing equation (7) the equilibrium pressure P, may be calculated.

6.2.3 Hutcheon, Froese and Gordon

Hutcheon, Froese and Gordon (1974) examined the two end member reactions as follows,

$2Fe_3Al_2Si_3O_{12} + 4Al_2SiO_5 + 5SiO_2 \rightleftarrows 3Fe_2Al_4Si_5O_{18}$ - reaction a

$2Mg_3Al_2Si_3O_{12} + 4Al_2SiO_5 + 5SiO_2 \rightleftarrows 3Mg_2Al_4Si_5O_{18}$ - reaction b

Assuming ideality, then at equilibrium ΔS° and ΔV° can be regarded as constant, then, for reaction a,

$$\Delta G_a = \Delta G_a^\circ - \Delta S_a^\circ(T - 298) + \Delta V_a^\circ (P - 1) + RT\ell nK_a = 0 \qquad \ldots. (9)$$

and for reaction b,

$$\Delta G_b = \Delta G_b^\circ - \Delta S_b^\circ(T - 298) + \Delta V_b^\circ(P - 1) + RT\ \ell nK_b = 0 \qquad \ldots.(10)$$

where ΔG = change in Gibbs Free Energy

R = Gas constant

ΔS = change in entropy

$$K_a = \frac{(a_f^c)^3}{(a_f^g)^2} \qquad \text{and} \qquad K_b = \frac{(a_m^c)^3}{(a_m^g)^2}$$

a_j^i = activity of component j in phase i

Since ideal ionic solution in garnet and cordierite is assumed, the activity is equal to the atomic fraction raised to a power equal to the number of lattice sites where mixing occurs. Hence

$$K_a = \left(\frac{\chi_F^c}{\chi_F^g}\right)^6 \qquad \text{and} \qquad K_b = \left(\frac{\chi_m^c}{\chi_m^g}\right)^6$$

where χ_j^i = mole fraction of component j in phase i.

Solving equations (9) and (10) for P and T

$$P = \frac{(\Delta G_a^\circ+298\Delta S_a^\circ-\Delta V_a^\circ)(R\ell nK_b-\Delta S_b^\circ)-(R\ell nK_a-\Delta S_a^\circ)(\Delta G_b^\circ+298\Delta S_b^\circ-\Delta V_b^\circ)}{(R\ell nK_a-\Delta S_a^\circ)\Delta V_b^\circ - (R\ell nK_b-\Delta S_b^\circ)\Delta V_a^\circ} \qquad \ldots.(11)$$

$$T = \frac{(\Delta G_a^o + 298\Delta S_a^o - \Delta V_a^o)\Delta V_b^o - (\Delta G_b^o + 298\Delta S_b^o - \Delta V_b^o)\Delta V_a^o}{(R\ell nK_b - \Delta S_b^o)\Delta V_a^o - (R\ell nK_a - \Delta S_a^o)\Delta V_b^o} \quad \ldots\ (12)$$

Knowing the composition of the coexisting garnet and cordierite it is possible to calculate K_a and K_b. The thermodynamic parameters ΔG^o, ΔS^o and ΔV^o for both reactions a and b were either assumed, calculated (using other known thermodynamic data) or obtained from other experimental workers by Hutcheon et. al. (1973).

All these parameters are placed in equations (11) and (12) to obtain P and T, the equilibrium pressure and temperature for a particular coexisting pair of cordierite and garnet.

6.3 DISCUSSION OF CALIBRATIONS

Unfortunately there is lack of agreement between the above-mentioned calibrations. It should be mentioned that both the calibrations of Hensen and Green and that of Currie are based on experimental work in which observed reactions were not reversed. However, Hensen (1972) reversed reaction (1) at 1000°C and 9 kilobars for one composition and found it roughly in agreement with the previously determined data of Hensen and Green.

The major difference between the calibration of Hensen and Green and that of Currie is that Currie predicts an increase in K_D with increasing temperature while Hensen and Green predict that K_D should decrease with increasing temperature.

Currie (1973) discusses this disagreement in defence of his own calibration. He questions the plausibility of the values of thermodynamic parameters (e.g. ΔS and ΔV) obtained from the experimental data of Hensen and Green. Further he examines some published analyses of co-existing cordierite and garnet from natural assemblages and the metamorphic environment in which these assemblages occur. He maintains that where an increase in temperature can be affirmed by separate evidence the K_D of the co-existing pairs increases, as he predicts. However the data of

Saxena and Hollander (1969) are not in accord with Currie's increasing K_D with increasing temperature. However, Saxena and Hollander (1969) obtained K_D values which were based on co-existing pairs taken from different metamorphic terrains and Currie (1971) states that their supposedly low grade (epidote - amphibolite facies) rocks are actually of a higher grade as they contain sillimanite.

Wood (1973) also discussed the conflict in experimental data shown by Hensen and Green, and Currie. He noted that the only real difference between the two experimental methods was the presence, or absence of water in the bombs. He suggested that it was this water which gave rise to the discrepancies. By making some assumptions and using published thermodynamic data he was able to compute the amount of water that could take part in the reaction (equation (1)) and the effect that this water would have on the equilibrium constant, K_D.

He found that for the anhydrous reaction the slope of log K_D against 1/T was positive, as obtained by Hensen and Green, who experimented under dry conditions. For the hydrous reaction, however, the slope was negative, as obtained by Currie, who experimented under wet conditions (Wood, 1973; Fig. 2). Thus Wood (1973) states ".... K_D might be regarded as a better measure of PH_2O operating during crystallization than of temperature".

In order to apply any of the calibrations to natural assemblages certain conditions need to be fulfilled:

(i) Equilibrium has been reached, at least in regard to partitioning between iron and magnesium.

(ii) The cordierite and garnet must be reasonably free from contaminants which would compete with Fe^{2+} and Mg^{2+} for lattice positions.

Hensen (1971) found that biotite does not act as a "sink" for cations and the presence of biotite in a cordierite, garnet, sillimanite assemblage does not effect the composition of the co-existing phase at constant P and T, but may alter their relative proportions.

Probably the most likely contaminant would be Mn^{2+}, although Ca^{2+}

must make some contribution, especially in garnet. Hutcheon et. al. (1974) make an attempt to correct for these contaminants in the calculation of K_a and K_b. However, their correction is not necessarily a valid one as they still need to assume that the partitioning of Fe^{2+} and Mg^{2+} is ideal and also that their estimates of thermodynamic parameters are based on pure end member reactions.

Recently Weisbrod (1973) has examined the effect of Mn on the Fe end member reaction equilibrium position. He notes that: ".... Consider a pelitic rock containing 2% garnet, excess quartz and sillimanite and having a bulk composition with 0.2 wt. % MnO, a typical value. Because Mn is dominantly contained in garnet, this mineral would contain about 25 mole % spessartite. At 750°C, the minimum stability pressure for Mn free garnet co-existing with quartz and sillimanite is 3.3 Kbar. Garnet containing 25 mole % spessartite could be stable, however, to 2.1 Kbar."

Thus, the garnet-cordierite pair must be used with some care when attempting to estimate conditions of metamorphism.

6.4 APPLICATION OF CALIBRATIONS TO NATURAL ASSEMBLAGES

6.4.1 Introduction

The assemblage biotite + cordierite + garnet + sillimanite is placed in the upper amphibolite facies by Winkler (1967) whereas DeWaard (1965) places it in the lower granulite facies. Binns (1964) and Heitenan (1967) however recognise this assemblage in both upper amphibolite and lower granulite facies.

In an attempt to determine which of the calibrations is more applicable to natural assemblage, a literature search was undertaken to find published analyses of co-existing cordierite and garnet with sillimanite and biotite. The equilibrium pressure and temperature of these pairs were calculated using the three different calibrations and related to various experimental stability curves pertinent to the upper amphibolite and lower granulite facies. The results of the literature search are detailed in Table 6.1 and plotted in Figure 6.1.

Source	Sample No.	CALIBRATION					
		CURRIE		HENSEN & GREEN		HUTCHEON FROESE & GORDON	
		P(Kbrs)	T°C	P(Kbrs)	T°C	P(Kbrs)	T°C
Reinhardt (1968)	D-28	6.6	677	8.6	790	6.0	737
	D-56	6.4	712	9.0	700	5.0	626
	D-87	5.6	652	7.1	840	5.9	866
	D-102	6.4	692	8.5	760	5.5	688
	D-175	6.1(5)	641	8.0	870	6.8	918
	R-114	6.1	711	7.9	750	4.7(5)	635
	R-124	6.5	717	9.3	705	5.1	709
	W-53	6.9	668	9.4	825	9.7	706
Hutcheon, Froese & Gordon (1973)	1	6.7(6)	713	10.0	770	5.5	625
	2	6.4	704	9.2	725	5.3	650
	3	6.8(6)	673	9.3	835	6.6	760
	4	6.2(5)	694	9.2	770	5.8	680
	5	6.9	675	9.5	825	6.6	750
Barker (1962)	2	6.2	698	8.6	750	5.7	774
Gable & Sims (1969)	EWT-90	5.9(6)	746	8.7	635	5.4	706
Wynne-Edwards & Hay (1963)	H29	6.3(5)	673	8.7	770	7.1	926
	H70	6.1	654	8.1	830	8.5	1182
Currie (1971)	69-117	5.7	627	7.4	825	5.9	864
	69-38	6.1(5)	652	8.0	760	5.6	745
	69-77	6.2	722	8.7	735	5.4	653
	69-6	6.4(5)	717	10.2	585	4.9	519
	69-29	6.7	732	10.8	580	5.0	501
Saxena & Hollander (1969)	6	6.4	810	9.9	550	3.9	428
	1	5.6	870	9.3	480	3.0	357
	12	5.6	823	9.1	510	3.3	412
	7	5.4	812	8.4	560	3.2(5)	396
	8	5.8	777	9.0	580	3.9	482
	4	6.0	762	9.0	620	4.2	512
	3	5.8	690	7.6	780	5.1	701
	9	5.9	690	8.2	760	5.3	703
	2	6.1	671	8.5	770	5.9	766
	5	6.0	607	7.3	940	8.0	1175
	10	6.4	632	8.5	870	7.5	965
Henry (1974)	2	6.4	727	9.5	665	5.0(5)	582
	3	6.7(5)	750	10.0	635	5.0(5)	534
	8	6.4	720	9.7	670	5.1(5)	608
	9	6.2	726	9.0	680	4.9	590
	10	6.1	747	9.2	620	4.5	539
	14	6.1	704	8.0	895	5.4	660
Blight (Windmill Islands)	335/19	5.9	760	8.7	640	3.9	516
	335/83	5.6	762	8.2	645	3.7	618
	335/274	6.4	762	9.6	605	7.3	890
	335/402	6.0	760	9.0	625	3.8	518
	335/519		780	8.9	560	3.3	459

TABLE 6.1: Estimated P-T conditions for co-existing garnet and cordierite obtained from the literature.

6.4.2 Hutcheon, Froese and Gordon

By examination of these data it can be seen that use of the calibration of Hutcheon, Froese and Gordon gives a very large temperature range (e.g. Saxena and Hollanders data taken from amphibolite to lower granulite facies rocks shows temperatures ranging from 350-1200°C, implying an unreal geothermal gradient). It appears that the determined temperature is sensitive to small changes in values of K_a and/or K_b. Since these temperatures are unrealistic the author examined the initial equation (12) to determine why the temperature is sensitive to small changes in K_a and/or K_b.

$$T = \frac{(\Delta G_a^\circ + 298\Delta S_a^\circ - \Delta V_a^\circ)\Delta V_b^\circ - (\Delta G_b^\circ + 298\Delta S_b^\circ - \Delta V_b^\circ)\Delta V_a^\circ}{(R\ell nK_b - \Delta S_b^\circ)\Delta V_a^\circ - (R\ell nK_a - \Delta S_a^\circ)\Delta V_b^\circ}$$

from Robie and Walbaum (1968) $\Delta V_a^\circ \simeq \Delta V_b^\circ$

$$\therefore \quad T = \frac{(\Delta G_a^\circ - \Delta G_b^\circ) + 298(\Delta S_a^\circ - \Delta S_b^\circ)}{R(\ell nK_b - \ell nK_a) + (\Delta S_a^\circ - \Delta S_b^\circ)}$$

$$\therefore \quad RT\,\ell n(K_b/K_a) + T(\Delta S_a^\circ - \Delta S_b^\circ) = (\Delta G_a^\circ - \Delta G_b^\circ) + 298(\Delta S_a^\circ - \Delta S_b^\circ)$$

$$\therefore \quad \ell n(K_b/K_a) = \frac{(\Delta G_a^\circ - \Delta G_b^\circ) + 298(\Delta S_a^\circ - \Delta S_b^\circ)}{R} \cdot \frac{1}{T} - \frac{(\Delta S_a^\circ - \Delta S_b^\circ)}{R}$$

Thus by plotting $\ell n(K_b/K_a)$ Vs. $\frac{1}{T}$ one should obtain a straight line with:

$$\text{slope} = \frac{(\Delta G_a^\circ - \Delta G_b^\circ) + 298(\Delta S_a^\circ - \Delta S_b^\circ)}{R}$$

and intercept on the $\ell n(K_b/K_a)$ axis $= \dfrac{-(\Delta S_a^\circ - \Delta S_b^\circ)}{R}$

In order to reduce the sensitivity of temperature on K_a and/or K_b (i.e. $\ell n\, K_b/K_a$), in the temperature range that we are concerned with (viz. 100-1000°C) the slope of $\ell n(K_b/K_a)$ must be increased.

This suggests that some or all of the thermodynamic parameters used by Hutcheon et. al. (1973) are incorrect. This is not surprising as some

of their assumed values are based on rather nebulous information. For example, in order to obtain a value for ΔG_b they estimated $\Delta G_b = 0$ at 1000^oC and 10 Kbars because ".... it allows the rocks from the Daly Bay Complex to fall into the stability field of sillimanite".

For the previously mentioned reasons, the calibration of Hutcheon et. al. (1973) is rejected.

6.4.3 Hensen and Green

Using the calibration of Hensen and Green (1973) most of the co-existing pairs suggest pressures in excess of 7 Kilobars, generally between 8 and 10 Kilobars. This is higher than the field of granulite facies suggested by the fluid inclusion studies of Touret (1971) and further, they suggest the stable aluminosilicate phase should be kyanite at temperatures below about 750^oC (Richardson et. al. 1969) and not sillimanite, as observed in the natural assemblages.

Newton (Newton 1972 and Newton et. al. 1974) suggests that the calibration of Hensen and Green (1973) gives anomalously high pressure estimates for the breakdown of Mg-cordierite because of the possibility of:

(i) sluggishness of breakdown reactions in dry systems;

(ii) any water present may be incorporated in the cordierite structure and thus stabilize the reaction by as much as 4 Kbars. above the true dry breakdown limit.

This second suggestion of Newton does not seem likely as the experiments of Hensen and Green were conducted under completely anhydrous conditions. Also the experimental observation of Newton (1972) that anhydrous Mg-cordierite breaks down at lower load pressures than the hydrous form is in conflict with the data of Hensen and Green (1971, 1972, 1973) and Currie (1971) as discussed by Wood (1973) (see Section 6.3).

6.4.4 Currie

When applied to the calibration of Currie (1973) the co-existing cordierite and garnet pairs obtained from the literature generally plot in the stability field of sillimanite, in the vicinity of the field,

suggested by the fluid inclusion studies of Touret (1971), of granulite facies. Also the temperatures suggested from this calibration are of the order expected from rocks of the upper amphibolite to lower granulite facies; namely, above the breakdown of muscovite (at low P_{H_2O}) and above the granite solidus, below the breakdown of hornblende and around the incoming of orthopyroxene (Fig. 6.1).

6.4.5 Conclusions

From the previous discussion it is felt that the calibration of the garnet - cordierite geothermometer and geobarometer devised by Currie (1971) is the most acceptable. However, until the role that water plays, in positioning the equilibrium reaction between garnet and cordierite is investigated fully, the quantitative answers supplied by the calibration of Currie must be accepted with reserve.

Dougan (1974) and Henry (1974) also prefer the calibration of Currie (1971).

6.5 APPLICATION TO THE ROCKS OF THE WINDMILL ISLANDS

Five co-existing cordierite garnet pairs were analysed from the rocks of the Windmill Islands (analytical details are presented in Appendix II). These analyses and the P-T estimates, using the three calibrations, are given in Table 6.2. Each pair is from the assemblage; quartz + garnet + plagioclase + cordierite + sillimanite + biotite (see section 2.2.3.5). Many of the cordierite grains have been extensively altered during a retrograde event (see section 2.5.6). Where the cordierite is not altered, the cordierite and garnet show reaction textures, the garnet and sillimanite nucleating in and around the cordierite.

The only significant contaminant in the pairs is manganese in the garnets. However the maximum percentage of Mn is equivalent to less than 15% spessartite rich and as such would affect the calibration only to a small extent, possibly reducing the estimated pressures by 0.5 Kbars.

	335/19	335/83	335/274	335/402	335/519
Whole Rock Analyses					
SiO_2	70.46	62.07	64.87	64.44	63.32
Al_2O_3	13.31	17.42	14.78	14.40	15.80
Fe_2O_3	2.15	5.10	4.16	3.66	2.78
Fe_2O	4.57	7.77	6.18	5.11	5.85
CaO	1.87	.80	2.02	1.25	1.95
N_2O	2.02	1.12	1.81	1.56	2.52
MgO	1.74	2.11	2.33	4.19	2.16
K_2O	2.79	2.78	2.00	3.07	3.25
TiO_2	.82	1.66	1.08	1.12	.99
MnO	.16	.16	.23	.17	.15
P_2O_5	.17	.23	.21	.16	.26
H_2O+	.50	.72	1.05	1.81	1.07
Total	100.56	100.94	100.72	100.94	100.10
Modal %'s					
Quartz	38	33	29	22	31
Plag	8	7	27	35	36
Kspar	-	2	3	8	-
Cordierite	24	17	13	11	9
Biotite	27	29	12	20	20
Sillimanite	trace	7	trace	1	1
Garnet	1	2	13	1	trace
Opaques	2	3	3	2	3
Mineral Analyses	Cord Gnt	Cord Gnt	Cord Gnt	Cord Gnt	Cord Gnt
SiO_2 wt.%	47.88 37.05	47.24 36.05	48.49 37.54	47.87 37.23	48.09 37.06
Al_2O_3	32.68 21.00	32.47 20.87	32.75 21.34	32.69 21.00	32.99 21.03
FeO	7.90 29.56	9.29 31.30	6.45 30.24	7.49 28.39	8.35 30.13
CaO	0.00 .75	.02 .93	.00 1.24	.03 .98	.02 1.12
MgO	7.85 3.97	7.22 3.27	9.01 5.64	7.69 3.94	7.64 3.28
MnO	0.32 4.20	.25 4.04	.12 1.94	.24 6.52	.45 5.61
Estimated P-T Conditions					
Currie P Kbrs	5.9	5.6	6.4	6.0	5.9
T °C	760	762	762	760	780
Hensen P Kbrs	8.7	8.2	9.6	9.0	8.9
& Green T °C	640	645	605	625	560
Hutcheon P Kbrs	3.9	3.7	7.3	3.8	3.3
et. al. T °C	516	618	890	518	459

TABLE 6.2: Data of the co-existing garnet and cordierite assemblages from the Windmill Islands.

The estimated pressures and temperatures of equilibration of cordierite and garnet from rocks of the northern part of the Windmill Islands are plotted in figure 6.2 along with other experimentally obtained breakdown curves. Samples 335-19, 335-83, 335-402 and 335-519 were collected from upper amphibolite facies rocks, north of the hypersthene isograd (fig. 2.16), where as 335-274 comes from the north side of Mitchell Peninsula, in the lower granulite facies. All basic rocks from these areas contain hornblende. Thus these rocks (viz. 335-19, 335-83, 335-274, 335-402 & 335-519) should plot close to the experimentally determined curve for the incoming of hypersthene on the low temperature side of the hornblende breakdown curve. If P_{H_2O} was between 0 and 3.0 Kbars the calibration of Currie satisfies these conditions. No rocks from the Windmill Islands contain primary muscovite, but contain sillimanite and K-feldspar (except late stage pegmatites and the quartz vein), hence the rocks should plot on the high temperature side of the muscovite breakdown curve. All cordierite bearing specimens were taken from regions abounding in migmatites suggesting that the P-T conditions these rocks experienced, must have been greater than that necessary for the beginning of melting of a granite. All of these rocks contain sillimanite and so should plot in the stability field of sillimanite.

From figure 6.2 it can be seen that the P-T estimates using the calibration of Currie (1971) are the only ones which fulfil the previously mentioned conditions.

The rocks of the north part of the Windmill Islands (viz. north of Sparkes Bay) are believed to have been re-crystallized under conditions of 5.5 - 6.5 Kbars pressure and temperatures about 760^{o}C with P_{H_2O} approximately 3.0 Kbars.

The rocks south of Sparkes Bay have been shown to have crystallized at higher temperatures than those in the north (see section 5.5) and there is some evidence that load pressures also increases southwards. The assemblage hypersthene + garnet + quartz on Herring Island (228-30) repre-

sents a pelitic rock which should contain cordierite, had P-T conditions been suitable (see section 2.14.2). This absence of cordierite from 288-30 can be accounted for in terms of its breakdown to garnet + sillimanite + quartz or hypersthene + garnet + quartz, reactions indicated by Hensen and Green (1971, 1972 & 1973) to be dominantly pressure sensitive. Thus load pressures, like temperatures, operating on the south Windmill Islands (viz. Herring, Ford & Cloyd Islands) rocks during metamorphism appear to have been higher than those in the north.

APPENDIX I

PETROGRAPHY OF ANALYSED ROCKS

Specimens and thin sections are housed in the Department of Geology and Mineralogy, University of Adelaide. Specimen locations are detailed in Fig. I.1.

335-1 Leuco Gneiss — Bailey Peninsula

Microstructure: Inequigranular, interlobate. Grain boundaries embayed to weakly lobate sutured. Average grain size, 1.0 mm.

Mineralogy: Plagioclase (23%) An 25, antiperthitic. Quartz (39%), graphically intergrown with plagioclase, and commonly as small inclusions. Biotite (2.5%), pleochroic laths. Accessories are Magnetite, Muscovite and Garnet.

335-12A Mafic Gneiss — Ford Island

Microstructure: Inequigranular, polygonal. Grain boundaries straight to weakly embayed. Average grain size, 0.6 mm.

Mineralogy: Plagioclase (42%) An 39. Biotite (23%) pleochroic laths. Clinopyroxene (21%), occasionally simply twinned, and Hypersthene (12%) are commonly larger in grain size. Opaques (2%). Trace of Apatite.

335-15 Aplite — Ford Island

Microstructure: Equigranular interlobate. Grain boundaries embayed to lobate sutured. Average grain size, 0.3 mm.

Mineralogy: Mesoperthite (54%) in band form, commonly poikiloblastic. Quartz (43%), strained. Microcline (2%), tartan twins. Biotite (1%), pleochroic laths with preferred orientation. Traces of Plagioclase, Magnetite and Apatite.

335-19 Migmatite Gneiss — Clark Peninsula

Microstructure: Inequigranular interlobate. Grain boundaries embayed to weakly sutured. Average grain size, 0.8 mm.

Mineralogy: Quartz (44%), commonly as inclusions. Cordierite (28%), multiply twinned, pleochroic halos about included zircons. Biotite (21%). Plagioclase (4%), An 31, patch form antiperthite, opaques (2%). Minor highly fractured Garnet and small prismatic Sillimanite needles.

335-21 Leuco Gneiss Bailey Peninsula

Almost identical microstructure and mineralogy to 335-1.

335-24 Weakly Layered Gneiss Bailey Peninsula

Similar to 335-1 but with slightly more Biotite (10%).

335-30 Leuco Gneiss Bailey Peninsula

Almost identical microstructure and mineralogy to 335-1.

335-32 Leuco Portion of Migmatite Gneiss Bailey Peninsula

Microstructure: Inequigranular, interlobate. Grain boundaries embayed to lobate sutured. Average grain size, 1.5 mm.

Mineralogy: Quartz (38%) strained, commonly as small inclusions. Plagioclase (44%) An 25, albite and pericline twinning, some antiperthitic in rod form. Microcline (16%), perthitic in stringlet or bead form. Traces of shattered Garnets, Biotite, Opaques and Zircon.

335-35 Leuco Gneiss Bailey Peninsula

Microstructure: Equigranular, interlobate. Grain boundaries embayed to lobate sutured. Average grain size, 1.0 mm.

Mineralogy: Quartz (62%), strain extinction, commonly as small inclusions. Plagioclase (27%), commonly has rims of plagioclase, extensively altered to sericite. Microcline (10%), tartan twinned, commonly perthitic. Minor pleochroic Biotite altering to Chlorite. Traces of Epidote and Zircon.

335-45 Layered Gneiss N.E. Bailey Peninsula

Microstructure: Equigranular, polygonal. Grain boundaries straight to slightly embayed. Average grain size, 0.4 mm.

Mineralogy: Plagioclase (39%) An 53, albite and pericline twins. Hornblende (25%). Hypersthene (7%), altered at edges to anthophyllite(?). Biotite (5%), pleochroic laths with a preferred orientation. Most Opaques (5%) are Magnetite with minor Pyrite and Chalcopyrite. Traces of Quartz as small rounded inclusions.

335-50 Layered Gneiss East side of Newcombe Bay

Microstructure: Inequigranular polygonal. Grain boundaries slightly curved to embayed. Average grain size, 1.0 mm.

Mineralogy: Quartz (37%) strained, commonly as small rounded inclusions. Plagioclase (44%), An 20, albite and pericline twins. Biotite (18%), pleochroic laths with preferred orientation concentrated into layers. Opaques (<2%). Traces of Zircon and Microcline.

335-73 Migmatite Gneiss Clark Peninsula

Microstructure: Inequigranular interlobate. Grain boundaries embayed to sutured. Average grain size, 1.0 mm.

Mineralogy: Quartz (19%) strained, commonly as small rounded inclusions. Cordierite (50%) nearly all altered to a fine grained mineral (pininite?). Biotite (16%), pleochroic laths with preferred orientation, commonly altering to Chlorite. Plagioclase (7%), approximately An 40, albite and pericline twins. Garnet (5%), large fractured idioblastic crystals. Sillimanite (<1%), idioblastic crystals with preferred orientation, folded. Opaques (3%), elongate grains probably Magnetite. Traces of Microcline and Zircon.

335-74 Leuco Portion of Migmatite Gneiss Clark Peninsula

Microstructure: Inequigranular, interlobate. Grain boundaries embayed to sutured. Average grain size, 1.3 mm.

Mineralogy: Quartz (15%), strained. Microcline (16%), tartan twinned. Plagioclase (64%), An 29, strongly antiperthitic in patch form. Retrograde Epidote and Muscovite (5%). Trace of Zircon and Garnet.

335-82 Layered Granite Gneiss Clark Peninsula

Microstructure: Inequigranular, interlobate. Grain boundaries embayed to sutured. Average grain size 0.8 mm. Very retrograded rock.

Mineralogy: Quartz (55%), strained, commonly as rounded inclusions. Microcline (22%), tartan twinned. Plagioclase (18%), albite twins, highly altered. Chlorite (7%), alteration of biotite(?), concentrated in layers. Trace of Epidote.

335-83 Migmatite Gneiss Clark Peninsula

Microstructure: Inequigranular, interlobate. Grain boundaries embayed to sutured. Average grain size, 1.0 mm.

Mineralogy: Quartz (22%). Cordierite (26%), multiple twins. Biotite (29%), thin pleochroic laths with preferred orientation. Sillimanite (7%), small idioblastic crystals with a preferred orientation. Plagioclase (7%) approximately An 10, strongly antiperthitic, confined to leuco veins. Porphyroblastic Garnet (2%). Opaque (3%). Traces of Microcline, Muscovite and Chlorite.

335-100 Ribbon Gneiss Pidgeon Island

Microstructure: Equigranular, polygonal to interlobate. Grain boundaries curved to slightly embayed. Average grain size, 1.5 mm.

Mineralogy: Quartz (42%), graphically intergrown with plagioclase. Microcline (39%) perthitic, partially rimmed by plagioclase. Plagioclase (9%), highly altered to sericite. Biotite (4%), altered partly to Chlorite. Magnetite (2%). Traces of Garnet, Zircon, Apatite and retrograde Epidote.

335-110 Mafic Gneiss N.E. Mitchell Peninsula

Microstructure: Equigranular polygonal. Grain boundaries straight to curved. Average grain size, 0.8 mm.

Mineralogy: Plagioclase (43%), approximately An 70. Hornblende (25%), elongate pleochroic laths with a preferred orientation. Clinopyroxene (11%), slightly elongate. Quartz (9%), confined to layers. Hypersthene (4%),

elongate, altered at rims to anthophyllite(?). Elongate Opaques (5%), probably Magnetite. Minor Biotite and Zircon.

335-113 Ribbon Gneiss Pidgeon Island

Microstructure: Equigranular, interlobate. Grain boundaries embayed to lobate sutured. Average grain size, 2.0 mm.

Mineralogy: Quartz (47%), strained. Plagioclase (42%), heavily altered, some graphically intergrown with quartz. Microcline (9%), also altered. Biotite (2%) altering to Chlorite. Minor Opaques and some retrograde Epidote.

335-114 Ribbon Gneiss Pidgeon Island

Almost identical in microstructure and mineralogy to 335-113 but contains slightly more Opaques (Magnetite)(5%).

335-115 Ribbon Gneiss Pidgeon Island

Microstructure: Equigranular, interlobate. Grain boundaries embayed to lobate sutured. Average grain size, 1.0 mm.

Mineralogy: Quartz (36%), strained, commonly as small rounded inclusions. Microcline (31%), tartan twins, some perthitic in string or bead form. Plagioclase (28%), approximately An 20, graphically intergrown with quartz. Biotite (4%), pleochroic laths some altering to Chlorite. Hypersthene (<1%), almost entirely altered to a green fibrous amphibole. Accessories are Opaques and Zircon.

335-122 Ribbon Gneiss Midgely Island

Similar in microstructure and mineralogy to 335-113 but mineral modes are different: Quartz (63%), Microcline (25%), Plagioclase (12%).

335-144 Granite Gneiss Warrington Island

Microstructure: Equigranular, interlobate. Grain boundaries embayed to lobate sutured. Average grain size, 2.0 mm.

Mineralogy: Quartz (37%), strained. Microcline (42%), very perthitic, sometimes only at rims, Plagioclase (21%), graphically intergrown with quartz. Accessories are Biotite, Opaques and Zircon.

335-151 Leuco Gneiss — Beall Island

Microstructure: Inequigranular, polygonal-interlobate. Grain boundaries embayed. Average grain size 4.00 mm.

Mineralogy: Microcline (50%), porphyroblastic, perthitic in stringlet and bead form. Quartz (30%), strained. Plagioclase (20%), some graphically intergrown with quartz. Traces of idioblastic Garnet, Biotite altering to Chlorite and retrograde Epidote.

335-160 Layered Gneiss — Haupt Nunatak

Microstructure: Inequigranular, polygonal to interlobate. Grain boundaries curved to embayed. Average grain size, 0.5 mm. Mineralogical layering.

Mineralogy: Plagioclase (61%), An 52. Quartz (23%). Hornblende (5%). Clinopyroxene (6%). Hypersthene (4%). Traces of Biotite and Opaques.

335-219 Aplite — Browning Peninsula

Microstructure: Inequigranular, interlobate. Grain boundaries embayed to lobate sutured. Average grain size, 3.0 mm.

Mineralogy: Quartz (38%) strained. Microcline (47%), some perthitic in stringlet form. Plagioclase (12%), An 34, graphically intergrown with quartz. Some Opaques and minor Zircon, Apatite and Muscovite.

335-254 Layered Gneiss — Bosner Island

Microstructure: Inequigranular, polygonal. Grain boundaries straight to weakly embayed. Average grain size, 0.7 mm. Mineralogical layering.

Mineralogy: Plagioclase (61%). An 50, larger grain size than other minerals. Clinopyroxene (17%). Biotite (12%), preferred orientation parallel to layers. Hypersthene (4%). Opaques (4%). Minor Apatite.

335-274 Migmatite Gneiss — North Mitchell Peninsula

Microstructure: Inequigranular, polygonal to interlobate. Grain boundaries embayed. Average grain size, 1.5 mm.

Mineralogy: Cordierite (12%), twinned, heavily altered to pininite. Garnet (13%), porphyroblastic. Quartz (29%), strained. Plagioclase (27%), An 39, antiperthitic. Biotite (13%), partially altered to Chlorite. Opaques (3%). Microcline (3%).

335-307 Amphibolite North Robinson Ridge

Microstructure: Inequigranular, polygonal. Grain boundaries straight to curved. Average grain size, 1.0 mm.

Mineralogy: Hornblende (85%), poikilitic, larger grain size than pyroxenes. Clinopyroxene (9%). Orthopyroxene (5%), altered at rims. Opaques (1%) commonly as inclusions in hornblende. (Mostly magnetite with minor pyrite and chalcopyrite).

335-308 Layered Gneiss North Robinson Ridge

Microstructure: Equigranular, polygonal to interlobate. Grain boundaries curved to embayed. Average grain size, 0.2 mm.

Mineralogy: Quartz (30%). Plagioclase (30%). Hornblende (18%). Clinopyroxene (17%). Hypersthene (5%), larger in grain size than other minerals, altering to a fibrous amphibole.

335-313 Layered Gneiss South Robinson Ridge

Microstructure: Equigranular interlobate. Grain boundaries embayed to lobate sutured. Average grain size, 0.8 mm.

Mineralogy: Quartz (27%). Plagioclase (35%), partially altered. Microcline (28%), tartan twins. Biotite (5%), retrograding to Chlorite. Minor Opaques.

335-321 Layered Gneiss South Robinson Ridge

Microstructure: Inequigranular, interlobate. Grain boundaries lobate sutured. Average grain size, 0.8 mm.

Mineralogy: Quartz (47%), flattened in preferred orientations, concentrated in layers. Plagioclase (44%), An 33, perthitic in patch and stringlet form. Hypersthene (5%), altering to anthophyllite, concentrated with quartz. Biotite (1%), pleochroic laths with preferred orientation, associated with hypersthene. Accessories are Opaques and Microcline.

335-324 Weakly Layered Gneiss Mitchell Peninsula

Microstructure: Inequigranular, interlobate. Grain boundaries embayed to lobate sutured. Average grain size, 2.0 mm.

Mineralogy: Quartz (52%), strained. Plagioclase (13%), some graphically intergrown with quartz. Microcline (33%), perthitic in stringlet form. Biotite (1%). Garnet (1%), poikiloblastic. Trace of retrograde fibrous amphibole and Epidote.

335-329 Layered Gneiss Mitchell Peninsula

Microstructure: Inequigranular interlobate. Grain boundaries lobate sutured. Average grain size, 2.0 mm.

Mineralogy: Quartz (65%), strained. Plagioclase (15%), An 40, antiperthitic in string form. Biotite (8%), preferred orientation. Hypersthene (7%), larger pleochroic grains. Idioblastic Garnet (2%). Opaques (3%) and minor Microcline.

335-375 Leuco Gneiss Mitchell Peninsula

Microstructure: Inequigranular, interlobate. Grain boundaries lobate sutured. Average grain size, 1.0 mm.

Mineralogy: Quartz (27%), strained. Plagioclase (35%), An 27, antiperthitic in patch form, graphically intergrown with quartz. Microcline (34%), perthitic in stringlet form. Biotite (2%) altering to Chlorite. Minor Sillimanite and Garnet.

335-380 Layered Gneiss Mitchell Peninsula

Leucocratic layer.

Microstructure: Equigranular interlobate. Grain boundaries embayed to sutured. Average grain size 3.5 mm.

Mineralogy: Quartz (40%), strained, graphically intergrown with plagioclase. Plagioclase (45%), An 23, antiperthitic in patch form. Microcline (15%), tartan twinned, perthitic in stringlet form.

Mafic layer.

Microstructure: Equigranular, interlobate. Grain boundaries embayed to sutured. Average grain size 1.0 mm.

Mineralogy: Quartz (44%), strained, graphically intergrown with plagioclase. Microcline (22%), tartan twinned, perthitic in stringlet form. Plagioclase (13%), An 23. Biotite (12%), pleochroic laths with preferred orientation

parallel to layering. Hypersthene (8%) confined to layers with biotite, strongly pleochroic. Minor Opaques and Apatite.

335-400B Aplite Clark Peninsula

Microstructure: Inequigranular, interlobate. Grain boundaries lobate sutured. Average grain size, 1.0 mm.

Mineralogy: Microcline (40%), perthitic in string form. Quartz (40%), strained. Plagioclase (19%), An 23, partially altered. Traces of Biotite, Opaques, Muscovite and Zircon.

335-402 Migmatite Gneiss Clark Peninsula

Microstructure: Inequigranular, interlobate. Grain boundaries embayed to sutured. Average grain size, 0.8 mm.

Mineralogy: Quartz (22%). Plagioclase (35%), An 34. Biotite (20%), nearly all retrograded to Chlorite. Cordierite (11%), altered. Microcline (7%). Sillimanite (1%), associated with cordierite. Garnet (1%), fractured. Opaques (2%) and minor Zircon.

335-445 Leuco Portion of Migmatite Gneiss Clark Peninsula

Microstructure: Inequigranular, interlobate. Grain boundaries lobate sutured. Average grain size, 2.0 mm.

Mineralogy: Quartz (30%), strained. Microcline (11%), tartan twins. Plagioclase (53%), An 22, antiperthitic in patch form. Small idioblastic Garnet (6%) grains. Traces of Biotite.

335-483 Basic Schist Clark Peninsula

Microstructure: Equigranular, polygonal to interlobate. Grain boundaries curved to embayed. Average grain size, 1.0 mm.

Mineralogy: Plagioclase (49%), An 38, albite and pericline twins. Biotite (23%), pleochroic laths with strong preferred orientation. Hornblende (17%), preferred orientation. Quartz (11%), small rounded inclusions in plagioclase and hornblende. Traces of Opaques and Apatite.

335-495 Leuco Gneiss Clark Peninsula

Microstructure: In equigranular, interlobate. Grain boundaries curved to embayed. Average grain size, 1.0 mm.

Mineralogy: Quartz (31%), strained. Plagioclase (27%), An 22, some antiperthitic, some graphically intergrown with quartz, partially altered. Microcline (39%), perthitic in string form, generally larger grain size. Biotite (3%), altering to Chlorite. Traces of Opaques and retrograde Epidote.

335-502 Pegmatite Clark Peninsula

Large (up to 20 cm.) Microcline crystals graphically intergrown with Quartz.

335-519 Migmatite Gneiss Clark Peninsula

Microstructure: In equigranular, interlobate. Grain boundaries lobate sutured. Average grain size, 1.0 mm.

Mineralogy: Quartz (40%). Plagioclase (35%), An 36. Biotite (20%) partially altering to Chlorite. Cordierite (4%), multiple twins, mostly altering to pininite(?). Sillimanite (1%), small idioblastic crystals with a preferred orientation. Traces of Opaques and Apatite.

335-601 Basic Gneiss N.E. Bailey Peninsula

Microstructure: Equigranular, polygonal. Grain boundaries curved to embayed. Average grain size, 0.7 mm.

Mineralogy: Hornblende (50%), preferred orientation. Hypersthene (12%), partially altered, concentrated in layers. Plagioclase (22%), An 58, antiperthitic. Biotite (7%), preferred orientation. Clinopyroxene (5%). Microcline (3%).

335-602 Basic Gneiss N.E. Bailey Peninsula

Microstructure: Equigranular polygonal. Grain boundaries curved to embayed. Average grain size, 1.0 mm.

Mineralogy: Hornblende (70%). Plagioclase (10%), An 54. Altered Hypersthene (10%) and Clinopyroxene (10%) form mineralogical layering. Traces of Opaques.

335-629 Layered Charnockite Peterson Island

Microstructure: Inequigranular, polygonal to interlobate. Grain boundaries embayed to sutured. Average grain size, 3.0 mm. Layered.

Mineralogy: Quartz (23%) strained. Plagioclase (37%), An 40, some graphically intergrown with quartz. Microcline (23%). Hornblende (12%). Biotite (2%). Hypersthene (1%) Clinopyroxene (5%). Opaques (4%). Minor Apatite and euhedral Zircon.

Throughout the rock are mafic rich (especially in hornblende) layers 3 or 4 crystals thick which are flanked by slightly thicker mafic poor layers.

335-640A Basic Gneiss Cloyd Island

Microstructure: Equigranular, polygonal. Grain boundaries straight to embayed. Average grain size, 0.5 mm.

Mineralogy: Plagioclase (42%), An 39. Quartz (19%). Biotite (21%), strong preferred orientation. Hypersthene (8%), altered at edges, strong preferred orientation. Clinopyroxene (9%), preferred orientation. Minor Opaques and Apatite.

335-641 Basic Gneiss Cloyd Island

Microstructure: Equigranular, polygonal. Grain boundaries straight to embayed. Average grain size, 0.7 mm.

Mineralogy: Plagioclase (57%), An 38. Quartz (8%). Biotite (10%), preferred orientation. Clinopyroxene (9%). Hypersthene (5%), altered at edges. Opaques (5%). Traces of Hornblende, Apatite and Zircon.

335-648 Basic Layered Gneiss Cloyd Island

Microstructure: Inequigranular, polygonal to interlobate. Grain boundaries curved to embayed. Average grain size, 0.7 mm.

Mineralogy: Quartz (22%), strained. Plagioclase (47%), An 52. Biotite (15%), preferred orientation. Clinopyroxene (9%), preferred orientation. Hypersthene (6%), preferred orientation, topotactic growth on clinopyroxene. Opaques (4%). Minor Zircon.

335-674 Porphyritic Granite Ford Island

Microstructure: Inequigranular, interlobate. Grain boundaries embayed to sutured. Porphyroblastic. Average groundmass grain size, 1.5 mm. Average porphyroblast grain size, 10.00 mm.

Mineralogy: Microcline (62%), large tubular, aligned porphyroblasts with a simple twin plane parallel to the preferred orientation, poikiloblastic, smaller grains perthitic in stringlet form. Plagioclase (10%), An 30, antiperthitic in stringlet form, some graphically intergrown with quartz. Quartz (21%) strained. Biotite (3%), altering to Chlorite, preferred orientation parallel to that of microcline. Hornblende (2%). Hypersthene (1%), retrograded at rims. Opaques (1%) are magnetite and pyrite. Traces of Garnet, Sillimanite, Zircon and Apatite.

335-716 Basic Gneiss Clark Peninsula

Microstructure: Equigranular, polygonal to interlobate. Grain boundaries embayed. Average grain size, 0.7 mm.

Mineralogy: Quartz (40%), strained. Plagioclase (34%), An 38, partially altered. Hornblende (22%), poikiloblastic with rounded quartz inclusions. Biotite (2%) altering to Chlorite. Minor Opaques, Limonite (after pyrite?), Apatite and Epidote.

335-717A Mafic Portion of Migmatite Gneiss Clark Peninsula

Microstructure: Equigranular, polygonal to interlobate. Grain boundaries embayed. Average grain size, 0.7 mm.

Mineralogy: Quartz (30%), strained. Plagioclase (51%), An 43. Biotite (18%) partially altered to Chlorite. Garnet (1%). Traces of Opaques, Apatite and retrograde Epidote.

AN71-313 Mafic Gneiss Herring Island

Microstructure: Inequigranular, polygonal. Grain boundaries straight to embayed. Average grain size, 0.6 mm.

Mineralogy: Plagioclase (40%), An 98. Hypersthene (23%). Clinopyroxene (27%). Opaques (10%). Minor Biotite and Apatite.

228-12 Leuco Gneiss Herring Island

Microstructure: Inequigranular, interlobate. Grain boundaries embayed to sutured. Average grain size, 0.7 mm.

Mineralogy Quartz (44%) strained. Microcline (46%), perthitic in stringlet form. Plagioclase (8%) graphically intergrown with quartz. Hypersthene (1%), strongly pleochroic, heavily altered. Trace of Biotite.

288-19 Basic Gneiss Herring Island

Microstructure: Equigranular, polygonal. Grain boundaries straight to curved. Average grain size, 1.0 mm.

Mineralogy: Plagioclase (55%), An 70. Hornblende (20%). Clinopyroxene (13%). Hypersthene (7%). Opaques (5%). Traces of Apatite and Zircon.

288-30 Weakly Layered Gneiss Herring Island

Microstructure: Inequigranular, interlobate. Grain boundaries embayed to sutured. Average grain size, 0.7 mm.

Mineralogy: Quartz (50%). Plagioclase (20%), An 35, altered. Microcline (20%), perthitic in stringlet form. Hypersthene (7%), strongly pleochroic. Biotite (2%), sometimes symplectically intergrown with Opaques. Opaques (1%). Trace of Garnet.

288-46 Basic Gneiss Herring Island

Microstructure: Inequigranular, polygonal to interlobate. Grain boundaries embayed. Average grain size, 0.8 mm.

Mineralogy: Microcline (38%), tartan twins. Quartz (24%). Plagioclase (18%), antiperthitic in rod form. Hypersthene (11%), strongly pleochroic. Clinopyroxene (6%). Biotite (2%). Opaques (2%). Minor Apatite.

288-76 Basic Gneiss Clark Peninsula

Microstructure: Equigranular polygonal. Grain boundaries straight to embayed. Average grain size 0.5 mm.

Mineralogy: Plagioclase (60%). Hornblende (40%). Minor Biotite altering to Chlorite. Traces of Opaques, Apatite and Zircon.

APPENDIX II

TECHNIQUES

1. Sample Preparation

Specimens selected for analyses were first cleaned of weathering products etc., with a cut off saw. The resultant slab weighed at least 500 grams. These slabs were then crushed in a fly press to small pea size fragments. Approximately 50 grams of this sample was separated out using a hopper type sample splitter. This 50 gram separate was crushed to a fine powder (<180 mesh) in a Siebteknik mill using a chrome steel grinding vessel. This powder was used for chemical analyses.

2. Chemical Analyses

Major elements (excluding FeO and Na_2O) were determined by X-Ray fluorescence using a modified Philips X-Ray Spectrograph PW/1540. Operating conditions are listed in Table II.1. The technique used is one modified from Norrish and Hutton (1969) by the Department of Geology and Mineralogy at the University of Adelaide. Various standards (G-2, SY-1, BCR-1 & PCC-1) were repeatedly analysed with the Windmill Islands samples to check on accuracy. Values of these standards was obtained from Flanagan (1973).

Na_2O and K_2O were determined using an EEL flame photometer. Samples were digested with hydrofluoric and perchloric acid in platinum crucibles. Blanks were run to check for contamination and, as with the X.R.F. analyses, standards were run to check the accuracy.

FeO was determined using the modified Pratt Method described in Maxwell (1968 page 416).

H_2O^+ was determined using the Penfield Method (Maxwell 1968 page 221).

Trace elemental concentrations were determined by X.R.F. techniques on pressed buttons of rock powder. Operating conditions are listed in Table II.1. The techniques used were modified from Norrish and Chappell (1967) and are detailed in The University of Adelaide, Department of Geology and Mineralogy unpublished reports 3/73 (Rb & Sr) and 6/74 (Th & Pb).

Mass absorption coefficient corrections for these trace element analyses were calculated from major element oxide weight percentages following the method described by Norrish and Chappell (1967).

Element	X-Ray Tube	Excitation Energy KV/ma	Analysing Crystal	2Θ	Background Θ	Spectral Line	Collimator	Counter
Major Elements								
Si	Cr	60/40	PE	79.06		Kα	Coarse	Flow Prop. ($Ar-10\%CH_4$)
Al	"	60/40	PE	115.06		"	"	"
Fe	"	50/30	LiF200	57.45		"	"	"
Ca	"	40/20	LiF200	113.01		"	"	"
Mg	"	50/45	ADP	106.47		"	"	"
P	"	60/40	Ge	110.00		"	"	"
Ti	"	60/40	LiF200	86.07		"	"	"
K	"	60/40	PE	20.46		"	"	"
Mn	Mo	50/30	LiF200	62.91		"	"	"
Trace Elements								
Rb	Mo	60/40	LiF220	37.66	36.60	$K\alpha_{1-2}$	Fine	Scintillation
Sr	"	"	"	35.54	36.60	$K\alpha_{1-2}$	Coarse	"
Pb	"	"	"	40.36	41.02	$L\beta_{1-2}$	Fine	"
Th	"	"	"	39.07	38.57	$L\alpha_1$	Fine	"

TABLE: II.1: X.R.F. Operating Conditions

REFERENCES CITED

Albee, A.L., 1965. Distribution of Fe,Mg and Mn between garnet and biotite in natural mineral assemblages. J.Geol., 73, 155-164.

Annersten, H., 1968. A mineral chemical study of a metamorphosed iron formation in Northern Sweden. Lithos., 1, 374-397.

Annersten, H. & Ekström, T., 1971. Distribution of major and minor elements in coexisting minerals from a metamorphic iron formation. Lithos., 4, 185-204.

Arriens, P.A., 1971. The Precambrian geochronology of Antarctica. Abstracts of the First Australian Geological Convention, page 97.

Atkins, F.B., 1969. Pyroxenes of the Bushveld intrusion, South Africa. J. Petrology, 10, 222-249.

Barker, Fred., 1962. Cordierite-garnet gneiss and associated microcline rich pegmatite at Sturbridge, Massachusetts and Union, Connecticut. Am. Miner., 47, 907-918.

Barth, T.F.W., 1966. Theoretical Petrology. 2nd Ed. John Wiley & Sons, Inc., 416pp.

Bell, T.H., 1973. Mylonite development in the Woodroofe Thrust, north of Amata, Musgrave Ranges, Central Australia. Unpublished Ph.D. thesis, Univ. Adelaide.

Binns, R.A., 1962. Metamorphic pyroxenes from the Broken Hill District, New South Wales. Miner. Mag., 33, 320-338.

Binns, R.A., 1964. Zones of progressive regional metamorphism in the Willyama Complex, Broken Hill District, New South Wales. J. geol. Soc. Aust., 11, 283-330.

Binns, R.A., 1965. The mineralogy of metamorphosed basic rocks from the Willyama Complex, Broken Hill District, New South Wales: Part 1. Hornblendes. Miner. Mag., 35, 306-326.

Binns, R.A., 1969a. Ferromagnesium minerals in high grade metamorphic rocks. Spec. Publs. geol. Soc. Aust., 2, 323-332.

Binns, R.A., 1969b. Hydrothermal investigations of the Amphibolite-Granulite facies boundary. Spec. Publs. geol. Soc. Aust., 2, 341-344.

Boyd, F.R. & England, J.L., 1960. Apparatus for phase-equilibrium measure-ments at pressures up to 50 kilobars and temperatures up to 1750°C. J. geophys. Res., 65, 741-748.

Boyd, F.R. & England, J.L., 1964. The system enstatite-pyrope. Carnegie Inst. Wash. Year b., 63, 157-161.

Burns, R.G., 1966. Origin of optical pleochrism in orthopyroxenes. Miner. Mag., 35, 715-719.

Butler, P. Jnr., 1969. Mineral compositions and equilibria in the metamorphosed iron formation of the Gagnon Region, Quebec, Canada. J. Petrology., 10, 56-101.

Byerly, G.R. & Vogel, T.A., 1973. Grain boundary processes and development of metamorphic plagioclase. Lithos., 6, 183-202.

Cameron, R.L., Goldich, S.S. & Hoffman, J.H., 1960. Radioactity age of rocks from the Windmill Islands, Budd Coast, Antarctica. Acta Univ. Stockh., 6, 1-6.

Chappell, B.W. & White, A.J.R., 1974. Two contrasting granite types. Pacific Geology, 8, 173-174.

Chinner, G.A., 1960. Pelitic gneisses with varying Ferrous/Ferric ratios from Glen Clova, Angus, Scotland. J. Petrology., 1, 178-217.

Chuboba, K., 1933. The determination of the feldspars in thin section. Thomas Murby & Co.

Collerson, K.D., 1972. High grade metamorphic and structural relationships near Amata, Musgrave Ranges, Central Australia. Unpublished Ph.D. thesis, Univ. Adelaide.

Collerson, K.D., 1974. Descriptive microstructural terminology for high grade metamorphic tectonites. Geol. Mag., 111, 313-318.

Collerson, K.D., 1975. Contrasting patterns of K/Rb distribution in Precambrian high grade metamorphic rocks from Central Australia. J. geol. Soc. Aust., 22, 145-158.

Currie, K.L., 1971. The reaction 3 cordierite - 2 garnet + 4 sillimanite + 5 quartz as a geological thermometer in the Opinicon Lake Region, Ontario. Contr. Miner. Petrology., 33, 215-226.

Currie, K.L., 1973. A note on the calibration of the garnet-cordierite geothermometer and geobarometer. Contr. Miner. Petrology., 44, 35-44.

Dahl, O., 1972. The effect of garnet cell volume on the distribution of Mg and Fe in garnet exchange equilibria. Lithos., 5, 33-56.

Davidson, L.R., 1968. Variations in ferrous iron - magnesium distribution coefficients of metamorphic pyroxenes from Quairading, Western Australia. Contr. Miner. Petrology., 19, 239-259.

Davidson, L.R., 1969. Fe^{2+} - Mg^{2+} distribution in co-existing metamorphic pyroxenes. Spec. Publs. geol. Soc. Aust., 2, 341-344.

Deer, W.A., Howie, R.A. & Zussman, J., 1963. Rock forming minerals: Vol. 1., Ortho and ring silicates. London; Longmans, Green and Co. Ltd., 435p.

Deer, W.A., Howie, R.A. & Zussman, J., 1966. An introduction to the rock forming minerals. London; Longmans, Green and Co. Ltd., 528p.

Didier, J., 1973. Granites and their enclaves. The bearing of enclaves on the origin of granites. (Developments in Petrology.3.)., Elsevier Scientific Publishing Co.

Dougan, T.W., 1974. Cordierite gneisses and associated lithologies of the Guri Area, Northwest Guayana Shield, Venezuela. Contr. Miner. Petrology., 46, 169-188.

Drury, S.A., 1973. The geochemistry of Precambrian granulite facies rocks from the Lewisian Complex of Tiree, Inner Hebrides, Scotland. Chem. Geol., 11, 167-188.

Engel, A.E.J. & Engel, C.G., 1962. Hornblendes formed during progressive metamorphism of Amphibolites, North West Adirondack Mountains, New York. Bull. geol. Soc. Am., 73, 1499-1514.

Eskola, P., 1957. On the mineral facies of Charnockites. J. Madras Univ., 27, 101-119.

Evans, B.W., 1965. Pyrope garnet-piezometer or thermometer? Bull. geol. Soc. Am., 76, 1295-1300.

Evans, B.W. & Leake, B.E., 1960. The composition and origin of the striped Amphibolite of Connemara, Ireland. J. Petrology., 1, 337-363.

Flanagan, F.J., 1973. 1972 values for international geochemical reference samples. Geochim. cosmochim. Acta., 37, 1189-1200.

Fleming, P.D., 1972. Mg-Fe distribution between co-existing garnet and biotite, and the status of fibrolite in the andalusite, staurolite zone of the Mt. Lofty Ranges, South Australia. Geol. Mag., 109, 477-482.

Gable, D.J. & Sims, P.K., 1969. Geology and regional metamorphism of some high grade cordierite gneisses, Front Range, Colorado. Geol. Soc. Am. Spec.Pap. 128.

Ghose, S., 1965. Mg^{2+}-Fe^{2+} order in orthopyroxene, Mg 0.93 $Fe_{1.07}Si_2O_6$. Z. Kristallogr., 122, 81-99.

Ghose, S. & Hafner, S.S., 1967. Mg^{2+}-Fe^{2+} distribution in metamorphic and volcanic orthopyroxenes. Z. Kristallogr., 125, 157-162.

Gilbert, M.C., 1966. Synthesis and stability relations of the hornblende ferropargasite. Am. J. Sci., 264, 698-742.

Goldsmith, J.R. & Heard, H.C., 1961. Subsolidus phase relations in the system $CaCO_3$-$MgCO_3$., J. Geol., 69, 46-71.

Green, D.H. & Ringwood, A.E., 1967. An experimental investigation of the gabbro to eclogite transformation and its petrological applications. Geochim. cosmochim. Acta., 31, 767-833.

Harrington, H.J., 1965. Geology and geomorphology of Antarctica. Biogeography and ecology in Antarctica. Monographic Biol., 15, 1-71.

Heier, K.S., 1964. Rb/Sr and Sr^{87}/Sr^{86} ratios in deep crustal material., Nature, 202, 477-478.

Heier, K.S., 1965a. Metamorphism and the chemical differentiation of the crust. Geol. Föreń. Stockh. Förh., 87, 249-256.

Heier, K.S., 1965b. Radioactive elements in the continental crust. Nature, 208, 479-480.

Heier, K.S., 1973a. Geochemistry of granulite facies rocks and problems of their origin. Phil. Trans. R. Soc., 273, 429-442.

Heier, K.S., 1973b. A model for the composition of the deep continental crust. Fortschr. Miner., 50, 174-187.

Heier, K.S. & Adams, J.A.S., 1965. Concentration of radioactive elements in deep crustal material. Geochim. cosmochim Acta., 29, 53-61.

Heier, K.S. & Thoresen, K., 1971. Geochemistry of high grade metamorphic rocks, Lofoten-Vesterålen, North Norway, Geochim cosmochim Acta, 35, 89-100.

Heitanen, A., 1967. On the facies series in various types of metamorphism. J. Geol., 75, 187-214.

Hensen, B.J., 1971. Theoretical phase relations involving cordierite and garnet in the system MgO-FeO-Al_2O_3-S_1O_2. Contr. Miner. Petrology., 33, 191-214.

Hensen, B.J., 1972. Cordierite-garnet equilibrium as a function of pressure, temperature, and iron-magnesium ratio., Carnegie Inst. Wash. Year b., 71, 418-421.

Hensen, B.J. & Green, D.H., 1969. Experimental data on the stability of garnet and cordierite in high grade metamorphic rocks. Spec. Publs. geol. Soc. Aust., 2, 345-347.

Hensen, B.J. & Green, D.H., 1970. Experimental data on coexisting cordierite and garnet under high grade metamorphic conditions. Phys. Earth & Planet Interiors., 3, 431-440.

Hensen, B.J. & Green, D.H., 1971. Experimental study of cordierite and garnet in pelitic compositions at high pressures and temperatures: I. Compositions with excess alumino-silicate. Contr. Miner. Petrology., 33, 309-330.

Hensen, B.J. & Green, D.H., 1972. Experimental study of cordierite and garnet in pelitic compositions at high pressures and temperatures:II. Compositions without excess alumino-silicate. Contr. Miner. Petrology., 35, 331-354.

Hensen, B.J. & Green, D.H., 1973. Experimental study of cordierite and garnet in pelitic compositions at high pressures and temperatures:III. Synthesis of Experimental data and geological applications. Contr. Miner. Petrology., 38, 151-166.

Henry, J., 1974. Garnet-cordierite gneisses near the Egersund-ogna anorthositic intrusion, southwestern Norway. Lithos., 7, 207-216.

Himmelberg, G.R. & Phinney, W.M.C., 1967. Granulite facies metamorphism, Granite falls Montevideo Area, Minnesota. J. Petrology., 8, 325-348.

Hollander, N., 1970. Distribution of chemical elements among phases in amphibolites and gneiss. Lithos, 3, 93-111.

Holmes, A., 1928. The nomenclature of Petrology. 2nd Ed. Thomas Murby & Co.

Howie, R.A., 1964. Pleochroism of orthopyroxenes. Nature., 204, 279.

Hubbard, F.H., 1967. Exsolution myrmekite. Geol. Föreń. Stockh. Förh., 89, 410-422.

Hubregtse, J.J.M.W., 1973. Distribution of elements in some basic granulite facies rocks. Eerste Reeks., Deel., 27, 1-68.

Hutcheon, I., Froese, E. & Gordon, T.M., 1974. The assemblage quartz-sillimanite-garnet-cordierite as an indicator of metamorphic conditions in the Daly Bay Complex, N.W.T. Contr. Miner. Petrology., 44, 29-34.

Joplin, G.A., 1968. A petrography of Australian metamorphic rocks. Angus and Robertson, 262p.

Van der Kamp, P.C., 1968. Geochemistry and origin of metasediments in the Haliburton-Madoc area, S.E.Ontario. Can. J. Earth Sci., 5, 1337-1372.

Kleeman, A.W., 1965. The origin of granitic magmas. J. geol. Soc. Aust., 12, 35-52.

Kretz, R. 1959. Chemical study of garnet, biotite and hornblende from gneisses of southwestern Quebec, with emphasis on distribution of elements in co-existing minerals. J. Geol., 67, 371-402.

Kretz, R., 1961. Some applications of thermodynamics to co-existing minerals of variable composition: Examples: Orthopyroxene-clinopyroxene and orthopyroxene-garnet. J. Geol., 69, 361-387.

Kretz, R., 1963. Distribution of magnesium and iron between ortho-pyroxene and calcic pyroxene in natural mineral assemblages. J. Geol., 71, 773-785.

Kretz, R., 1964. Analysis of equilibrium in garnet-biotite-sillimanite gneisses from Quebec. J. Petrology., 5, 1-20.

Lambert, I.B. & Heier, K.S., 1967. The vertical distribution of Uranium, Thorium and Porassium in the Continental crust. Geochim. cosmochim. Acta., 31, 377-390.

Lambert, I.B. & Heier, K.S., 1968a. Geochemical Investigations of deep seated rocks in the Australian Shield. Lithos., 1, 30-53.

Lambert, I.B. & Heier, K.S., 1968b. Estimates of crustal abundance of Thorium, Uranium and Potassium. Chem. Geol., 3, 233-238.

Lambert, I.B. & Wyllie, P.J., 1972. Melting of gabbro (quartz eclogite) with excess water to 35 kilobars, with geological applications. J. Geol., 80, 693-708.

Lange, I.M., Reynolds, R.C.Jnr. & Lyons, J.B., 1966. K/Rb ratios in co-existing K feldspar and biotites from some New England granite and metasediments., Chem. Geol., 1, 317-322.

Leake, B.E., 1963. Origin of amphibolite from north west Adirondacks, New York. Bull. geol. Soc. Am., 74, 1193-1202.

Leake, B.E., 1964. The chemical distinction between ortho and para amphibolites. J. Petrology., 5, 238-254.

Leake, B.E., 1966a. The relation between tetrahedral aluminium and the maximum possible octahedral aluminium in natural calciferous and sub-calciferous amphiboles. Am. Miner., 50, 843-851.

Leake, B.E., 1965b. The relationship between composition of calciferous amphibole and grade of metamorphism; in Pitcher, W.S. & Flinn, G.W. (Eds) Controls of Metamorphism. Oliver and Boyd, Edinburgh, 299-318.

Leake, B.E., 1969. Tje discrimination of ortho and para charnockitic rock, anorthosites and amphbolites. Indian Mineralogist., 10, 89-104.

Leake, B.E., 1971. On aluminous and edenitic hornblendes Miner. Mag., 38, 389-407.

Lewis, J.D. & Spooner, C.M., 1973. K/Rb ratios in Precambrian granulite terrains. Geochim cosmochim. Acta., 37, 1111-1118.

Lindh, A., 1974. Manganese distribution between co-existing pyroxenes. Neues Jb. Miner. Mh., 8, 335-344.

Lyons, J.B. & Morse, S.A., 1970. Mg/Fe partitioning in garnet and biotite from some granitic, pelitic and calcic rocks. Am. Miner., 55, 231-245.

McLeod, I.R. & Gregory, C.M., 1966. Geological investigations along the Antarctic coast between longitude 108°E and 166°E. A.N.A.R.E. Scientific Reports, Series A(iii) Geology, Publ. 83.

Mason, B., 1958. Principles of Geochemistry. 2nd Ed. John W. Ley & Sons Inc., 310pp.

Maxey, L.R. & Vogel, T.A., 1974. Compositional Dependence of the co-existing pyroxene iron-magnesium distribution coefficient. Contr. Miner. Petrology., 43, 295-306.

Maxwell, J.A., 1968. Rock and Mineral Analysis. Interscience Publishers, 584p.

Moore, A.C., 1970. Descriptive terminology for the textures of rocks in granulite facies terrain. Lithos, 3, 123-127.

Mueller, R.F., 1960. Compositional characteristics of equilibrium relations in mineral assemblages of a metamorphosed iron formation. Am. Miner., 21, 449-497.

Mueller, R.F., 1961. Analysis of relations among Mg,Fe and Mn in certain metamorphic minerals. Geochim. cosmochim Acta., 25, 267-296.

Newton, R.C., 1972. An experimental determination of the high-pressure stability limits of magnesium cordierite under wet and dry conditions. J. Geol., 80, 398-420.

Newton, R.C., Charlu, T.V. & Kleppa, O.J., 1974. A calorimetric investigation of the stability of anhydrous magnesium cordierite with application to granulite facies metamorphism. Contr. Miner. Petrology., 44, 295-311.

Nockolds, S.R., 1954. Average chemical composition of some igneous rocks. Bull. geol. Soc. Am., 65, 1001-1052.

Norrish, K. & Chappell, B.W. 1967. X-Ray Fluorescence Spectrography; in Zussman, J.(ed), Physical methods in Determinative Mineralogy. Academic Press, London. 514p.

Norrish, K. & Hutton J.T., 1969. An accurate X-Ray spectrographic method for the analysis of a wide range of geological samples. Geochim cosmochim. Acta., 33, 431-453.

Offler, R., 1966. The structure and metamorphism of the Pewsey Vale area north-east of Williamstown, S.A. Unpublished Ph.D. thesis Univ. Adelaide.

Oliver. R.L., 1970. Some aspects of Antarctica-Australian geological relationships; in Antarctic Geology and Geophysics; Adie R.J. (ed), 859-864.

Pettijohn, F.J., 1957. Sedimentary Rocks. 2nd ed. Harper and Brothers, 718p.

Phadke, A.V. & Powar, K.B., 1972. On the biotite-garnet-cordierite -sillimanite association from the Sausar Group. Curr. Sci., 141, 779-780.

Phillips, E.R., 1974. Myrmekite - One hundred years later. Lithos., 7, 181-194.

Raase, P., 1974. Al and Ti contents of hornblendes, indicators of pressure and temperature of regional metamorphism. Contr. Miner. Petrology, 45, 231-236.

Ramberg, H., 1952. The origin of metamorphic and metasomatic rocks. University of Chicago Press.

Ramberg, H., 1962. Intergranular precipitation of albite formed by unmixing of alkali feldspars. Neues. Jb. Miner. Ab., 98, 14-34.

Ramberg, H. & DeVore, G.W., 1951. The distribution of Fe^{2+} and Mg^{2+} in co-existing olivines and pyroxenes. J. Geol., 68, 110-113.

Ravich, M.G., 1960. The rocks of Grearson Hills and the Windmill Islands (Greason Oasis). In collected papers Antarctic Geology, Pt 2, Scientific Research Institute of Antarctic Geology, 113, 53-81.

Ravich, M.G. & Voronov, P.S., 1958. Geological structures of the coast of the East Antarctica continent (between 55^{o}E and 110^{o}E longitude). Sov. Geol., 2, 3-26.

Ravich, M.G., Klimov, L.V. & Solovev, D.S., 1965. The Precambrian of East Antarctica. Transactions of the Scientific Research Institute of Geology of the Arctic, of the State Geological Comittee of the U.S.S.R.

Ray, S. & Sen, S.K., 1970. Partitioning of major exchangeable cations among orthopyroxene, calcic pyroxene and hornblende in basic granulites from Madras. Neues Jb. Miner. Abh., 114, 61-88.

Reinhardt, E.W., 1968. Phase relations in cordierite bearing gneisses from the Gananoque area, Ontaria. Can. J. Earth. Sci., 5, 455-482.

Richardson, S.W., 1968. Staurolite stability in part of the system Fe-Al-Si-O-H. J. Petrology, 9, 467-488.

Richardson, S.W., Gilbert, M.C. & Bell, P.M., 1969. Experimental determination of kyanite-andalusite and andalusite-sillimanite equilibria; The aluminosilicate triple point. Am. J. Sci., 267, 259-272.

Rickwood, P.C., 1968. On recasting analyses of garnet into end member molecules. Contr. Miner. Petrology., 18, 175-198.

Rivalenti, G. & Rossi, A., 1973. Amphiboles and biotites of the hornblende gneisses in an area to the north east of the Fjord Qagssit, Frederikshåb district, south-west Greenland. Tschermaks miner. petrogr. Mitt., 20, 13-27.

Robertson, R., 1961. Preliminary report on the bedrock geology of the Windmill Islands. I.G.Y. Glaciological Reports, 4, 1-26.

Robie, R.A. & Waldbaum, D.R., 1968. Thermodynamic properties of minerals and related substances at 298.15°K (25.0°C) and one atmosphere (1.013 bars) pressure and at higher temperatures. Bull. geol. Soc. Am., 1259, 256p.

Saxena, S.K., 1968. Crystal chemical aspects of distribution of elements among certain rock forming silicates. Neues Jb. Miner. Abh., 108, 292-323.

Saxena, S.K., 1969a. Silicate solid-solutions and geothermometry: 3. Distribution of Fe and Mg between co-existing garnet and biotite. Contr. Miner. Petrology, 22, 259-267.

Saxena, S.K., 1969b. Distribution of elements in co-existing minerals and the problem of chemical disequilibrium in metamorphosed basic rocks. Contr. Miner. Petrology, 20, 177-197.

Saxena, S.K., 1971. Mg^{2+}-Fe^{2+} order-disorder in orthopyroxene and the Mg^{2+}-Fe^{2+} distribution co-existing minerals. Lithos, 4, 345-354.

Saxena, S.K. & Ghose, S., 1971. Mg^{2+}-Fe^{2+} order-disorder and the thermodynamics of the orthopyroxene crystalline solution Am. Miner., 56, 532-559.

Saxena, S.K. & Hollander, N.B., 1969. Distribution of iron and magnesium in co-existing biotite, garnet and cordierite. Am. J. Sci., 267, 210-216.

Scharbet, H.G. & Kurat, G., 1974. Distribution of some elements between co-existing ferromagnesium minerals in Moldanubian granulite facies rocks, Lower Austria. Tschermaks miner. petrogr. Mitt., 21, 110-134.

Schreyer, W., 1965a. Zür stabilität des ferrocordierits. Beitr. Miner. Petrogr., 11, 297-322.

Schreyer, W., 1965b. Upper pressure stability limit of Mg-cordierite Carnegie Inst. Wash. Year b., 66, 387-388.

Schreyer, W. & Schairer, J.F., 1961. Compositions and structural states of anhydrous Mg cordierites: A re-investigation of the central part of the system $MgO-Al_2O_3-SiO_2$. J. Petrology., 2, 324-406.

Schreyer, W. & Seifert, F., 1969a. Compatibility relations of the aluminium silicates in the systems $MgO-Al_2O_3-SiO_2-H_2O$ and $K_2O-MgO-Al_2O_3-SiO_2-H_2O$ at high pressures. Am.J. Sci., 267, 371-388.

Schreyer, W. & Seifert, F., 1969b. High pressure phases in the system $MgO-Al_2O_3-SiO_2-H_2O$. Am. J. Sci., Schrairer Volume, 407-443.

Schreyer, W. & Yoder, H.S., 1960. Instability of anhydrous Mg-cordierite at high pressures. Carnegie Inst. Wash. Year b., 59, 90-91.

Schreyer, W. & Yoder, H.S., 1964. The system Mg-cordierite-H_2O and related rocks. Neues Jb. Miner. Abh., 101, 271-342.

Sen, S.K., 1970. Magnesium-iron compositional variance in hornblende pyroxene granulite. Contr. Miner. Petrology, 29, 76-88.

Sen, S.K., 1973. Compositional relations among hornblende and pyroxenes in basic granulites and an application to the origin of garnets. Contr. Miner. Petrology., 38, 299-306.

Sen, S.K. & Chakraboty, K.R., 1968. Magnesium-iron exchange equilibrium in garnet-biotite and metamorphic grade. Neues Jb. Miner. Abh., 108, 181-207.

Shaw, D.M., 1968. A review of the K-Rb fractionation trends by covariance analysis. Geochim. cosmochim. Acta, 32, 573-601.

Shaw, D.M., 1972. The origin of the Apsley Gneiss, Ontario. Can. J. Earth. Sci., 9, 18-35.

Shaw, D.M. & Kudo, A.M., 1965. A test of the discriminant function in the Amphibolite problem. Miner. Mag., 34, 423-435.

Sheraton, J.W., 1970. Origin of the Lewisian gneiss of northwest Scotland, with particular reference to the Drumbeg area, Sutherland. Earth Plan. Sci. Lett., 8, 301-310.

Sighinolfi, G.P., 1970. Investigations into the deep levels of the continental crust: Petrology and chemistry of the granulite facies terrains of Bahia (Brazil). Processi verb. Soc. tosc. Sci. nat. Pisa., 77, 327-341.

Sighinolfi, G.P., 1971. Investigations into deep crustal levels: Fractionation effects and geochemical trends related to high-grade metamorphism. Geochim. cosmochim. Acta., 35, 1005-1021.

Spry, A., 1969. Metamorphic textures. Permagon Press Ltd. 370p.

Starik, I.E., Ravich, M.G., Krylov, A.J. & Silin, J.I., 1959. On absolute age of rocks of the Eastern Antarctic Platform Dokl. Akad. Nauk. SSSR., 126, 144-146.

Starik, I.E., Ravich, M.G., Krylov, A.J., Silin, J.I., Atrashenok, L.J. & Lovcjus, A.V., 1960. New data on the absolute ages of rock of the Eastern Antarctic continent. Dokl. Akad. Nauk. SSSR., 134, 1441-1443.

Talbot, J.L. & Hobbs, B.E., 1968. The relationship of metamorphic differentiation to other structural features at three localities. J. Geol., 76, 581-586.

Taylor, S.R., 1965. The application of trace element data to problems in petrology. Phys. Chem. Earth., 6, 133-213.

Tobi, A.C., 1971. The nomenclature of the charnockite rock suite. Neues Jb. Miner. Mh., 5, 193-205.

Touret, J., 1971a. Les facies granulite en Norvege Meridionale: I. Les associations mineralogiques. Lithos, 4, 239-249.

Touret, J. 1971b. Les facies granuilite en Norvege Meridionale: II Les fluides inclusions. Lithos., 4, 423-436.

Trail, D.S., 1963. Low-grade metamorphic rocks from the Prince Charles Mountains, East Antarctica. Nature., 197, 548-550.

Turner, F.J., 1958. Mineral assemblages of individual metamorphic facies. in Fyfe, W.S., Turner, F.J. & Verhoogen, J. Metamorphic reactions and metamorphic facies: Mem. geol. Soc. Am., 73, 199-239.

Turner, F.J., 1968. Metamorphic Petrology: Mineralogical and field aspects. Published by McGraw Hill, 403p.

Turner, F.J. & Weiss, L.E., 1963. Structural analysis of metamorphic tectonites. McGraw Hill, New York. 545p.

Virgo, D., 1966. Some elemental distributions between co-existing feldspars in metamorphic rocks. Unpublished Ph.D. thesis Univ. Adelaide.

de Vore, C.W., 1955. The role of adsorption in the fractionation and distribution of elements. J. Geol., 63, 159-190.

Voronov, P.S. & Krasik, A.M., 1963. Brief geological and geophysical characteristics of Grearson Oasis and the Budd Coast area in East Antarctica. Inf. Byull. sov. antarkt. Eksped. 42, 5-11.

de Waard, D., 1965. A proposed subdivision of the granulite facies. Am. J. Sci., 263, 455-461.

Webb, A.W., McDougall, I. & Cooper, J.A., 1963. Potassium-Argon dates from the Vincennes Bay region and Oates Land, Antarctica in Adie, R.J. (ed) Antarctic Geology., 597-600.

Weisbrod, A., 1973. Cordierite-garnet equilibrium in the system Fe-Mn-Al-Si-O-H. Carnegie Inst. Wash. Year b., 72, 515-518.

White, A.J.R., 1966. Genesis of migmatites from the Palmer region of South Australia. Chem. Geol., 1, 165-200.

Whitney, P.R., 1969. Variations of K/Rb ratio in migmatitic paragneisses of the northwest Adirondacks. Geochim. cosmochim. Acta., 33, 1203-1211.

Winkler, H.G.F., 1967. Petrogeneses of metamorphic rocks. 2nd Ed. Springler-Verlag, 237p.

Wones, D.R. & Eugster, H.P., 1965. Stability of biotite: Experiment theory and application. Am. Miner., 50, 1228-1272.

Wood, B.J., 1973. Fe^{2+}-Mg^{2+} partition between co-existing cordierite and garnet: A discussion of experimental data. Contr. Miner. Petrology, 40, 253-258.

Wood, B.J., 1974. The solubility of alumina in orthopyroxene co-existing with garnet. Contr. Miner. Petrology., 46, 1-15.

Wynne-Edwards, H.R. & Hay, P.W., 1963. Co-existing cordierite and garnet in regionally metamorphosed rocks from the Westport area, Ontario. Can. Mineralogist., 7, 453-478.

Yoder, H.S. Jnr. & Tilley, C.E., 1962. Origin of basalt magmas: An experimental study of natural and synthetic rock systems. J. Petrology., 3, 342-532.